A geomagnetic polarity timescale for the Permian, calibrated to stage boundaries

Mark W. Hounslow[1] (m.hounslow@lancs.ac.uk) & Yuri P. Balabanov[2] (balabanov-geo@mail.ru)

[1]. Palaeomagnetism, Environmental Magnetism, Lancaster Environment Centre, Lancaster Univ. Lancaster, Bailrigg, LA1 4YW, U.K.

[2]. Kazan Federal University, Kazan, Russia

Abstract: The reverse polarity Kiaman Superchron has strong evidence for three, probably four normal magnetochrons during the early Permian. Normal magnetochrons are during the early Asselian (base CI1r.1n at 297.94±0.33 Ma), late Artinskian (CI2n at 281.24±2.3 Ma), mid Kungurian (CI3n at 275.86±2.0 Ma) and Roadian (CI3r.an at 269.54 ±1.6 Ma). The mixed polarity Illawarra Superchron begins in the early Wordian at 266.66 ±0.76 Ma. The Wordian to Capitanian interval is biased to normal polarity, but the basal Wuchiapingian begins the beginning of a significant reverse polarity magnetochron LP0r, with an overlying mixed polarity interval through the later Lopingian. No significant magnetostratigraphic data gaps exist in the Permian geomagnetic polarity record. The early Cisuralian magnetochrons are calibrated to a succession of fusulinid zones, the later Cisuralian and Guadalupian to a conodont and fusulinid biostratigraphy and Lopingian magnetochrons to conodont zonations. Age calibration of the magnetochrons is obtained through a Bayesian approach using 35 radiometric dates. 95% confidence intervals on the ages and chron durations are obtained. The dating control points are most numerous in the Gzhelian-Asselian, Wordian and Changhsingian intervals. This significant advance should provide a framework for better correlation and dating of the marine and non-marine Permian.

Igneous and sedimentary rocks record the earth's magnetic field at the time of their formation, via their small content of mostly Fe-oxides. This is recorded as a remanent magnetisation, which needs to be both stable with time, resist potential later re-magnetisation events, and be subsequently extracted using palaeomagnetic measurements. The first study of remanent magnetisation of Permian rocks was Mercanton (1926) using volcanic rocks from near Kiama on the New South Wales coast in Australia. This followed earlier studies on much younger rock by Brunhes (1906), in which the remanent magnetisation directions recorded, had orientations similar to the modern field, which is now defined as having *normal* polarity. However, some volcanic rocks recorded a remanent magnetisation direction opposite to the modern field (*reverse* polarity), which Matuyama (1929) suggested recorded a reversal in the main (i.e. dipole) component of the Earth's magnetic field (see discussion of these early developments in Jacobs 1963). Mercanton (1926) was the first to identify remanent magnetisation in Permian rocks with a reverse polarity, but science did not recognise the significance of these Australian volcanics until the re-study of the New South Wales coastal sections by Irving & Parry (1963). The reverse polarity of other early Permian volcanics were studied earlier by Creer *et al.* (1955), and red-bed sediments by Doell (1955), Graham (1955) and Khramov (1958).

The pioneer in our understanding of using changes in the polarity of the earth's magnetic field for correlation and dating was A. N. Khramov, who in Khramov (1958), outlined a rudimentary polarity stratigraphy from late Permian and early Triassic sections in the Vyatka River region of the Moscow Basin, with details of this work later appearing in Khramov (1963a). Khramov (1958) discussed issues of data quality and cross-validation by exploring the concepts of utilising data from multiple sections, with minimum sampling requirements to define intervals (magnetozones) of single polarity, concepts which are now embodied in the magnetostratigraphic quality criteria proposed by Opdyke & Channel (1996).

Irving & Parry (1963) later defined a polarity stratigraphy from the late Carboniferous through the Permian, and into the Triassic, using Permian palaeopole-type palaeomagnetic data coming from sedimentary, volcanic and igneous units from most of the major continents. They proposed to use the name Kiaman (from Mercanton's early work near Kiama), for the predominantly reverse polarity interval from the late Carboniferous until the mid Permian. Later Irving (1971) suggested substituting the more cumbersome 'late Palaeozoic Reversed Interval' for the Kiaman interval, based on limiting proliferation of new names, for geomagnetic chron intervals (see longer discussion in Klootwijk *et al.* 1994). This work will refer to this long duration polarity interval as the Kiaman Superchron (as opposed to the more cumbersome ‘Permo-Carboniferous quiet interval’ or superchron of Irving & Pullaiah 1976). The start of the reverse and normal polarity interval following the end of the Kiaman Superchron in the mid Permian, Irving & Parry (1963) referred to as the ‘Illawarra reversal’; a confusing terminology, since the ‘reversal’ by definition is the base of the first major overlying normal magnetozone, which they hypothesized occurred in ca. 100 m of unsampled strata. We like others (e.g. Klootwijk *et al.* 1994), refer to this interval beginning in the mid Permian as the Illawarra Superchron (hyperchron in Russian literature; Molostovsky *et al.* 1976), composed of normal and reverse polarity intervals, extending into the Triassic (Hounslow & Muttoni 2010). Although perhaps from historical precedent, a better term for this interval might be the ‘Volga-Kama superchron’ since the best type area and first identification of the Illawarra Superchron was in these Russian river basins. In Australian sections the first normal polarity in the Narrabeen Shale, originally defining the upper boundary of the ‘Illawarra reversal’ of Irving and Parry (1963), was studied by Embleton & McDonnell (1980) in the Kiama area and shown to be Triassic in age. Later studies of the units equivalent to the Illawarra Coal Measures, however do appear to show both reverse and normal polarity in the Illawarra Superchron (Klootwijk *et al.* 1994).

Development of a Permian geomagnetic polarity timescale

There have been several previous attempts at a construction of a Permian polarity stratigraphy, such as Khramov (1963a,b, 1967), McElhinney & Burek (1971), Irving & Pullaiah (1976), Molostovsky *et al.* (1976), Klootwijk *et al.* (1994), Opdyke (1995), Jin (2000) and Molostovsky (2005). The latest comprehensive attempt for the mid and late Permian is that of Steiner (2006), with Shen *et al.* (2010), Henderson *et al.* (2012) and Hounslow (2016) attempting integration with geochronology to produce a geomagnetic polarity timescale (GPTS). The 2012 Permian polarity timescale (Henderson *et al.* 2012), uses data from only a small number of key sections, plus several of the pre-1996 composites.

Over the half century since the first Permian magnetostratigraphy, palaeomagnetic methods that extract the original remanent magnetisation (i.e. characteristic remanence) of the geomagnetic field have improved. There has been increasing focus on improving the sensitivity of magnetometers (Kirschvink *et al.* 2015), the magnetic cleaning techniques (i.e. demagnetisation), and the rate of specimen measurements (Kirschvink *et al.* 2008). Measurements on Permian sediments in the 1960’s- 1980’s often focussed on red-bed successions, since these provided both large remanent magnetisation intensity, and stable magnetisations, but often lacked detailed biochronology. This evolved during the 1990’s to examination of carbonate and non-red clastic rocks, with weaker characteristic remanences, but often much better biochronology. These improvements need to be borne in mind when considering Permian magnetostratigraphic data; it is not that early datasets are necessarily more unreliable than recent data, it is that they need to be considered in this wider improvement in palaeomagnetic techniques and associated chronology.

In this work, we primarily utilise the original magnetostratigraphic or palaeomagnetic datasets, rather than rely on previously constructed composites. Some of the section magnetozones boundaries have been modified from the original publications, to maintain a consistent data style. The associated biochronology and correlations have been supplemented by additional available biostratigraphic data since the original publication. Finally, a GPTS for the Permian in constructed using radiometric dates where available, starting from the section composting procedures in Hounslow (2016).

A magnetochron labelling scheme

Naming conventions for pre-late Jurassic magnetochrons have not been standardized, with Permian conventions based on either stage-abbreviation-number labels (Ogg *et al*. 2008, Ogg 2012), or labelling individual magnetochrons (Creer *et al.* 1971; Davydov *et al.* 1992; Steiner 2006). The mid to late Permian Russian labelling system is perhaps the most widely used (Molostovsky 1996), but not easily adaptable to the early Permian, or to areas outside Russian sections, since correlations are somewhat debatable. Like the Triassic (Hounslow & Muttoni 2010), the stability in the stage-boundary dating of Permian magnetochrons has not solidified sufficiently at this time, so it is not always crystal clear what stage every magnetochron belongs to. Hence, applying the stage-abbreviation-number labels of Ogg *et al.* (2008), could require major future changes, whereas stability with respect to Series is more stable. For ease of description, the Permian magnetozones have been formally numbered in couplets (i.e. a normal with overlying reverse) for each of the Permian Series, from CI1 to CI3 (Cisuralian), GU1 to GU3n (Guadalupian), and LP0r to LP3 (Lopingian, to not confuse with the Lower Ordovician, LO; Hounslow 2016). The basal Triassic magnetochron labelling is after Hounslow & Muttoni (2010). Chrons are grouped according to polarity dominance in the section data, except in the Cisuralian (see Murphy & Salvador 1999, for chronostratigraphic definition of magnetochrons and their sub-divisions). Sub-magnetochron labelling is applied (i.e. n.1r or r.1n), to less dominant chrons or those with less supporting data, but seen in multiple sections. Tentative sub-chrons are labelled .ar and .an if the subchron is considered to possess insufficiently strong evidence from multiple sections. This hierarchical labelling gives a clue to the strength of evidence available, and allows easier re-labelling in later studies. The chron numbering is in the opposite direction (i.e. younger magnetochrons given larger number) to the Cenozoic and late Mesozoic chron labelling (Ogg 2012), which starts from 0 Ma. This follows the procedure suggested by Kent & Olsen (1999), but widely adopted in other Mesozoic and Palaeozoic studies since the studies of Khramov (1967) and McElhinney & Burek (1971).

The early Permian and the Kiaman Superchron

The early Permian is characterised by the Kiaman Superchron, the interval of predominantly reverse polarity, well known from studies in the 1960's and 1970's (Irving & Parry 1963; Irving & Pullaiah 1976). The main issue for defining the nature of the GPTS for the early Permian is therefore the age and duration of any normal polarity magnetozones in the Kiaman Superchron. There have been a great many (in excess of 400) palaeomagnetic studies of the early Permian, primarily focussing on palaeopole type studies (i.e. defining tectonic motions etc). These have shown that if there are normal polarity magnetozones in the early Permian, they are likely to be short in duration (Irving & Pullaiah 1976; Opdyke 1995). Sampling density and stratigraphic dating issues with palaeopoles-type studies often mean that stratigraphic relationships between samples may be poorly defined, ages poorly defined, sampled horizons may be few, and widely spread out through a large stratigraphic range, so they cannot be used to build a reliable polarity stratigraphy (but can indicate polarity bias). However, sampled sites with normal polarity from such studies, do give strong evidence for the presence of a limited number of normal polarity magnetozones in the Kiaman Superchron (Table 1). In spite of the very large number of early Permian palaeomagnetic palaeopole-type studies, there is a much small number of conventional magnetostratigraphic studies in this interval, that have used closely-spaced stratigraphic sampling.

In spite of an often perceived lack of normal magnetozones in the Kiaman, expressed in polarity composites like Opdyke (1995), there are sufficient datasets that show a consistent pattern of normal magnetozones in the early Permian, which are reasonably well-dated (Table 1). These data suggest at least three probably four normal magnetozones in the early Permian, during the early Asselian (CI1r.1n), late Artinskian (CI2n), mid Kungurian (CI3n) and mid Roadian (C3r.1n). As a result of the occasional difficulty in distinguishing CI1r.1n from a normal magnetozone in the underlying (Carboniferous) late Gzhelian strata (CI1n), we discuss the data relating to CI1n and CI1r.1n together. We take the late Gzhelian CI1n normal magnetochron as the start of the labelled Permian chrons, since the CI1n-CI1r.1n interval straddles the Carboniferous-Permian boundary.

Gzhelian and Asselian magnetochrons CI1n and CI1r.1n

The study of Khramov (1963b) was the first to identify a likely normal polarity magnetozone in the Kiaman Superchron (here called CI1n), from the Donets Basin, located in the Kartamysh Suite (Kartamyshskaya Formation), in the upper Gzhelian between limestones Q4 and Q8 (Davydov & Leven 2003; Fig. 1). In spite of it being established with many specimens (Table. 1), it was only located in the Suhoj-Jaz section, with the specimens not subject to conventional modern demagnetisation techniques. Fusulinids found in marine analogues of the Kartamyshskaya Formation (Fm) in the Predonets Trough suggest correlation of limestones Q1-Q6 with the late Gzhelian *Ultradaixina bosbytauensis-Schwagerina robusta* fusulinid zone and limestones Q7-Q12 with the early Asselian *Sphaeroschwagerina vulgaris-Sch. fusiformis* fusulinid zone (Davydov *et al.* 1992). However, the palaeo-pole type study of Iosifidi *et al.* (2010), which sampled this same formation and the same section, failed to find evidence of normal polarity. However, this may relate to the wide sample spacing used, indicating that the equivalent of CI1n found by Khramov (1963b) is brief in duration, as suggested by other studies.

The base Permian GSSP section at Aidaralash contains a tentative normal magnetozone that is restricted to the *U. bosbytauensis-Sch. robusta* fusulinid zone, directly below the Carboniferous- Permian Boundary (Fig. 1). This normal magnetozone, which was named the "*Kartamyshian*" by Davydov & Khramov (1991) has also been detected in the Nikolsky section of the southern Urals, the Belaya River section of the Northern Caucasus, and the Ivano-Darievka section of the Donets Basin (Khramov 1963b; Khramov & Davydov 1984; Davydov *et al.* 1998; Davydov & Leven 2003). A study with widely-spaced samples, from three overlapping sections (Dzhingilsaj, Uchbulak and Dastarsaj), in Ferghana (Uzbekistan; Davydov & Khramov 1991), identified four normal polarity intervals (all based on single samples, multiple specimens) in the Gzhelian - Asselian, dated by a fusulinid zonation (Fig. 1). The data from the oldest section (Dzhingilsaj) being the best defined, with the closest spaced sampling in the Gzhelian parts of these sections. Like the Suhoj-Jaz, Nikolsky and Aidaralash sections, the S. Ferghana Uchbulak section contains a tentative normal magnetozone approximately within age-equivalent foraminifera zones, indicating substantive evidence for CI1n.

Higher in the Aidaralash section, a normal magnetozone, CI1r.1n (defined by 2 sample level), occurs in the early Asselian *Sph. vulgaris - Sch. fusiformis* Zone (equivalent to *Sph. aktjubensis – Sph. fusiformis* Zones of Schmitz & Davydov 2012). The youngest tentative normal polarity magnetozone in the S. Ferghana, Dastarsaj section, is in the *Sph. sphaerica- Sch. firma* zone, equivalent to the late Asselian *Sph. gigas* Zone of Schmitz & Davydov (2012). Hence, it is not clear if this is the same magnetozone as at the

Aidaralash section, in spite of Davydov & Leven (2003) 'moving' the Dastarsaj section normal magnetozone into the early Asselian. The interval containing the equivalent *Sp. vulgaris - Sc. fusiformis* Zone in the Dastarsaj section has not closely samples, so it is possible the equivalent of CI1r.1n was unsampled.

Nawrocki & Grabowski (2000) collected some 300 samples, supporting a detailed magnetostratigraphy through the early Permian in Spitsbergen (Fig. 2). Three short normal polarity intervals occur, one within the base of the Tyrrellfjellet Member (Mb), one in the lower parts of the Svenskegga Mb and a probable third in the base of the Hovtinden Mb (Fig. 2; data of Nawrocki & Grabowski 2000, but using the lithostratigraphy in Hounslow & Nawrocki 2008). The normal magnetozone in the Tyrrellfjellet Mb is just below the *Palaeoaplysina* build-ups in the upper part of the Brucebyen Beds . At levels below the top of the Brucebyen Beds, there are a succession of Gzhelian fusulinid zones, with the boundary between the *Zigarella furnishi* and the *Sch. robusta* zones marking the probable Gzhelian-Asselian boundary (Nilsson & Davydov 1997; Davydov *et al.* 2001). In the underlying Cadellfjellet Mb the conodont *Streptognathodus alekseevi* also indicates a Gzhelian age (Nakrem *et al.* 1992; Fig. 2). However, in contrast the conodont *Str. barskovi* (Fig. 2) is normally considered indicate of the mid Asselian in the Urals (Nakrem *et al.* 1992). The overlying part of the Tyrrelfjlellet Mb has two further Asselian foraminifera zones (*Sch. princeps* and *Sch. sphaerica*), with the uppermost *Eoparafusulina paralinearis* assigned to the Sakmarian by Nilsson & Davydov (1997). This suggests the normal magnetozone in the Tyrellfjellet Mb, probably represents the equivalent of the late Gzhelian normal magnetozone CI1n (Fig. 2). If the Asselian magnetozone CI1r.1n is present it is rather too brief to have been detected by the ca. 5-10 m spaced samples of Nawrocki & Grabowski (2000). There is a notable disparity between the foraminifera based ages in the upper part of the Tyrrellfjellet Mb and the presence of *Sweetognathus* sp., which usually suggests an Artinskian age (Nakrem *et al.* 1992), although there are taxonomic issues with *Sw. inornatus* (Mei *et al.* 2002).

Several studies have examined the reversal stratigraphy through the Lower Rotliegend, which should include the Gzhelian-Asselian interval (Fig. 2). Menning *et al.* (1988) summarised and synthesized these studies, which appear to show a tentative normal polarity interval in the mid parts of the Manebach Fm in non-red mudstone samples from locality 'Hinteres schulzental', isolated with AF demagnetisation (Menning, 1987; Menning *et al.* 1988). Representatives of the insect zone *Sysciophlebia ilfeldensis* occur as fragments in the Manebach Fm suggesting the formation spans the Gzhelian - Asselian boundary

(Schneider *et al.* 2013), so it is not totally clear if this normal polarity magnetozone represents CI1n or CI1r.1n, although it is most likely to be equivalent to CI1n (see below).

The CI1r.1n magnetozone may have been detected in the Nohfelden and Donnersberg rhyolites in the Saar-Nahe Basin (Berthold *et al.* 1975). More recent dating of associated extrusives and intrusives associated with these volcanic centres, using Rb-Sr, K-Ar and ^{40}Ar-^{39}Ar radiometric ages from rhyolites, yields ages of 300 to 290 Ma (Schmidberger & Hegner 1999), suggesting an Asselian age.

The coal-bearing Dunkard Group in West Virginia was reconnaissance sampled by Helsley (1965), with his lowest sample level ~8 m above the Washington Coal, with data displaying tentative normal polarity using undemagnetised samples (Fig. 2). Gose & Helsley (1972) subsequently demagnetised these normal polarity samples and found 2 of the 3 samples to be stable to demagnetisation, which indicates the good likelihood of a normal magnetozone. The highest resolution biochronology data for these units appears to be spiloblattinid insects with *Sysciophlebia balteata* occurring in the earliest part of the Dunkard Group (Schneider *et al.* 2013), suggesting the entire Dunkard Group is early Permian. This probably places the Dunkard normal magnetozone in the Asselian, equivalent to CI1r.1n. The parts sampled by Helsley (1965), which did not include the youngest Dunkard Group, probably extend into the Sakmarian (Di Michel *et al.* 2013; Lucas 2013). The occurrence of *S. ilfeldensis* in the German Manebach Fm of the Lower Rotliegend, places the Dunkard Grp normal magnetozone as probably younger than that in the Manebach Fm (Fig. 2).

The study of Diehl & Shive (1979) on the Ingleside Fm in northern Colorado (in Owl Canyon), tried to locate normal polarity intervals in the early Permian by collecting samples through this formation at an average spacing of 0.28 m. In the original study the Ingleside Fm was assigned to the early Permian, however, the fusulinid *Triticites ventricosus* in the base of the formation (Hoyt & Chronic 1961) suggests a Virgilian age (late Gzhelian), according to Gomez-Espinosa *et al.* (2008) and Wahlman & West (2010). The formations younger age is not clear, since it is overlain unconformably by the Owl Canyon Fm of early Permian age, although the formation presumably covers the Carboniferous- Permian boundary interval into the Sakmarian (Sweet *et al.* 2015). However, Diehl & Shive (1979) failed to find normal polarity samples in the complete 70 m of the formation, which should have covered magnetochron interval CI1n - CI1r.1n.

Sakmarian- Artinskian

The Sakmarian is consistently reverse polarity in all studies. The earliest study to detect the equivalent of normal magnetochron CI2n in the Artinskian was the palaeopoles-type study of Peterson & Nairn (1971) on the Garber Fm of Oklahoma, who performed thermal demagnetisation up to 600^{o}c to isolate normal polarity in 7 specimens (Table 1). According to Giles *et al.* (2013) the Garber Fm is mid Artinskian in age based on regional correlation of the laterally equivalent Hennessey Shale. A younger age straddling the Artinskian-Kungurian boundary was suggest by May *et al.* (2011), based on vertebrate (dissorophids) ranges. Other palaeopole-type studies in red-beds of Artinskian age with normal polarity intervals, are from the Pictou Grp of Prince Edwards Island, Canada (Symons 1990). The Pictou Group data were from megasequence IV (Orby Head Fm, Ziegler *et al.* 2002) with nine specimens from three blocks, demagnetised to 650^{o}C, showing apparently two normal polarity intervals. One of these is from near the base of the formation, but with most of the normal polarity data from two sites near the top of the formation. Plant fossil data suggests a late Artinskian age for the Orby Head Fm (Zeigler *et al.* 2002). Considering the uncertainty in age assignment for the Orby Head Fm, it is possible the lower normal polarity level is CI2n and the upper one CI3n.

Irving & Monger (1987) found normal polarity samples in their palaeopole-type study of the volcanic units of the Asitka Group (British Columbia). Modern demagnetisation techniques were employed, and normal polarity was found in multiple specimens (Table 1). The Asitka Group is dated, by overlying limestones, containing Sakmarian and Artinskian conodonts (MacIntyre *et al.* 2001), but fusulinids suggests a late Sakmarian to early Artinskian age (Ross & Monger 1978). This suggests the magnetochron detected in the Asitka Group is probably CI2n.

Palaeopole and magnetostratigraphic studies of Valencio *et al.* (1977), Sinito *et al.* (1979) and Valencio (1980) measured a predominantly reverse polarity stratigraphy through the La Colina Fm from the Paganzo Basin in Argentina. Based on palynological and radiometric dating, their data likely ranges in age from the Asselian to Artinskian (Césari & Gutiérrez 2000; Césari *et al.* 2011). Valencio *et al.* (1977) detected a single normal polarity interval, which is correlated Artinskian CI2n. Normal polarity samples below this level were detected by Sinito *et al.* (1979), but are less reliably located stratigraphically and appear to have less reliable palaeomagnetic data. In the same area, normal polarity samples measured by Thompson (1972) were from the overlying Amana Fm, which is now assigned to the Triassic (Césari *et al.* 2011).

The magnetostratigraphic data from Spitsbergen of Nawrocki & Grabowski (2000), through the upper part of the Tyrrellfjellet Mb into the Gipshuken Mb shows only reverse polarity. The Tyrrellfjellet Mb contains the conodont *Sweetognathus inornatus*, indicating a Sakmarian-Artinskian age, whereas the rich fusulinid assemblages suggest age ranges from the Asselian to Sakmarian (Nakrem *et al.* 1992). The more restricted range of conodont and foraminifera faunas from the Gipshuken Fm suggests a probable age range into the Artinskian. A regional hiatus is widely concluded at the base of the overlying Kapp Starostin Fm (Blomeier *et al.* 2011), but the age gap is below the resolution of biostratigraphy. Nawrocki & Grabowski (2000) found normal polarity in three specimens from the lower part of the Svenskegga Mb (above the Vøringen Mb), two at Kapp Wijk (30 m from the base of the Kapp Starostin Fm; Fig. 2) and one at Trygghamna, which probably represents the equivalent normal magnetozone. The normal magnetozone in the lower parts of the Svenskegga Mb is CI2n (Table 1). The Vøringen Mb contains a diverse marine fauna, with conodonts including *Sweetognathus whitei* and *S. clarki*, indicating a probable late Artinskian age (Nakrem *et al.* 1992; Nakrem 1994). A Sr-isotope value of 0.70746 from the Vøringen Mb also suggests an Artinskian age (Ehrenberg *et al.* 2010). The overlying mid and upper parts of the Svenskegga Mb contain foraminifera assigned to the *Gerkeina komiensis* assemblage zone (Sosipatrova, 1967; Nakrem *et al.* 1992), correlated to the Iren Horizon in the Uralian successions, where it is assigned a mid Kungurian age (Lozovsky *et al.* 2009). This suggests the Artinskian-Kungurian boundary occurs in the lower-mid parts of the Svenskegga Mb (Fig. 2).

Kungurian to Roadian

Graham (1955) was the first to identify a normal polarity interval in the Kungurian. His palaeopole type study (using undemagnetised specimens) identified both reverse and normal polarity in samples, from the Supai Group in the Oak Creek and Carrizo Creek sections in Arizona. Although precise details of stratigraphic levels sampled are not clear, both these locations have good sections through the upper part of the ‘Supai’ (Corduroy, Big A Butte members, Esplanade Sandstone, Hermit Fm; Winters 1962; Blakey & Middleton 1987), which probably locate Graham’s samples in the upper-most Supai Group and overlying Schnebly Hill Fm, using the modern lithostratigraphy (Blakey 1990). Conodonts within the Fort Apache Mb of the Schnebly Hill Fm date Graham’s data to the mid Leonardian (Blakey 1990; Eagar & Peirce 1993), which is early-mid Kungurian (Henderson *et al.* 2012). The study of Graham (1955) has not been re-evaluated using modern palaeomagnetic techniques.

Wynne *et al.* (1983) performed a palaeopole-type study of the Esayoo Volcanic Fm on Ellesmere Island, N. Canada, which they initially assumed was Artinskian in age, but has been re-dated as Kungurian (Table 1). The Esayoo Volcanic Fm is sandwiched between the Great Bear Cape and the overlying Sabine Bay formations (Morris 2013), although no data on stratigraphic position in the lava succession is described by Wynne *et al.* (1983). Le Page *et al.* (2003) suggested the sediments overlying the Esayoo Volcanics are mid to late Kungurian based on plant megafossils, and the youngest part of the Sabine Bay Fm is late Kungurian based on conodonts such as *Mesogondolella idahoensis* (Henderson & Mei 2000). The youngest part of the Great Bear Cape Fm, underlying the Esayoo Volcanic Fm, is earliest Kungurian in age (Mei *et al.* 2002), suggesting the normal polarity interval is early-mid Kungurian.

In the Spitsbergen magnetostratigraphic data of Nawrocki & Grabowski (2000), the best quality data showing normal polarity in these Permian successions is in cherts from the base of the Hovtinden Mb at Trygghamna (Hounslow & Nawrocki 2008). Brachiopod and bryozoans faunas from the youngest parts of the Kapp Starostin Fm suggest equivalence with Ufimian and Kazanian faunas from Greenland and Novaya Zemlya, suggesting possible late Kungurian to Roadian ages (Stemmerik 1988; Nakrem *et al.* 1992). Foraminiferal and coral assemblages suggest Kungurian - Ufimian ages when compared to the Urals successions (Nakrem *et al.* 1992; Chwieduk 2007). A conodont fauna of *Mesogondolella idahoensis* and *Merrillina* sp. from the upper most part of the Kapp Starostin (Nakrem *et al.* 1992) suggests, the latest Kungurian- early Roadian. Since reverse polarity dominates to the topmost part of the Kapp Starostin Fm (Fig. 2; Hounslow *et al.* 2008), without major intervals of normal polarity, it suggests, like the faunal data, that most of the Wordian, Capitanian and late Lopingian (and their normal polarity intervals) are missing on Spitsbergen. This suggests the Hovtinden Mb normal magnetozone is probably Kungurian in age. However, ~70 m above this normal magnetozone, an interpreted late Capitanian low in Sr-isotope data has been detected (Ehrenberg *et al.* 2010; Bond *et al.* 2015), which contradicts the faunal and magnetostratigraphic data. This occurs prior to a brachiopod extinction and negative excursion in $\delta^{13}C_{org}$ in the Kapp Starostin Fm, which occur ca. 45 m below the top of the formation (Bond *et al.* 2015). A partial reconciliation of the magnetostratigraphic and Sr-isotope data is if the normal polarity intervals in the Wordian and Capitanian are missing, so the reverse polarity in the early Wuchiapingian (to preserve lows in Sr-isotope, and early Wuchiapingian $\delta^{13}C$ excursion) sits on Roadian or late Kungurian strata in the upper part of the Hovtinden Mb. However, this option remains incompatible with the key conodont data, and there is no evidence of a major mid Permian hiatus in the Barents Sea (Ehrenberg *et al.* 2001). The Spitsbergen brachiopod extinction is quite dramatic, and using the age model proposed here, likely corresponds instead with a latest Kungurian bivalve extinction event seen in NE Asia (Biakov 2012).

The detailed magnetostratigraphy from the Adz'va River section in the Pechora Basin through the Tal'bei and upper-most Inta formations (Balabanov 1988) shows the Illawarra Superchron in the *Phylladoderma* beds, underlain by predominantly reverse polarity down into the Inta Fm (Fig. 1). The biostratigraphic ages of these units in the Pechora Basin has been much debated (Rasnitsyn *et al.* 2005; Lozovsky *et al.* 2009; Kotylar 2015). Based on floral, fish and insect remains the Inta Fm is probably placed in the Ufimian (late Kungurian?). This suggests the tentative normal polarity interval in the lower part of the Seida Fm may be the equivalent of CI3n (Fig. 1). There is tentative (single sample) evidence for a normal polarity magnetozone in the Tal'bei Fm (CI3r.1r) that may equate with a tentative normal polarity level in the Trygghamna section from Spitsbergen (Figs 1, 2), although other extensive data through the Russian Ufimian-Kazanian sections show no substantiated evidence of normal polarity (Burov *et al.* 1998).

The age of CI3n is perhaps best constrained in the Esayoo Volcanic Fm, by the over and underlying sedimentary units with conodont ages, along with its relationship to the magnetostratigraphy from Spitsbergen sections, which suggests the age of CI3n is mid Kungurian.

Other normal polarity intervals in the early Permian?

The palaeopole type study of Rakotosolofu *et al.* (1999) found normal polarity in the lower Sakamena and Lower Sakoa formations from Madagascar, originally allocated to the Permian. However, the basal tillites sampled from the Lower Sakoa Group are probably early Pennsylvanian in age (Wescott & Diggens 1998) and the those from the lower Sakamena Formation are from the late Permian (Illawarra Superchron) according to palynological dating (Wescott & Diggens 1998).

Halvorsen *et al.* (1989) published work on dual polarity magnetisations from the Karkonosze Granite, SW Poland, which was originally dated to the 305 to 281 Ma interval, but now has a more precise chronology (Kryza *et al.* 2014) with a main intrusion age of 311 ± 3 Ma, placing it in the Moscovian.

Creer *et al.* (1971) reported normal polarity in 31 Permian andesitic and basaltic specimens from the San Rafael area of Argentina. These are now assigned to the Cerro Carrizalito Fm of the upper part of the Choiyoi volcanics (Rocha-Campos *et al.* 2011), and dated using SHRIMP U–Pb zircon ages to the mid

Guadalupian and younger (265±2.9Ma to 252±2.7 Ma), not so different from the K-Ar age (263±5 Ma) determined by Creer *et al.* (1971). These indicate these normal polarity data are from the Illawarra Superchron.

There have been several other reported normal polarity sample-sets in the Permian (e.g. Klootwijk *et al.* 1983, Geuna & Escosteguy 2004; Pruner 1992; Vozárová & Túnyi 2003). These share the characteristics of having very poor age control and a very wide spacing of stratigraphic sampling, in palaeopole type studies, so it is impossible to evaluate their usefulness for construction of a magnetostratigraphy.

McMahon & Strangway (1968) identified normal polarity samples in the red-bed Maroon Fm in Colorado, but with inadequate AF demagnetisation. These were in the lower parts of the Maroon Fm and underlying (Pennsylvanian) Minturn Fm (Fig. 2). The youngest age of the Maroon Fm is constrained by the overlying State Bridge Fm, which contains Guadalupian fossils (Johnson *et al.* 1990). The youngest detrital zircons from the Maroon Fm suggest an age no older than Wolfcampian (Soreghan *et al.* 2015). However, large age uncertainties from the zircon populations and similar mean ages (~293.1 ±4.5 Ma), from the top and bottom of the formation, do not help constrain its age duration, but rather suggest it is restricted to a Sakmarian age. The Maroon Fm sits unconformably on the mid Pennsylvanian Minturn Fm, so the Gzhelian-Asselian boundary interval may be missing. A later ca. 1 m spaced magnetostratigraphic sampling of the Maroon Fm by Deon (1974) found that 99.2% of the samples were of reverse polarity, with only three specimens of interpreted normal polarity (but not in adjacent strata). Miller & Opdyke (1985) purposefully re-sampled the Red Sandstone Creek section used by McMahon & Strangway (1968) to try to locate the tentative normal polarity intervals, but found no normal polarity samples. These data may indicate, like the zircon populations, that the Maroon Fm occupies the reverse polarity late Asselian- early Artinskian interval (Fig. 2).

North American early Permian studies

Red-bed and limestone bearing Permian strata in the American SW in Utah, Colorado and Wyoming have a distinct absence of early Permian normal polarity intervals, in spite of several detailed studies, and apparently appropriate ages of strata. We critically examine this data, since it clearly has a bearing on the reliability of these studies, and opens the question of the reliability of the normal polarity intervals in the Cisuralian, seen in studies outside the American SW. These studies have critically influenced the conventional hypothesis of the reverse-only character of the Permian part of the Kiaman Superchron.

In the marine sandstone and limestone beds in the Casper Fm of Wyoming (at Horse Creek), Diehl & Shive (1981) sampled 190 m in total of the 220 m of this formation at 0.33m spacing and found only reverse polarity. The age of the Casper Fm sampled is Desmoinesian (late Moscovian) to Wolfcampian (Sakmarian?), based on brachiopod, fusulinids and conodonts. Red-bed units of the Cutler Group at Moab in Utah were also extensively sampled (Fig. 2), at close stratigraphic spacing by Gose & Helsely (1972) but again failed to find normal polarity samples, through a Wolfcampian (possibly Virgilian; Soreghan *et al. 2*002; Condon 1997; Scott 2013) to Leonardian interval (i.e. Gzhelian- Kungurian). Based on vertebrate data Scott (2013) has suggested the Carboniferous Permian boundary is in the lower 10 m of the Halgaito Fm in SE Utah (Fig. 2). Vertebrates from the Organ Rock Shale indicate a Seymouran land vertebrate zone (Lucas 2006), implying the section sampled by Gose & Helsley (1972) at Moab may extend into the Kungurian. However, this does not seem to be borne out by the detailed sampling showing only reverse polarity (Fig. 2), which implies the section may end before the Artinskian. Reasons for the absence of normal polarity in the Cutler Group are unclear, possibly due to unsampled intervals in the Halgaito Fm, unsuspected hiatus, and a shorter age range than anticipated, not extending into the Artinskian-Kungurian.

Farther east in northern Colorado, the magnetostratigraphic study of the red-beds of the Ingleside Fm (Diehl & Shive 1979), specifically tried to find the normal polarity intervals in the Gzhelian-Asselian interval, but failed. The same study-targeting issue applied by Miller & Opdyke (1985) to the Maroon Fm in Colorado. Steiner (1988) also sampled extensively the lower and central portions of the Laborcita Formation (Gzhelian- early Asselian; Krainer *et al.* 2003) and about 1/3rd of the overlying Abo Fm (Asselian to late Sakmarian) in New Mexico, but found only reverse polarity.

The reasons for these studies on North American sections inability to detect the brief early Permian normal polarity intervals, seen in other areas are not clear; but there may be several possibilities:

1) The stratigraphic complexity and often poor-dating resolution in the red-beds may mean that the Carboniferous-Permian boundary interval, containing the latest Gzhelian- early Asselian, may be missing (though this does not apply to the Laborcita Fm; Krainer *et al.* 2003). Likewise, in some cases the red-bed units may not extend up to the CI2n magnetochron, as usually implied by the low resolution biochronology from these strata.
2) Issues with diagenetically delayed magnetisations (Turner 1979; Kruiver *et al.* 2003; Van der Voo & Torsvik 2012) or late Kiaman remagnetisations (e.g. Magnus & Opdyke 1991) may be more common in these units than currently realised. In the front ranges of the Rocky Mountains, Kiaman-

age remagnetisations, carried by haematite, appear to be widespread and associated with modest burial, connected with deformation of the ancestral Rocky Mountains (Geissman & Harlan 2002). It is not clear if this situation in Colorado applies also to the Permian in the Paradox Basin in Utah, or the Casper Fm of Wyoming. However, there have been suggestions that a late Permian-Triassic remagnetisation may be affecting some datasets from the North American Craton (Steiner 1988; Pan & Symonds 1993).

Guadalupian

Age of the start of the Illawarra Superchron

The chronostratigraphic age of the end of the Kiaman Superchron is in the early Wordian. The first normal polarity magnetochron of the Illawarra Superchron, appears to be shown in the mid and upperparts of the back-reef Grayburg Fm (and overlying Queen Fm) in the Guadalupe Mts in W. Texas (Steiner 2006). The Grayburg Fm is inferred to be early Wordian in age, based on its lateral relationship to conodont and fusulinid dated units. This is based on the basinal to back reef stratigraphic correlations of Lambert *et al.* (2007), Barnaby & Ward (2007), Olszewski & Erwin (2009), Rush & Kerans (2010). Nicklen (2011) has suggested the Queen and Grayburg formations correlate to the basinal South Wells Mb (of the Cherry Canyon Fm), which has an associated U-Pb ID-TIMS date (using EARTHTIME standards) of 266.5±0.24Ma, potentially directly dating the start of the Illawarra Superchron. Alternatively, Olszewski & Erwin (2009) correlate the South Wells Mb to a level higher than the Queen Fm. Normal and reverse polarity intervals in the Manzanita Mb of the Cherry Canyon Fm in the Guadalupe Mts (Burov *et al.* 2002) derive from the late Wordian (Olszewski & Erwin 2009), probably corresponding to the GU2 magnetochron (Fig. 6). Nicklen (2011) suggested the zircon U-Pb date of 265.3±0.2Ma of Bowring *et al.* (1998) provides a date for the bentonites in the Manzanita Mb.

The end of the Kiaman Superchron is also shown in the Kyushu sections in Japan (Fig. 4), occurring in the *Neoschwagerina craticulifera* fusulinid assemblage zone (Kirschvink *et al.* 2015). *N. craticulifera* has its first appearance in the late Roadian (Henderson *et al.* 2012), but Kasuya *et al.* (2012) correlate the *N. craticulifera Zone* in these Japanese sections to the early Wordian.

The end of the Kiaman Superchron is very well-defined in numerous sections from Russia, in the upper Urzhumian Stage within the Biarmian Series (Molostovsky 1996; Molostovsky *et al.* 1998; Burov *et al.* 1998). The base of the underlying Kazanian Stage and the Biarmian Series, is marked by the first occurrence of the Roadian conodont *Kamagnathus khalimbadzhae*, and this is further emphasised by an assemblage of ammonoids, slightly above the base of the Kazanian, which dates it to the Roadian (Silantiev *et al.* 2015a). The regional stages Urzhumian, Severodvinian and Vytakian are demarcated by the first occurrence of non-marine ostracod species in continuous phylogenetic lineages (Tverdokhlebova *et al.* 2005; Silantiev *et al.* 2015a). These series are also sub-divided by detailed freshwater bivalve, tetrapod and fish biozonations (Tverdokhlebova *et al.* 2005; Silantiev *et al.* 2015a). As such the Biarmian and Tatarian Series have a very detailed internal biozonation, but wider correlation to the international stages is reliant on Eurasian-wide correlation of these non-marine faunas (Kotlyar, 2015). Multiple sections, borehole cores and studies through the Kazanian (Silantiev *et al.* 2015c) and lower Urzhumian have failed to substantiate any normal polarity intervals below the Russian NRP mixed polarity magnetozone (Fig. 3), so the top of the Kiaman Superchron is very clearly expressed (Burov *et al.* 1998). However, the Russian regional stages have long been problematic to correlate in detail to marine sections with conodont and fusulinid zonations, but the Wordian is widely inferred to correlate approximately to the Urzhumian (Lozovsky *et al.* 2009; Henderson *et al.* 2012; Kotlyar 2015). Although not commonly discussed its clear, that at least locally there are a number of hiatus or unconformities in the Tatarian successions (of unknown duration) such as Urzhumian erosion contact on the Kazanian, and the locally the Vyatkian on the Severodvinian (Tverdokhlebova *et al.* 2005). Integration of sequence stratigraphic concepts in these successions with the magnetostratigraphy needs to evolve in this respect, to better understand issues of missing strata.

In the Monastyrski Ravine (Monastery Ravine, type section of the basal Severodvinian) section (Fig. 3) the base of the Illawarra Superchron corresponds to the *Paleodarwinula tuba–P. arida–P. torensis* ostracod Zone (Mouraviev *et al.* 2015; Kotlyar 2015). The better biostratigraphic dating of the end of the Kiaman from the sections in Texas and Japan, suggest the base of the NRP magnetozone (in the late Urzhumian) is slightly older than commonly inferred (e.g. Golubev 2015), and should equate to the earliest Wordian or latest Roadian.

Other more poorly dated, non-marine sections, also probably displaying the end of the Kiaman Superchron are the Taiyuan section in China, within the lower member of the Upper Shihhotse Fm (Embleton *et al.* 1996; Stevens *et al.* 2011). This occurs between two floral extinction events. The earlier one in the Lower Shihhotse Fm (inferred to be Roadian). Two later extinction events in the middle and upper members of the Upper Shihhote Fm, are inferred to be late Guadalupian (Stevens *et al.* 2011; Fig. 4).

The start of the Illawarra Superchron is present in European red-bed successions in the German Upper Rotliegend, Parchim Fm (Langereis *et al.* 2010; Fig 7), and in southern England in the Exeter Group (Hounslow *et al.* 2016). The biostratigraphic age dating of these units is low resolution, largely based on tetrapods (Rotleigend only), footprints and occasionally long-ranging palynomophs such as *Lueckisporites virkkiae* (Edwards *et al.* 1997; Słowakiewicz *et al.* 2009). Generally, the end of the Kiaman provides a higher resolution-dating tool in these successions. The base of the Illawarra Superchron has also probably been detected in Kansas (USA) in the Rebecca K Bounds core (Soreghan *et al.* 2015), in a succession which lacks independent evidence of age, but whose age is approximately constrained by sub-surface regional relationships (Sawin *et al.* 2008).

In the type region of the Illawarra Superchron in Australia, magnetic polarity details and ages are less clear. The base of the Illawarra Superchron is thought to be within the Mulbring Siltstone in the Hunter Valley region of New South Wales (Idnurum *et al.* 1996; Foster & Archibold 2001). The Mulbring Siltstone correlates to the Broughton and underlying Berry formations of the southern Sydney Basin in SE Australia around the Kiama area, because of the *Echinalosia wassi* brachiopod range zone and palynological zones, in these two areas (Campbell & Conaghan 2001; Cottrell *et al.* 2008). The lateral equivalent to the Broughton Fm (Campbell & Conaghan 2001) is the lower part the Gerringong Volcanics (Blowhole, Bumbo, Dapto and Cambewarra flows), which is reverse polarity and widely considered to be within the end of the Kiaman Superchron (Irving & Parry 1963; Cottrell *et al.* 2008). Irving & Parry (1963) also found reverse polarity in the youngest, Berkeley flow, of the Gerringong Volcanics. This suggests the base of the Illawarra Superchron may be within the laterally equivalent and overlying Pheasants Nest Fm (of the Illawarra Coal measures, Campbell & Conaghan 2001; Metcalfe *et al.* 2014) in the southern Sydney Basin. Foster & Archibold (2001) infer the brachiopod faunas of the Broughton Fm have similarity to latest Ufimian to Kazanian brachiopod assemblages. However, the Mulbring Siltstone has U-Pb SHRIMP ages of ca. 264 ±2.2 Ma (Retallack *et al.* 2011), and the laterally equivalent uppermost part of the Broughton Fm has a U-Pb IDTIMS date of 263.5 ±0.31 Ma (Metcalfe *et al.* 2014), suggesting an early Capitanian age in the timescale of Henderson *et al.* (2012), and that proposed here. These inconsistencies probably indicate the Sydney Basin brachiopod fauna's are of little use for international correlation (as suggested by Metcalfe *et al.* 2014) and the new radiometric dates suggest the reverse polarity Gerringong Volcanics may not be within the Kiaman Superchron, but instead correlate to GU2r?

Guadalupian data from marine sections

The Nammal Gorge section (Hagg & Heller 1991) is a key marine section for the mid Permian magnetostratigraphy, since it has an associated conodont biostratigraphy, but in its original publication had very little supporting biostratigraphic detail (Fig. 4). However, based on nearby sections (Saidu Wali, Kotla Lodhian, Zalucj Nala, Chihidru Nala and Kathwai sections) conodont ranges (Fig. 4), can be related to the magnetostratigraphic data in the Nammal Gorge section (Wardlaw & Pogue 1995, Wardlaw & Mei 1999). These conodont ranges are correlated onto the magnetostratigraphy, using the lithostratigraphy and bed numbers from published sedimentary logs (Baud *et al.* 1995; Waterhouse 2010). A hiatus in the Nammal Gorge section is present in the late Capitanian (i.e. missing conodont zones) between the Lakriki and the Sakesar members of the Wargal Fm (Mei & Henderson 2002; Mertmann 2003; Waterhouse 2010). This hiatus separates dominantly normal polarity below from reverse polarity in the upper part of the Wargal Fm (Fig. 4). Hence, the oldest normal polarity interval in the original published data (Haag & Heller 1991) is probably magnetozone GU2n in the late Wordian to earliest Capitanian. No magnetostratigraphy was measured from the underlying Amb Fm, which posses an array of conodonts indicating a Wordian age (Wardlaw & Mei 1999). The early Wordian to Capitanian fusulinid *Neoschwagerina margaritae* is found in unit 2 of the Wargal Fm (Jin *et al.* 2000; Waterhouse 2010; Fig. 4).

The Shangsi section magnetostratigraphy has key for radiometric date for age calibration of the Lopingian, and the section probably extends down into the Capitanian. Unfortunately, the three studies of the Permian magnetostratigraphy (Heller *et al.* 1988; Steiner *et al.* 1989; Glen *et al.* 2009) in this section, display differences in the interpretations of the polarity (Fig. 5). A composite magnetostratigraphy was constructed using the agreement between these, based on the sampling positions. The study of Glen *et al.* (2009) has many sampling levels in the Wujiaping Fm which failed to yield polarity information, whereas the study of Steiner *et al.* (1989) yielded a relatively simple polarity pattern through this formation. The age of the lower part of the Wujiaping Fm is not clear from the faunal data due to a barren interval (Sun *et al.* 2008). ID-TIMS U-Pb radiometric dates (260.4±0.8Ma; 259.1±0.9Ma), which appear to be from reworked material from the Emeishan volcanics (Zhong *et al.* 2014), suggest a maximum age, but are consistent with the normal polarity interval in bed-7 being of late Capitanian age. The underlying Maokou Fm at Shangsi contains the late Roadian through Wordian to earliest Capitanian, with a major hiatus at the base of the Wujiaping Fm (Sun *et al.* 2008). The cyclostratigraphy at Shangsi suggests large changes in sedimentation rates (Fig. 5). The biostratigraphy of the Maokou Fm in the Wulong section is based on unattributed conodont data in Jin *et al.* (2000).

Details of the Guadalupian and Wordian magnetostratigraphy are generally poorly-defined from marine sections alone, but show both polarities in the early Wordian and early Capitanian (Figs. 4, 6). The upper Capitanian is normal polarity dominated as the chron GU3n (the 'Capitan-N' chron of Steiner 2006). This is shown by the data from the Wulong section (Heller *et al.* 1995), the Emeishan Basalts (Zheng *et al.* 2010; Liu *et al.* 2012), and data from the *Yabiena* through *Lepodolina* fusulinid zones from Kyushu in Japan (Fig. 4). The Ebian county magnetostratigraphy through the Emeishan basalts, and overlying units (Ali *et al.* 2002) together with the radiometric dates suggest a mid to late Capitanian age for the Emeishan Basalts (He *et al.* 2007; Zheng *et al.* 2010; Liu *et al.* 2012). This is supported by the mid to late Capitanian age suggested by the conodonts *J.altudaensis* (conodont zone G5) and *J. xuanhanensis* (zone G7) from the few metres of the Maokou Fm that underlie the Emeishan Basalts (Sun *et al.* 2010). The predominantly normal polarity Emeishan Basalts continue into an overlying reverse polarity magnetozone (Ali *et al.* 2002), which is inferred to be the latest Capitanian LP0r (Fig. 4).

Guadalupian data from non-marine sections

Magnetic polarity data from Russian sections through the Urzhumian and early parts of the Severodvinian provide detail through the earliest parts part of the Illawarra Superchron, suggesting the Wordian-Capitanian interval has a bias towards normal polarity (Fig. 3). The Russian NRP mixed polarity magnetozone appears to show two major reverse polarity intervals, the upper one of which is sub-divided by a normal polarity sub-magnetozone. In these sections the structure of the earliest normal magnetozones in the Illawarra Superchron are best represented by the thick Cheremushka section (Silantiev *et al.* 2015b), which is the parastratotype of the Urzhumian. Similar polarity structure, is shown in other Russian sections, such as Tetyushi, Monastyrski and Murygino (Burov *et al.* 1998; Gialanella *et al.* 1997; Balabanov 2014), which allow a division into two major normal magnetochrons (GU1n and GU2n), most clearly seen in the Murygino core and Khei-yaga River section (Fig. 3). However, the NRP polarity interval has problems of partial normal overprints, making magnetozones in the NRP zone difficult to define (Westfahl *et al.* 2005; Silantiev, 2015b). However, normal polarity intervals detected in the many sections in the upper Urzhumian, suggests a Permian geomagnetic signature, rather than a later overprint.

Like the marine-section data, and the Russian sections, the dominance of normal polarity through the later parts of the Guadalupian (i.e. GU3n) are well-displayed in other non-marine sections, such as the

Whitehorse Fm in Kansas (Fig. 6) and the Havel Subgroup, and Exeter Mudstone and Sandstone Fm in the Rotliegend equivalent in Europe (Fig. 7).

Options for the Magnetostratigraphy of the Wordian

A key problem in comparing marine and non-marine sections in the earliest part (i.e. Wordian) of the Illawarra Superchron, in that there are two likely magnetic polarity models for this interval, a 'long-GU1r' option and a 'brief-GU1r' option:

Long-GU1r option: In sections such as at Wulong, Taiyuan and those in W. Texas (Figs. 4, 6), thicker intervals of reverse polarity are displayed, compared to the associated normal magnetozones in the GU1 to GU2 interval. Sections through the Abrahamskraal Fm in the lowermost Beaufort Group (South Africa) have similar characteristics. Crucially the South African sections have SHRIMP U/Pb dates, which overlap the ID-TIMS radiometric dates from the Guadalupian type area, allowing fuller integration of the geochronology and magnetostratigraphy. This is the option used here in the Permian GPTS, but Hounslow (2016) uses the 'brief GU1r option'

Brief-GU1r option: This is exemplified by the Russian Urzhumian data (Fig. 3), where there is dominance of normal polarity in the earliest parts of the Illawarra (GU1- GU2 interval), and the reverse polarity magnetozones appear generally briefer than the normal magnetozones (e.g. Russian composite; Fig. 3). The Wargal Fm, Whitehorse Fm and the SW English coast data share similar characteristics (Figs. 4, 6, 7).

Lanci *et al.* (2013) measured a magnetostratigraphy through the Waterford Fm (Ecca Grp) and the overlying lower parts of the Abrahamskraal Fm (Beafort Grp) and interpreted these data as evidence of the base of the Illawarra Superchron because of three normal polarity magnetozones (N1 to N3, Figs. 1, 6). They interpreted N3 magnetozone (identified in two separate sections), as the start of the Illawarra Superchron. Normal polarity dominates the overlying argillaceous mid-parts of the Abrahamskraal Fm in the Buffels River area (Tohver *et al.* 2015; Fig. 6). Tohver *et al.* (2015) estimated the base of the Abrahamskraal Fm is some 340 m below their lowest sampled levels, suggesting the youngest polarity data in the Ouberg Pass study of Lanci *et al.* (2013) is approximately equivalent with the oldest strata sampled by Tohver *et al.* (2015) at Buffels River (Fig. 6). A correlation more likely than that proposed by Lanci *et al.* (2013) is that magnetozone interval N2-N1 is the equivalent of GU1n, marking the base of the Illawarra Superchron (Fig. 1), indicating one reverse subzone (GU1n.1r) in GU1n. This 'long-GU1r' option suggests magnetozone N3 is the magnetochron CI3r.1n (Figs. 1, 6). In the same general area as the study of Tohver *et al.* (2015), Jirah & Rubidge (2014) measured the total stratigraphic thickness of the Abrahamskraal Fm as 2565 m, suggesting the upper-most sampled levels of Tohver *et al.* (2015) at Buffel River are ca. 920 m from the base of the Abrahamskraal Fm. These upper samples are therefore approximately at the upper range of the *Eodicynodon* Assemblage Zone (Jirah & Rubidge 2014). The 'long-GU1r' option is supported by the similarity in U-Pb SHRIMP dates of 266.4 ±1.8 Ma (Lanci *et al.* 2013) from near the base of N2 (GU1n) and from the ID-TIMS date 266.5 ±0.24 Ma near the base of the Wordian in Texas/New Mexico sections (Bowring *et al.* 1998; Fig. 6). The youngest U-Pb SHRIMP date in the Ouberg Pass section of 264.4 ±1.9 Ma indicates a level in GU1r. Zircon ID-TIMS dates from ca. 1.5 km higher in the Beaufort Group, than the Buffels River magnetostratigraphy (Fig. 6), suggests the Capitanian-Wuchiapingian boundary (at ca. 260 Ma) approximates the boundary between the tetrapod *Tropidostoma* and *Pristerognathus* Assemblage Zones (Rubidge *et al.* 2013). Using this date and the 'long-GU1r' option suggest that the bulk of this additional 1.5 km of strata is predicted to be normal polarity, corresponding to most of GU3n (Fig. 6).

Palynological zonations of the underlying Ecca Group generally support the 'long-GU1r' option suggesting the youngest parts may be late Cisuralian or possibly Roadian in age (Modie & Le Hérissé 2009). This is largely based on correlation of the Ecca Group assemblage zones (in upper half of the Ecca Group) to the *Lueckisporites virkkiae* Interval Zone of the Parana Basin, where in Argentina the base of the interval zone is dated (using SHRIMP U/Pb on zircons) to 278.4 Ma (Modie & Le Hérissé 2009), placing its base in the Kungurian. This is a similar position to the first occurrence of *L. virkkiae* in the Svalbard sections (Fig. 2).

Tetrapod fauna of the Beaufort Group *Eodicynodon* Assemblage Zone, forms the key components of the Kapteinskraalian land vertebrate faunachron (LVF) of Lucas (2006). The fauna of this LVF is most similar to the Ocher and part of the Mezen tetrapod assemblages from Russia (Lucas, 2006), which occur within the Shesmian (upper interval of Ufimian) to Kazanian to the mid Urzhumian (Goulbev 2015). In Russian sections this interval is reverse polarity only (Figs. 1,3), whereas the assumed equivalent *Eodicynodon* Assemblage interval is associated with both polarities. Hence, the 'long-GU1r' option indicates diachroneity of the Kapteinskraalian LVF, with the Russian faunas being the oldest representatives of this LVF.

The alternative ‘brief-GU1r’ option places the start of the Illawarra Superchron c. 400 m above in the mid parts of the Abrahamskraal Fm (Buffels River section), at the base of the interval of normal polarity dominance (Fig. 6). This option suggests the Ouberg Pass section N2-N3 magnetozones represent the Kungurian magnetochron CI3n, and magnetozone N3 is possibly CI2n (or a tentative magnetozone between CI2n and CI3n; Fig. 1). This ‘brief-GU1r’ option is compatible with the normal polarity dominance in the mid parts of the Abrahamskraal Fm in the Buffels River area (Fig. 6). However, it requires the overlying 1.5 km of strata to the Wuchiapingian boundary in the Beaufort Group to be largely normal polarity corresponding to the younger part of GU3n. This option makes the correlations between the Russian and South African expression of the Kapteinskraalian LVF more consistent in terms of the reverse polarity dominance, in the inferred late Ufimian to mid Urzhumian age for the *Eodicynodon* Assemblage Zone. However, it does push the base of the *Eodicynodon* Assemblage Zone into the Kungurian potentially as early as the Kungurian- Artinskian boundary, which is counter to current thinking which suggests tetrapod assemblages yielding “bona fide therapsids” are mid Permian (Lucas 2006). The two older Littlecrotian and Redtankian LVF’s (Lucas, 2016) have little independent age control. The older LVF the Redtankian, has equivalent tetrapod fauna from the Garber Fm (in which CI2n has been inferred; Table 1), suggesting that the Waterford Fm magnetozone N3 is a good deal younger than late Artinskian. Supporting evidence for the ‘brief-GU1r’ option is the re-assessment of the detrital zircon SHRIMP ages (due to suspected lead loss) from the top of the Ecca Group (Tohver *et al.* 2015) which suggest ages as old as 275 Ma (i.e. Kungurian) for deposition of the upperparts of the Ecca Group.

Broadly, the ‘long-GU1r’ option implies polarity dominance over the GU1 magnetochron is poorly represented by the Russian Urzhumian dataset (Fig. 3), supporting suspected normal polarity overprints in this dataset. It also implies a large diachroneity of the Kapteinskraalian LVF. The crucial supporting data are the age overlap between the radiometric dates from the Abrahamskraal Fm and those from the Guadalupian type area (Fig. 6).

The ‘brief-GU1r’ option relies on the large wealth of data from the Russian sections through the Urzhumian, and requires that the U-Pb SHRIMP ages from the Abrahamskraal Fm are too young, probably impacted by lead loss (e.g. Tohver *et al.* 2015). It also indicates the Kapteinskraalian LVF extends into the Kungurian, counter to vertebrate workers hypotheses.

Lopingian and the Permian-Triassic boundary

The key part of the Lopingian magnetochron pattern is the reverse polarity dominated early Wuchiapingian (i.e. LP0r), a key feature clearly seen in many marine and non-marine datasets. This reverse polarity interval and its transition from GU3n, is seen by the relatively thick LP0r, overlying a relatively thick GU3n in many sections. The LP0r is followed through the late Wuchiapingian and Changhsingian, by a pattern of reverse and normal magnetozones with similar relative thickness (Figs. 3, 4).

Biochronological control of the magnetic polarity changes across the Guadalupian-Lopingian boundary is probably best defined in the Kyushu sections (Kirschvink *et al.* 2015), where an extinction level and change to the Wuchiapingian fusulinid *Codonofusiella - Reichelina* Zone is seen (Fig. 4). The extinction level appears to be located in a ca. 2-3 m thick normal polarity interval (LP0r.1n), within an interval of predominant reverse polarity. There are tentative brief normal polarity intervals in other sections (e.g. Wulong, Shangsi, Sukhona River) at around this level following GU3n (Figs. 3,4), but none of them have a better biochronology. Magnetostratigraphic studies on the Laibin section (and the Wuchiapingian GSSP section) by M. Menning and S. Shen have only recovered remagnetisations (Jin *et al.* 2006b).

The normal magnetochron LP0r.2n is clearly shown in the Wulong and Linshui section in China, and tentatively in the Shangsi and Nammal Gorge sections. This magnetozone is the 'P3' normal chron of Steiner (2006). It occurs within the range of the conodont *Clarkina asymmetrica* (L3 standard conodont zone) in the Nammal Gorge section, placing it in the early Wuchiapingian. The age of unit 5 of the Longtan Fm in the base of the Linshui section, is based on regional correlations of brachiopod assemblages, suggesting a late Wuchiapingian age (Chen *et al.* 2005). This age is supported by the presence of the conodont *C. liangshanensis* (equivalent to conodont zones L6-L7; Shen *et al.* 2010) in the basal beds of the Longtan Fm, ca. 300 m below the measured magnetostratigraphy (pers comm. Shuzhong Shen 2010). Equivalents to magnetochron LP0r.2n also occur in the Rustler Fm in New Mexico, and the Littleham Mudstone Fm in England (Figs. 6, 7).

The base of magnetochron LP1n is a clear stratigraphic marker in many Lopingian marine sections, following the LP0r chron (Fig. 4). In non-marine sections in Russia and Europe, this is a very clear boundary to an overlying interval with several major normal polarity intervals (Fig. 3, 7). The base of

LP1n is within the range of the Wuchiapingian conodont *C. guangyuanensis* (L5 standard conodont zone) at Nammal Gorge, with LP1n extending to near the top of the late Wuchiapingian *C. transcaucasica* Zone (conodont zone L6) at the Shangsi section (Fig. 4).

The interval LP1n to base LP2r shows a pattern of polarity changes, which tend are dominated by normal polarity in marine sections, yet include regular reverse polarity intervals. This interval is the 'Chang-N' chron of Steiner (2006). The Linshui section (which has a high accumulation rate), displays this interval particularly well, whereas the Wulong, Shangsi and Nammal Gorge sections do not display the intervening reverse magnetozones well. In New Mexico, the Quartermaster and Dewey Lake formations clearly show a pattern of three major reverse magnetozone (Fig. 6), like the Linshui section. The upper boundary of the LP2n.3n magnetochron is within the Changhsingian *C. subcarinata* Zone (L9) at the Abedah section, but probably within the *C. changxingensis* Zone (L10) at the Shangsi section.

The three studies on the Changhsingian and Induan GSSP's at Meishan (Fig. 8) show a poor degree of similarity in the magnetic polarity through the section (Li & Wang 1989; Liu *et al.* 1999, Meng *et al.* 2000). An additional summary in Yin *et al.* (2001) shows some additional details, although the source data is not published. The low degree of consistency between the magnetostratigraphic data does suggests a normal polarity interval (the LP2n.2n-LP2n.3n interval?) in the *C. wangi*- *C. subcarinata* zones (L8-L9) and mixed polarity in the *C. changxingensis* Zone; possibly corresponding to the LP2r-LP3r interval (Fig. 8).

Lopingian Non-marine sections

Magnetic polarity data from marine sections display more detail in magnetozones through the Lopingian, than the Russian non - marine sections (Figs. 3, 4). The simplest interpretation of this is the absence of most of the late Changhsingian often inferred in Russian sections (Lozovsky 1998; Tverdokhlebov *et al.* 2005; Lozovsky *et al.* 2014). The oldest units of the Vetlugian (i.e. Vokhmian, considered early Triassic) have a transitional latest Changhsingian flora and reverse polarity (i.e. upper part of LP3r), clearly resting on an eroded surface of the late Vyatkian (Lozovsky *et al.* 2001). The Permian-Triassic boundary is therefore clearly within the basal-most Vokhmian.

In Russian Tatarian sections the uppermost normal polarity parts of magnetozone R_3P (i.e. n_1R_3P and n_2R_3P) are missing from some sections, but are clearly present at the Oparino and Boyevaya Gora sections and other sections shown in Burov *et al.* (1998). This likely reflects the variable erosion at the base of the Vokhmian. Both in the marine and non-marine sections, the three reverse magnetochrons in the magnetochron interval LP1- LP2 vary greatly in thickness (Figs. 3, 4). Some of this variation in the Russian sections may be due to channel bodies, which can give variable accumulation rates, together with likely local hiatus, features that are being investigated in more detail (Arefiev *et al.* 2015).

In Europe magnetostratigraphic studies in the Upper Rotliegend of the southern Permian Basin (well Mirow 1/1a/74, Menning *et al.* 1988; Langereis *et al.* 2010), and wells in Poland (Nawrocki 1997) clearly show the reverse polarity LP0r. Above this is a mixed polarity interval, which includes the Zechstein (Fig. 7). The incomplete sampling of the normal and reverse magnetozones in the Notec and Hannover formations, are more fully represented by studies from the laterally equivalent Lower Leman Sandstone from the Johnston and Jupiter gas fields in the southern North Sea (Turner *et al.* 1999; Lawton & Roberson 2003). In the Southern Permian Basin, these European-wide correlations are strongly constrained by the overlying Zechstein, the base of which is usually inferred to be an isochronous lithostratigraphic marker. In the southern German Obernsees core, normal polarity dominates the Z1 to Z3 interval (Szurlies 2013), with a briefer reverse polarity magnetozone near the base of the Z1 interval, which may correlate to the upper-most tentative reverse seen in the Polish Czaplinkek, Pila and Jaworzna IG-1 well (Fig. 7). Like the Everdingen-1 and Schlierbachswald-4 wells the Z4-Z6 interval is dominated by normal polarity in the Obernsees core (Szurlies 2013).

Correlations in Fig. 7 imply that the base of the Zechstein (basal Z1 cycle) occurs in the oldest parts of magnetochron LP2n.3n in the mid Changhsingian. The equivalent of LP2n.3n seems to be exceptionally thick in the Zechstein successions (ca. Z1-Z3 interval), which may be explained by the rapid infilling of the Zechstein Basin upon initial flooding. Additional support for the Changhsingian age of the Zechstein comes from Sr-isotope data, which indicates a short duration for the Zechstein of ca. 2 Ma, and an age range in the interval 255-251.5 Ma, placing it firmly in the Changhsingian (Denison & Peryt 2009). Attempts at direct dating of the Kupferschiefer (the base of the Zechstein- Z1 cycle) have failed to yield consistent results, with Re-Os ages giving wide 95% confidence intervals (Pašava *et al.* 2010). The Changhsingian age conflicts with conventional age interpretation of the basal Zechstein, which is usually assigned to the early Wuchiapingian (Szurlies 2013). This is primarily based on the conodonts *Merrillina divergens* and *Mesogondolella britannica* from the Kupferschiefer and Zechsteinkalk of the Z1 Formation (Swift 1986; Korte *et al.* 2005; Legler *et al.* 2005; Słowakiewicz *et al.* 2009; Szurlies 2013), since according to Kozur in Szurlies (2013), *Mer. divergens* occurs in the range interval of *Clarkina leveni* (conodont L4 standard zone) in Iran. However, *Mer. divergens* is found from the uppermost

Alibashi Fm in the Changhsingian *C. yini–C. zhangi* Zone in Iran (Kozur 2007), and from Wordian, Capitanian and late Cisuralian strata (Swift 1986; Nakrem *et al.* 1991). Therefore, Zechstein conodont faunas do not provide a precise biochronology- due to differences between cold and warm water faunas they only provide an approximate Lopingian age (Henderson & Mei 2000).

The Permian-Triassic boundary

The late Changhsingian transition towards the Permian-Triassic boundary has been well documented in terms of magnetic polarity in both marine (Gallet *et al.* 2000; Glen *et al.* 2009; Li *et al.* 2016) and non-marine successions (Glen *et al.* 2009; Hounslow & Muttoni 2010; Szurlies 2013), where a reverse polarity dominated interval (LP2r-LP3r) occupies the late Changhsingian. This occupies the *C. yini* (L11) and *C. meishanensis* (L12) conodont zones (and parts of the *C. changxingensis* in some sections), prior to the main extinction event in the latest Changhsingian. In spite of the well-studied nature of this interval, the conodont zonal boundaries are not consistently located with respect to the polarity boundaries, perhaps indicating placement issues with the conodont standard zones. In this interval the normal magnetozone LP3n is the ‘P5’ chron of Steiner (2006), and is clearly seen in several marine and non-marine sections (Figs. 4, 7).

In the Induan GSSP at Meishan (Fig. 8), the exact relationship between the polarity stratigraphy and the first occurrence of *Hindeodus parvus* is not clear, but the Shangsi and Abedah sections indicate the inferred base of the Induan is consistently in the lower part of the LT1n.1n magnetochron (Glen *et al.* 2009; Hounslow & Muttoni 2010; Szurlies 2013). The Shangsi section probably provides the most precise placement of the Permian-Triassic boundary interval with respect to the magnetostratigraphy (Fig. 9). At Shangsi the base of LT1n is near the base of the *C. meishanensis* conodont zone, within 0.5 m of the extinction event bed (Glen *et al.* 2009). A variety of CA-ID-TIMS U/Pb radiometric dates indicates ca. 252.3Ma for the age of the base of LT1n, in the latest Changhsingian (Fig. 9). At Shangsi, the precisely correlated base of the Induan (base of *H. eurypyge* Zone; Shen *et al.* 2011) is based on CONOP correlation and the occurrence of *H. changxingensis* rather than *H. parvus,* whose first occurrence is younger in the section (Metcalfe *et al.* 2007).

In Russian Platform sections, there is dispute about the continuity of the successions across the Permian-Triassic boundary with some preferring a lack of hiatus (Sennikov & Golubev 2006; Krassilov & Karasev 2009; Taylor *et al.* 2009) but others suggesting hiatus (Lozovsky *et al.* 1998; Tverdokhlebov *et al.* 2005); much depends upon the stratigraphic resolution of the dating tools. However, it is clear in the magnetostratigraphy from the Russian sections, there are insufficient magnetozones following LP1n (N_2P in Russian magnetozones, Fig. 3) to accommodate the entire Lopingian, indicating a major hiatus at the base of the Vokhmian, or locally in the Vyatkian. The basal Vokhmian typically shows a magnetite abundance increase, expressed by increases in magnetic susceptibility and remanence intensity (Burov *et al.* 1998; Lozovsky *et al.* 2014), which appears to be associated with an enhanced volcanic ash contribution (Burov 2004). In some other sections, where magnetozone n_2R_3P is not seen, the late Permian magnetozones are variably removed by erosion at the base of the Vokhmian, indicating that Russian magnetozone n_2R_3P is the equivalent of LP2n.3n (Fig. 3). However, in the Yug River basin, the transition of LP3r into LT1n (or perhaps LT1n.1r into LT1n.2n), and the transition into the Triassic may be preserved in the Nedubrovo Member. This member has plant and spore remains typical of the Tatarian and the Zechstein, as well as megaspores *Otynisporites eotriassicus* and *O. tuberculatus* typical of the earliest Triassic (Burov, 2004; Lozovsky *et al.* 2014; Arefiev *et al.* 2015).

In sections (East and West Lootsberg Pass and Komandodriftdam sections) from the Karoo Basin (S. Africa), the turnover in vertebrate assemblages is seen just below the Balfour Fm - Katburg Fm boundary (Fig. 9). This change is inferred to represent the Permian-Triassic boundary, because of association between the vertebrate biochronology, expected magnetostratigraphy (Fig. 9) and negative $^{13}C_{org}$ isotopic excursions (De Kock & Kirschvink 2004; Ward *et al.* 2005). However, magnetostratigraphy and U-Pb ID-TIMS dating from the nearby Old Lootsberg Pass (Gastaldo *et al.* 2015) suggest these supposed boundary successions are older, and likely Changhsingian in age around 253.2 ±0.15Ma (Fig. 9). This may relate to difficulties in defining the Permian-Triassic boundary based on tetrapods alone (Lucas, 2006). However, there are serious disagreements about the polarity in the upper part of the Balfour Fm, which either indicate problems with local hiatus (Gastaldo *et al.* 2015), or issues in the palaeomagnetic data from Old Lootsberg Pass, in distinguishing the present day overprints from the normal polarity Permian directions, which are similar to modern field directions (De Kock & Kirschvink 2004). It is not clear how these magnetic polarity datasets relate to each other, but there is not sufficiently strong evidence to invalidate the original interpretations of Ward *et al.* (2005).

There have been many magnetostratigraphic studies on the Siberian Traps (Gurevitch *et al.* 2004; Fetisova *et al.* 2014), and several attempts at a synthesis (Steiner 2006; Fetisova *et al.* 2014; Burgess and Bowring 2015). The successions indicate a simple pattern of magnetic polarity changes, dominated by normal polarity in the Noril'sk region, but with reverse magnetozones in the Kotui River region and at the base of the successions in the Ivaninsky and Khardakh formations (Fig. 9). Inadequately described fossil spores, pollen and brachiopod remains, constrain the succession into an older Permian and younger Triassic set of units (Fetisova *et al.* 2014). Based on the combination of biostratigraphic data, radiometric dating evidence and palaeomagnetic data, Fetisova *et al.* (2014) suggest the oldest units, the Ivakinsk (at Noril'sk) and Khardakh formations, are late Permian. The overlying, predominantly normal polarity basalts at Noril'sk likely correspond to LT1n.1n (Fig. 9). The Syverma to Nadezhda suites of the Noril'sk succession record the transitional geomagnetic field behaviour, across the boundary of the LP3r and LT1n.1n magnetochrons (Gurevitch *et al.* 2004), implying these units have a rapid (6-20 m/kyrs) accumulation rate. This transitional field interval is not shown in the Motui River sections, suggesting there may be a hiatus (or poorly sampled interval) at the base of the Ary-Dzhang Fm (Fetisova *et al.* 2014; Kamo *et al.* 2003). Radiometric data have consistently indicated the brief duration of the Siberian traps, which are constrained by dates from perovskite of 252.2±0.2 Ma from the Khardakh basal flows (Kamo *et al.* 2003) to 251.4±0.29Ma for the Daldykansky intrusion which cuts the lava flows in the Noril'sk region. Burgess & Bowring (2015) argue that the lava eruptions were ca. 0.8 Ma in duration with some 2/3rds of the volume erupted in the 0.3 Ma prior to the end-Permian extinction. The Permian-Triassic boundary is therefore within the mid to upper parts of the flood basalt succession at Noril'sk (Burgess & Bowring 2015).

A calibrated Permian geomagnetic polarity timescale

To generate a Permian geomagnetic polarity pattern in a million year scale, we firstly utilise the section compositing method proposed by Hounslow (2016). This first produces a magnetic polarity composite using numerical optimisation, in a composite scaled to relative height (Fig. 10b,e). This is in effect a numerical version of the hand drawn composites, produced by syntheses such as Opdyke (1995), Steiner (2006) and Hounslow & Muttoni (2010). The optimised composite utilises the proxy for time embedded in the relative height of magnetozones in the data from the source sections, and so smooth's the between-section sedimentation rate changes, by averaging magnetozone boundary positions across sections (Fig. 10b,e). This requires simple choices about relative sedimentation rates in the sections.

Secondly, the resulting optimised composite is scaled to million years, using appropriate radiometric data (i.e. an age model is applied to the optimised scale), from which an age estimate of the magnetochron bases is determined (Table 2; Figs. 10c, 11). To construct the age model we use the Bayesian-based approach of Haslett & Parnell (2008), Parnell *et al.* (2008) as implemented in the Bchron functions in R (Chambers 1998). This constructs an age model based on piecemeal linear segments constructed by simulating the sedimentation process by small increments random in both duration and sedimentation rate. The method handles radiometric date uncertainties (as normally distributed values) and uses the procedure of Christen & Perez (2009) to deal with radiometric date outliers, which flags the dates with a probability of being an outlier (P_{out} in Table 2). Uncertainties in placing the radiometric date onto the optimised polarity composite are handled as a defined range ('sample depth' range in Parnell *et al.* 2008) in the composite scale, in which the date occurs ($\pm e_s$; Table 2), and treated as coming from a uniform distribution. Stratigraphic (e_s; Hounslow 2016) and radiometric uncertainties (σ_R) on the dates are listed in Table 2 and Supplementary Table 2 of Hounslow (2016).

Confidence intervals on the magnetochron ages are obtained from the Monto Carlo simulations used in Bchron, using the limits of the 95% highest posterior density region (HPD) from the age model (Haslett & Parnell, 2008; Fig. 10c). Although, confidence intervals derived from Bchron may be overly pessimistic in intervals without age control points (Blaauw & Christen 2011). In the age models the measure of uncertainty (i.e. σ_T; Hounslow, 2016; Table 3) in the position of the magnetochrons in the optimised composite scale, is also included (Fig. 10a,d), as the 'uniform range' (d_{max}-d_{min} of Parnell *et al.* 2008), corresponding to $\pm\sigma_T$. The method therefore takes account of all the major uncertainties in the GPTS. The Permian optimised composite (Table 3) is scaled to age in two segments, because no sections span the CI1r.1n to CI2n interval.

Gzhelian-Asselian age scaling

The Gzhelian-Asselian magnetozone optimised composite, used the Karachatyr, Nikolskyi and Aidaralash sections. These can be tied together since they have a well defined fusulinid zonation, which is also utilised in the scaling (Fig. 10b). Linear rate scaling for the sections (Hounslow 2016) was used in the optimised composite. The Kapp Schoultz section from Svalbard was unused, since the relationships between the biostratigraphy and the magnetostratigraphy are not sufficiently well-defined to accurately identify positions of either biozones or stage boundaries with respect to the polarity, or to the biozones in the Uralian sections. The ID-TIMS U-Pb radiometric ages from the Usolka section were used (Table 2), directly related to the Urals foraminifera zones, via the conodont ranges in the Usolka section, and the conodont-foraminiferal biozonal correlations in Schmitz & Davydov (2012). The optimised composite scale was when related to the radiometric ages using Bchron (Fig. 10c). None of the radiometric dates were flagged as potential outliers (Table 2). The 95% HPD regions from Bchron show bowing and pinching related to the distribution of age control points, expressing the greater uncertainty between the more widely spaced dates (Fig. 10c), which is also expressed in the chron uncertainty (C_{95}, Table 3).

Kungurian- earliest Induan age scaling

A Kungurian-Capitanian optimised magnetozone composite (CI2n to GU3n) was constructed using the Paganzo, Ouberg Pass (Long GU1r option), Adz'va (Fig. 1), Kapp Wijk/Trygghamna (Fig. 2), the W. Texas (Fig. 6), the Taiyuan sections (Fig. 4) along with the Russian Khei-yaga, Muygino, Monastrski, Tetyushi and Cherumuska sections (Figs. 3, 10e). The optimisation tends to 'compress' the composite scale in the CI3r.1n to GU2n interval, due to the higher number of data points and magnetozones in this interval. Scale compression was controlled by expressing the minimised value E_{tot} (Hounslow, 2016) as E_{tot}/ divided by the median chron duration. Linear rate scaling (Hounslow 2016) was used for all but the Monastrski, Tetyushi and Cherumuska sections in which transgressive rate functions were used. Transgressive rate functions account for the apparently condensed GU1n (Fig. 3). Overall the optimised component produces a poorer model (large D_s) than the Gzhelian-Asselian model, due to the widely varying relative durations of chrons in the Wordian, which is shown as larger σ_T and D_j values (Fig. 10d,e).

The Cisuralian part of this range is sparse in radiometric dates. One ID-TIMS date from an ash in the base of the La Colina Fm was used (Gulbranson *et al.* 2010; Table 2), together with the Kungurian-Roadian boundary age from Henderson *et al.* (2012), inferred to coincide with the brachiopod extinction, and $\delta^{13}C$ excursion in the Hovtinden Mb on Spitsbergen (Figs. 2, 10f). The Artinskian-Kungurian boundary has an array of dates (Henderson *et al.* 2012), but cannot be clearly related to the polarity in any section. To constrain the Cisuralian, the Artinksian-Kungurian boundary age from Henderson *et al.* (2012) was used for the base of the Kungurian in the mid part of the Svenkegga Mb at Kapp Wijk/Trygghamna (Fig. 2). In the Wordian-Capitanian, zircon SHRIMP dates from the Abrahamskaal Fm are supplemented by additional radiometric, dates from the Texas sections of Nicklen (2011) and Bowring *et al.* (1998). These radiometric dates have been placed onto the magnetostratigraphy (Table 2; Fig. 11b), using the magnetic polarity data of Burov *et al.* (2002) and stratigraphic relationships discussed by Nicklen (2011).

The late Capitanian to earliest Triassic optimised composite (GU3n- LT1n.2n) is that derived by Hounslow (2016). This uses the magnetozone data from the Khei-yaga, Murygino, Monastyrki, Boyevaya Gora, Tuyembetka, Sambullak, Tetyushi, Cheremushka, Sukhona, Pizhma, Oparino, W.Texas, Linsui, Wulong, Shangsi, Taiyuan, Nammal Gorge and Abadeh sections to construct the optimised composite. This optimised composite is joined to that from the CI2n to GU3n interval at the base of GU3n (Fig. 11). This compound optimised composite is then scaled to age with Bchron using 28 dates (upper 11 ones in Table 2), plus the 17 ID-TIMS listed in Supplementary Table 2 of Hounslow (2016). Bchron identified two probable outliers in the age model at 252.1 Ma and 253.47 Ma (P_{out} of 0.992 and 0.998 respectively; Fig. 11).

Two intervals giving possibly unrealistic age estimates are the LP0r-LP1r and LP2n.2r-LP2n.3n intervals, since the Bchron age scaling does not match well the relative durations of section chrons in these two intervals. The former interval is strongly influence by the late Wuchiapingian date at 257.79 Ma from the Shangsi section (Figs. 5, 11), that gives a probable too-brief LP0r chron. This date may be incorrectly located with respect to the polarity stratigraphy. Attempts at correcting the later 'unrealistic' interval by excluding the possible outlier at 253.47 Ma, failed to produce much improvement, since the age model from Bchron already accounts for its outlier status.

Chron and stage ages and relationship to biozones

The earliest Permian age model (Figs. 10c, 12) gives an age for the base of fusulinid zone 10 (correlated base Asselian) of 298.41±0.36 Ma, similar to the 298.9±0.15 Ma proposed by Schmitz & Davydov (2012). The age differences likely relate to assumptions of conformity of fusulinid and conodont zonal boundaries (Schmitz & Davydov 2012), the different means of scale compositing (range top and bottom scaling in CONOP) and the method of scaling the composite to age. The derived Ma dates of the magnetochrons (Table 3) are broadly what would be expected based on the biozonal-stage-Ma age relationships proposed by Henderson *et al.* (2012). This is not surprising considering we largely use the same sets of controlling radiometric dates, and we have pinned the base Roadian and base Kungurian to that inferred by Henderson *et al.* (2012). However, our age control through the Wordian is considerably improved over the 2012 timescale, and we estimate the base Wordian at c. 266.7Ma and base Capitanian at c. 263.5 Ma, significantly displaced from the 2012 timescale by c. 2 Ma (Table 3). The base of the Lopingian stages and the Induan are similar to those inferred in the 2012 timescale, since there are many radiometric dates in this interval. Like the Asselian, the small differences likely relate to the different methods used.

The relationships between the stage-biozones and the magnetochrons have a variable amount of precision through the Permian. In the earliest part of the Cisuralian, the relationships between CI1r.1n and the Urals foraminifera biozones is fairly well defined (Fig. 12), but becomes much less precise for CI2n and CI3n, where relationships to conodonts zones seem to hold the best future promise for refinement (Figs. 1, 2). For the mid Permian there is a slightly more refined biozone-magnetochron relationship. The Lopingian has a comparatively well defined conodont biozone to magnetochron relationship (Figs. 4, 12).

Chron duration uncertainties

Apparent magnetozone durations (and zonal intervals in Ma) in the sections can be 'back-calculated' from the relationship between optimised composite chron duration and age. If the duration (in Ma) of a magnetochron (or chron interval) is C_m in the GPTS, and the pseudo-height in the composite of this interval is Y_m, then the apparent duration (C_S in Ma) of the equivalent magnetozone (or zonal interval) in the section can be estimated by $C_s= C_m *(Y_s/Y_m)$. Y_s is the pseudo-height of the magnetozone (or interval) in the section in the units of the optimised composite. Linear scaling is appropriate, since the segment age-models are approximately linear at a time-scale comparable to the magnetochron intervals used. This gives a cloud of points (Fig. 13a), which expresses the apparent age duration of chrons in the sections, visually showing the scatter in the original data, which for each chron is also expressed by σ_T.

Uncertainties on the chron durations can also be determined by the 95% HPD intervals derived directly from the differences in the simulated age-determinations for each chron ('events' in Bchron; Parnell *et al.* 2008; Fig. 13a). However, these Bchron 95% HPD estimates more express a prediction interval than a confidence interval on the 'mean' age-model, since they only consider the simulated data from a single magnetochron duration (rather than the whole age model; Dybowski & Roberts 2001). This can be seen in that the HPD bands largely encompass the cloud of points from the section estimates (Fig. 13a).

One estimate of the confidence intervals (D_{95}) on the durations (i.e. on C_m) can be determined from a conventional regression of C_s versus C_m (a 'section-estimate'; Fig. 13a). This approach is conceptually similar to that used by Agterberg (2004) for estimating confidence intervals on stage ages, since the estimated magnetozone duration in the section (C_s) is an independent estimate compared to that 'average' derived from the optimised chron scale. Statistically it is preferable to utilise a log-log regression for this 'section-estimate', since durations are typically exponentially distributed (Lowrie & Kent 2004). For shorter chron durations the percentage uncertainty increases (Fig. 13b), because there is proportionally a larger impact of changes in deposition rates in sedimentary systems (Sadler & Strauss, 1990; Talling and Burbank, 1993) and sampling density (i.e. fluctuations in the sedimentation rate and palaeomagnetic sampling density section, introduces additional variance in the section chrons duration). However, for longer chrons the log-log regression produces unrealistically large confidence intervals, because of the spreading of the confidence bands at the tails (Fig. 13b), and a linear C_s- C_m relationship is probably more appropriate (shown as linear model in Fig. 13b). Uncertainty on longer chrons is more impacted by the uncertainty in the age model from the radiometric dates (σ_R in Table 2) and their uncertainty of position with respect to the magnetochrons (i.e. e_s in Table 2). However, neither of these 'section-estimates' (i.e. log or linear models in Fig. 13b) takes account of uncertainty in the age model.

Agterberg (2004) proposed an estimate of D_{95} can be obtained from the confidence interval on a regression of calculated radiometric age versus actual radiometric age derived from the age model. A 'sample point distribution' correction factor should also be applied to correct for the Ma range of the age model (Agterberg, 2004). We determined this 'Agterberg estimate' using the data for the Wordian-early Triassic (i.e. data in Fig. 11, from 269-251 Ma) interval, since the larger number of dates in this interval probably best expresses the uncertainty in the age model. This estimate gives values for $\%D_{95}$ similar to the linear-model 'section-estimates' at chron durations >1 Ma (Fig. 13b). The final confidence interval on durations is a joint model (Fig. 13b; $\%D_{95}$ in Table 3) which adds the 'Agterberg estimate' (for the age model uncertainty) to the log and linear model 'section-estimates' for chron durations (Fig. 12b). This gives a balanced estimate that includes both uncertainty from the optimised polarity and from uncertainty in the age model.

Conclusions

A robust geomagnetic polarity timescale is constructed through the Permian, with no major intervals with missing polarity data (Fig. 12). The statistical compositing method of Hounslow (2016) allows construction of a numerical magnetochron composite using data from many sections. This composite is calibrated against radiometric dates, using Bayesian principles applied in the program Bchron, using two segments, one for the Carboniferous-Permian boundary and a Kungurian-earliest Triassic interval. The Artinskian, Kungurian and Roadian interval are the least well constrained in terms of controlling radiometric dates, so two previous estimates of stage boundary age are utilised for this interval. Estimates of the 95% confidence intervals on the chron-base ages and chron durations are derived.

In spite of a long held belief, by many, that the early Permian contains no substantiated normal polarity intervals, there is good evidence the Cisuralian contains at least two, probably four brief normal magnetochrons, and a further normal in the latest Carboniferous (latest Gzhelian). The Asselian magnetochron CI1r.1n (base at 297.94±0.33 Ma), and CI3r.1n (base at 269.54±0.70 Ma) are least well validated of these, whereas CI2n (base at 281.24±2.3 Ma) and CI3n (base at 275.86±2.0 Ma) in the Artinskian and Kungurian are rather better identified in more studies. The age-calibration of these clearly shows these magnetochrons are brief (ca. 81 ka - 506 ka) in duration, which has added to their difficulty in detection in the dominantly reverse polarity Kiaman Superchron. The presence of these magnetochrons holds promise as high-resolution time markers in the Cisuralian.

The start of the mixed polarity Illawarra Superchron is at 266.7±0.76 Ma in the early Wordian, long known to be a major chronostratigraphic marker in the mid Permian. The European Russian upper Tatarian (Vyatkian) magnetostratigraphic data appear incomplete in comparison to the better dated marine successions, indicating a part of the Changhsingian is missing from the European Russian sections. Magnetostratigraphic data from the European Upper Rotliegend and Zechstein clearly indicate the presence of the Guadalupian and Lopingian in these non-marine basins. However, magnetostratigraphic correlations suggest the Zechstein represents a much shorter age interval than conventionally inferred, occupying only the mid to late Changhsingian. The magnetic polarity with respect to the many high-resolution stratigraphic studies across the Permian-Triassic boundary is well defined and the best expressions of the linked polarity to faunal changes are in the Shangsi section in China. Radiometric and magnetostratigraphic data suggest the voluminous Siberian traps where erupted rapidly, starting in the latest Permian magnetochron LP3r, into and through the earliest Triassic normal chron LT1n.

Key uncertainties and future refinements of the Permian GPTS needed are:

1) Sub-magnetochrons CI1r.1n (early Asselian) and chron CI3r.1n (early Roadian) are the least well defined of the Permian chrons in the Kiaman Superchron, and need further work to consolidate understanding of these. Permian sections on Svalbard or in the Urals may hold the best promise for better calibration of these against biostratigraphy. High resolution studies of North American sections through the Laborcita Fm may aid investigations of chrons at the Carboniferous- Permian boundary.
2) Other Permian chrons in the Kiaman Superchron, CI2n and CI3n, are magnetically well-defined, but not well calibrated to biostratigraphy or radiometric dates. The arctic Permian sections seem to hold the best promise for a better intercalibration of magnetochrons and biochronology.
3) Detail of the polarity through Wordian which includes GU1 and GU2 have two alternative scenarios, firstly a long GU1r model (the one preferred here), based on fragmentary marine, and non-marine sections in the Beaufort Grp from South African. Secondly, a brief- GU1r model with more normal-polarity dominance, largely defined by the datasets from European Russian sections. The later scenario depends on the reliability of normal magnetozones in the Russian NRP mixed-polarity magnetozone and how to correlate marine and non-marine

magnetostratigraphies in the Wordian. Detailed magnetostratigraphic data from the back reef facies in the type region of the Guadalupian would help in this uncertainty.

4) The interval LP1n to LP2n.3n (late Wuchiapingian- mid Changhsingian) is normal polarity dominated in many sections, but the relative duration of reverse polarity magnetozones in this interval vary greatly between sections, particularly for LP1r. Better integration of regional sedimentological, cyclostratigraphic, radiometric and magnetostratigraphic studies in both marine and non-marine would help refine an improved polarity timescale through this interval.
5) Radiometric date control points for age scaling of the GPTS, appear to severely distort the relationship between apparent relative duration of chrons in the sections in the early Wuchiapingian and mid Changhsingian. Acquisition of more dates, and/or re-assessment of either the radiometric dates, or their position with respect to the composite magnetostratigraphy is needed to unravel the apparent conflict.

Acknowledgements

Vassil Karloukovski assisted with Russian translations. Andrew Parnell provided useful guidance on using Bchron. The reviewers Jim Ogg and Spencer Lucas provided much constructive comment, improving the text.

References

ALI, J.R. THOMPSON, G.M., SONG, X. & WANG, Y. 2002. Emeishan basalts (SW China) and the end-Gudalupian crisis: magnetobiostratigraphic constraints. *Journal Geol. Soc. London*. **159**, 21-29.

AGTERBERG, F.P. 2004. Statistical procedures. *In:* Gradstein, F., Ogg, J. & Smith, A. (eds), *A geologic Time Scale,* Cambridge University Press, Cambridge.

AREFIEV, V, GOLUBEV, V.K. BALABANOV, YU.P. KARASEV, E.V. MINIKH, A.V. MINIKH, M.G. MOLOSTOVSKAYA, I.I. YAROSHENKO, O.P. & ZHOKINA-NAUMCHEVA, M.A. 2015. *Type and reference sections of the Permian–Triassic continental sequences of the East European Platform: main isotope, magnetic, and biotic events*. XVIII International Congress on Carboniferous and Permian, August 4–10, Paleontological Institute of the Russian Academy of Sciences, Moscow.

BALABANOV, YU. P. 1988. Paleomagnetic rock sequence and the magnetic properties of the Permian coal-bearing rocks and Triassic basalts in the Adz'va River area. *In*: *The Permian System: Stratigraphy and the History of the Organic World*, Kazan University Press, Kazan, 126-134 [in Russian].

BALABANOV, YU. P. 1998. Paleomagnetic Characterization of the Permian–Triassic Boundary Deposits in the Northwestern Timan-Pechora Plate, in Permian–Triassic Boundary in Continental Series of Eastern Europe. *In*: V. R. LOZOVSKY & N. K. ESAULOVA (eds) *Upper Permian Stratotypes of the Volga Region*, GEOS, Moscow, 148–162 [in Russian].

BALABANOV, YU. P., 2014. Paleomagnetic characterization of the Middle and Upper Permian deposits based on the results from the key section in the Monastery Ravine. *In*: *Carboniferous and Permian Earth Systems, Stratigraphic Events, Biotic Evolution, Sedimentary Basins and Resources*, Kazan Golovkinsky Stratigraphic Meeting, Kazan. Federal Univ., Kazan, 14–17.

BARNABY, R.J. & WARD, W.B. 2007. Outcrop analog for mixed siliciclastic–carbonate ramp reservoirs—stratigraphic hierarchy, facies architecture, and geologic heterogeneity: Grayburg Formation, Permian basin, USA. *Journal of Sedim. Res.* **77**, 34–58.

BAUD, A., ATUDOREI, V. & SHARP, Z. 1995. The Upper Permian of the Salt Range area revisited: new stable isotope data. *Permophiles*, **27**, 39-41.

BECKER, R.A., CHAMBERS, J.M. & WILKS, A.R. 1988. The new S language. Chapman & Hall, New York.

BERTHOLD, G., NAIRN, A. E. M., & NEGENDANK, J. F. W. 1975. A palaeomagnetic investigation of some of the igneous rocks of the Saar-Nahe Basin. *Neues Jahrbuch für Geologie und Paläontologie, Monatshefte*, 134-150.

BIAKOV, A. S. 2012. Permian biospheric events in Northeast Asia. *Stratigraphy and Geological Correlation*, **20**, 199-210.

BLAAUW, M. & CHRISTEN, J. A. 2011. Flexible paleoclimate age-depth models using an autoregressive gamma process. *Bayesian Analysis*, **6**, 457-474.

BLAKEY, R. C. 1990. Stratigraphy and geologic history of Pennsylvanian and Permian rocks, Mogollon Rim region, central Arizona and vicinity. *Geological Society of America Bulletin*, **102**, 1189-1217.

BLAKEY, R. C. & MIDDLETON, L. T. 1987. Late Paleozoic depositional systems, Sedona-Jerome area, central Arizona. *In*: Davies, G.H. & VandenDolder, E.M. (eds). *Geologic diversity of Arizona and its margins: excursions to choice areas*, Arizona Bureau of Geology & Mineral Technology, Special Paper, **5**, 143-157.

BLOMEIER, D., DUSTIRA, A., FORKE, H. & SCHEIBNER, C. 2011. Environmental change in the Early Permian of NE Svalbard: from a warm-water carbonate platform (Gipshuken Formation) to a temperate, mixed siliciclastic-carbonate ramp (Kapp Starostin Formation). *Facies*, **57**, 493-523.

BOND, D. P., WIGNALL, P. B., JOACHIMSKI, M. M., SUN, Y., SAVOV, I., GRASBY, S. E., BENOIT BEAUCHAMP, B. & BLOMEIER, D. P.G. 2015. An abrupt extinction in the Middle Permian (Capitanian) of the Boreal Realm (Spitsbergen) and its link to anoxia and acidification. *Geological Society of America Bulletin*, **127**, 1411-1421.

BOWRING, S.A., ERWIN, D.H., JIN, Y.G. MARTIN, M.W., DAVIDEK, K. & WANG, W. 1998. U-Pb Zircon geochronology and Tempo of the End-Permian Mass extinction. *Science*, **280**, 1039-1045.

BRUNHES, B. (1906). Recherches sur la direction d'aimantation des roches volcaniques. *J. Phys. Theor. Appl.*, **5**, 705-724.

BURGESS, S. D. & BOWRING, S. A. 2015. High-precision geochronology confirms voluminous magmatism before, during, and after Earth's most severe extinction. *Science Advances*, **1(7),** e1500470.

BURGESS, S. D., BOWRING, S. & SHEN, S. Z. 2014. High-precision timeline for Earth's most severe extinction. *Proceedings of the National Academy of Sciences*, **111**, 3316-3321.

BUROV, B. V. 2004. Boundary between the Permian and Triassic rocks in the Moscow Syneclise reconstructed from the rock sequences exposed in the Kichmenga River basin. *Russian Journal of Earth Sciences*, **7**, 1–8.

BUROV, B.V. ZHARKOV, I.Y., NURGALIEV, D.K. BALABONOV, Y.P., BORISOV, A.S. & YASONOV, P.G. 1998. Magnetostratigrphic characteristivs of Upper Permian sections in the Volga and the Kama areas. *In:* ESAULOVA, N.K., LOZOVSKY, V.R. & ROZANOV, A.Y. (eds) *Stratotypes and reference sections of the Upper Permian in the region of the Volga and Kama Rivers* GEOS, 236-270.

BUROV B.V., ESAULOVA, N. K. ZHARKOV, I. YA. YASONOV, P.G. & NURGALIEV, D.K. 2002. Tentative palaeomagnetic data on the Permian Lamar and Manzanita members of the upper part of the Guadalupian Series, Guadalupe and Apache Mountains (Texas, USA) and their comparison with the east European magnetostratigraphic scale. *International Journal of Georesources* **6**, 24-28, Kazan State Univ, Tatarstan.

CAMPBELL, L. M. & CONAGHAN, P. J. 2001. Flow-field and palaeogeographic reconstruction of volcanic activity in the Permian Gerringong Volcanic Complex, southern Sydney Basin, Australia. *Australian Journal of Earth Sciences*, 48, 357-375.

CÉSARI, S. N. & GUTIÉRREZ, P. R. 2000. Palynostratigraphy of upper Paleozoic sequences in central-western Argentina. *Palynology*, **24**, 113-146.

CÉSARI, S. N., LIMARINO, C. O. & GULBRANSON, E. L. 2011. An Upper Paleozoic bio-chronostratigraphic scheme for the western margin of Gondwana. *Earth-Science Reviews*, **106**, 149-160.

CHAMBERS, J. M. 1998. Programming with Data. Springer, New York.

CHEN, H-H., SUN, S. & LI, J-L. 1994. Permo Triassic magnetostratigraphy in Wulong area, Sichuan, China. *Science in China (series B)* **37**, 203-212.

CHEN, Z-Q., CAMPI, M.J., SHI, G.R. & KAIHO, K. 2005. Post extinction brachiopod faunas from the Late Permian Wuchiapingian coal series of South China. *Acta Palaeontol. Polonica* **50**, 343-363.

CHRISTEN, J. A. & PEREZ, S. 2009. A new robust statistical model for radiocarbon data. *Radiocarbon*, 51, 1047-1059.

CHWIEDUK, E. 2007. Middle Permian rugose corals from the Kapp Starostin Formation, South Spitsbergen (Treskelen Peninsula). *Acta Geologica Polonica*, **57**, 281-304.

CONDON, S. M. 1997. *Geology of the Pennsylvanian and Permian Cutler Group and Permian Kaibab limestone in the Paradox Basin, southeastern Utah and southwestern Colorado*. U.S. Geological Survey Bulletin 2000, Denver.

COTTRELL, R. D., TARDUNO, J. A. & ROBERTS, J. 2008. The Kiaman Reversed Polarity Superchron at Kiama: Toward a field strength estimate based on single silicate crystals. *Physics of the Earth and Planetary Interiors*, **169**, 49-58.

CREER, K. M., IRVING, E., RUNCORN, S. K. 1955. The direction of the geomagnetic field in remote epochs in Great Britain. *J. Geomagn. Geoelect.,* **6**, 163-168.

CREER, K. M., MITCHELL, J. G., & VALENCIO, D. A. 1971. Evidence for a Normal Geomagnetic Field Polarity Event at 263+/-5 my BP within the Late Palaeozoic Reversed Interval. *Nature*, **233**, 87-89.

DAVYDOV, V. I. & KHRAMOV, A. N. 1991. Paleomagnetism of Upper Carboniferous and Lower Permian in the Karachatyr region (southern Ferghana) and the problems of correlation of the Kiama hyperzone. *In:* Khramov A.N. (ed), *Paleomagnetizm i paleogeodinamika territorii SSSR* (Palaeomagnetism and palaeogeodynamics of the territory of USSR), Transactions of the VNIGRI, 45-53. [in Russian]

DAVYDOV, V. I. & LEVEN, E. J. 2003. Correlation of Upper Carboniferous (Pennsylvanian) and Lower Permian (Cisuralian) marine deposits of the Peri-Tethys. *Palaeogeography, Palaeoclimatology, Palaeoecology*, **196**, 39-57.

DAVYDOV, V. I., BARSKOV, I. S., BOGOSLOVSKAYA, M. F., LEVEN, E. Y., POPOV, A. V., AKHMETSHINA, L. Z. & KOZITSKAYA, R. I. 1992. The Carboniferous-Permian boundary in the former USSR and its correlation. *International Geology Review*, **34**, 889-906.

DAVYDOV, V. I., GLENISTER, B. F., SPINOSA, C., RITTER, S. M., CHEMYKH, V. V., WARDLAW, B. R. & SNYDER, W. S. 1998. Proposal of Aidaralash as global stratotype section and point (GSSP) for base of the Permian System. *Episodes*, **21**, 11-18.

DAVYDOV, V. I. NILSSON, I. & STEMMERIK, L. 2001. Fusulinid zonation of the Upper Carboniferous Kap Jungersen and Foldedal formations, southern Amdrup Land, eastern North Greenland. *Bulletin of the Geological Society of Denmark*, **48**, 31-77.

DE KOCK, M. & KIRSCHVINK, J. 2004.Paleomagnetic constraints on the Permian– Triassic boundary in terrestrial strata of the Karoo Supergroup,SouthAfrica:implications for causes of the end-Permian extinction event. *Gondwana Res.***7**, 175–183.

DEON, C. F. 1974. *A paleomagnetic investigation of the Permo-Carboniferous Maroon and upper Permian-Lower Triassic State Bridge formations in north central Colorado*. Unpubl. PhD thesis, Univ. of Texas at Dallas.

DENISON, R. E. & PERYT, T. M. 2009. Strontium isotopes in the Zechstein (Upper Permian) anhydrites of Poland: evidence of varied meteoric contributions to marine brines. *Geological Quarterly*, **53**, 159-166

DIEHL, J. F. & SHIVE, P. N. 1979. Palaeomagnetic studies of the Early Permian Ingelside Formation of northern Colorado. *Geophysical Journal International*, **56**, 271-282.

DIEHL J. F. & SHIVE, P.N. 1981. Paleomagnetic results from the Late Carboniferous/Early Permian Casper Formation: implications for northern Appalachian tectonics. *Earth and Planetary Science Letters*, **54**, 281-292.

DI MICHELE, W. A., KERP, H., SIRMONS, R., FEDORKO, N., SKEMA, V., BLAKE, B. M. & CECIL, C. B. 2013. Callipterid peltasperms of the Dunkard Group, Central Appalachian Basin. *International Journal of Coal Geology*, **119**, 56-78.

DOELL, R. R. 1955. Palaeomagnetic study of rocks from the Grand Canyon of the Colorado River. *Nature* **176**, 1167.

DYBOWSKI, R., ROBERTS, S. J. 2001. Confidence intervals and prediction intervals for feed-forward neural networks. *In:* Dybowski R. & Gant ,V. (eds) *Clinical applications of artificial neural networks*, pp. 298-326, Cambridge University Press.

EAGAR, R.M.C. & PEIRCE, H.W. 1993. A nonmarine pelecypod assemblage in the Pennsylvanian of Arizona and its correlation with a horizon in Pennsylvania. *Journal of Paleontology*, **67**, 61-70.

EDWARDS, R.A., WARRINGTON, G., SCRIVENER, R.C., JONES, N.S., HASLAM, H.W. & AULT, L. 1997. The Exeter Group, south Devon, England: a contribution to the early post-Variscan stratigraphy of northwest Europe. *Geological Magazine*, **134**, 177-197.

EHRENBERG, S.N., PICKARD, N.A.H., HENRIKSEN, L.B., SVÅNÅ, T.A., GUTTERIDGE, P. & MCDONALD, D. 2001: A depositional and sequence stratigraphic model for cold-water, spiculitic strata based on the Kapp Starostin Formation (Permian) of Spitsbergen and equivalent deposits from the Barents Sea. *American Association of Petroleum Geologists Bulletin,* **85**, 2061–2087.

EHRENBERG, S. N., MCARTHUR, J. M. & THIRLWALL, M. F. 2010. Strontium isotope dating of spiculitic Permian strata from Spitsbergen outcrops and Barents sea well-cores. *Journal of Petroleum Geology*, **33**, 247-254.

EMBLETON, B. J. J. & MCDONNELL, K. L. 1980. Magnetostratigraphy in the Sydney Basin, southeastern Australia. *Journal of geomagnetism and geoelectricity*, 32(Supplement 3), SIII1-SIII10.

EMBLETON, B.J.J., MCELHINNY, M.W., ZHANG, Z. & LI, Z.X. 1996. Permo-Triassic magnetostratigraphy in China: the type section near Taiyuan, Shanxi Province, North China .*Geophys. J. Int.* **126**, 382–388.

FETISOVA, A. M., VESELOVSKII, R. V., LATYSHEV, A. V., RAD'KO, V. A. & PAVLOV, V. E. 2014. Magnetic stratigraphy of the Permian-Triassic traps in the Kotui River valley (Siberian Platform): New paleomagnetic data. *Stratigraphy and Geological Correlation*, **22,** 377-390.

FOSTER, C.B. & ARCHIBOLD, N.W. 2001. Chronologic anchor points for the Permian Early Triassic of the eastern Australian basins. *In*: Weiss, R.H. (ed) *Contributions to the geology and palaeontology of Gondwana in honour of Helmut Wopfner,* University of Cologne Geological Institute, 175-197.

GALLET, Y., KRYSTYN, L., BESSE, J., SAIDI, A. & RICOU, L-E. 2000. New constraints on the upper Permian and Lower Triassic geomagnetic polarity timescale from the Abadeh section (central Iran). *Journal of Geophysical Research*, **105**, 2805-2815.

GASTALDO, R. A., KAMO, S. L., NEVELING, J., GEISSMAN, J. W., BAMFORD, M. & LOOY, C. V. 2015. Is the vertebrate-defined Permian-Triassic boundary in the Karoo Basin, South Africa, the terrestrial expression of the end-Permian marine event? *Geology*, **43**, 939-942.

GEISSMAN, J. W. & HARLAN, S. S. 2002. Late Paleozoic remagnetization of Precambrian crystalline rocks along the Precambrian/Carboniferous nonconformity, Rocky Mountains: a relationship among deformation, remagnetization, and fluid migration. *Earth and Planetary Science Letters*, **203**, 905-924.

GEUNA, S. E. & ESCOSTEGUY, L. D. 2004. Palaeomagnetism of the Upper Carboniferous—Lower Permian transition from Paganzo basin, Argentina. *Geophysical Journal International*, **157**, 1071-1089.

GIALANELLA, P. R., HELLER, F., HAAG, M., NURGALIEV, D., BORISOV, A., BUROV, B., JASONOV, P., KHASANOV, D., IBRAGIMOV, S. & ZHARKOV, I. 1997. Late Permian magnetostratigraphy on the eastern Russian platform. *Geologie en Mijnbouw* **76,** 145–154.

GILES, J.M. SOREGHAN, M. J., BENISON, K. C., SOREGHAN, G. S., & HASIOTIS, S. T. 2013. Lakes, loess, and paleosols in the Permian Wellington Formation of Oklahoma, U.S.A.: implications for paleoclimate and paleogeography of the Midcontinent. *Journal of Sedimentary Research*, **83**, 825–846.

GLEN, J.M., NOMADE, S., LYONS, J.L, METCALFE, I., MUNDIL, R. & RENNE, P.R. 2009. Magnetostratigraphic correlations of Permian-Triassic marine and terrestrial sediments from western China. *Journal of Asian Earth Sciences* **36**, 521–540.

Golubev, V. K. 2015. Dinocephalian stage in the history of the Permian tetrapod fauna of eastern Europe. *Paleontological Journal*, **49**, 1346–1352.

GOMEZ-ESPINOSA, C., VACHARD, D., BUITRÓN-SÁNCHEZ, B., ALMAZÁN-VAZQUEZ, E. & MENDOZA-MADERA, C. 2008. Pennsylvanian fusulinids and calcareous algae from Sonora (Northwestern Mexico), and their biostratigraphic and palaeobiogeographic implications. *Comptes Rendus Palevol*, **7**, 259-268.

GOSE, W. A. & HELSLEY, C. E. 1972. Paleomagnetic and rock-magnetic studies of the Permian Cutler and Elephant Canyon Formations in Utah. *Journal of Geophysical Research*, **77**, 1534-1548.

GRAHAM, J. W. 1955. Evidence of polar shift since Triassic time. *Journal of Geophysical Research*, **60**, 329-348.

GULBRANSON, E. L., MONTAÑEZ, I. P., SCHMITZ, M. D., LIMARINO, C. O., ISBELL, J. L., MARENSSI, S. A. & CROWLEY, J. L. 2010. High-precision U-Pb calibration of Carboniferous glaciation and climate history, Paganzo Group, NW Argentina. *Geological Society of America Bulletin*, **122**, 1480-1498.

GUREVITCH, E.L., HEUNEMANN, C. RAD'KO, V., WESTPHAL,M., BACHTADSE, V., POZZI, J.P. & FEINBERG, H. 2004. Palaeomagnetism and magnetostratigraphy of the Permian–Triassic northwest central Siberian Trap Basalts. *Tectonophysics*, **379**, 211 –226.

HAAG, M. & HELLER, F. 1991. Late Permian to Early Triassic magnetostratigraphy. *Earth Planet. Sci. Lett*. **107**, 42–54.

HALVORSEN, E., LEWANDOWSKI, M. & JELEŃSKA, M. 1989. Palaeomagnetism of the Upper Carboniferous Strzegom and Karkonosze Granites and the Kudowa Granitoid from the Sudet Mountains, Poland. *Physics of the Earth and Planetary Interiors*, **55**, 54-64.

HASLETT, J. & PARNELL, A., 2008. A simple monotone process with application to radiocarbon-dated depth chronologies. *Royal Statistical Society Journal, series C*, **57**, 399–418.

HE, B., XU, Y-G, HUANG, X-L, LUO, Z-Y, SHI, Y-R, YANG, Q-J. & YU, S-Y. 2007. Age and duration of the Emeishan flood volcanism, SW China: Geochemistry and SHRIMP zircon U–Pb dating of silicic ignimbrites, post-volcanic Xuanwei Formation and clay tuff at the Chaotian section. *Earth and Planetary Science Letters* **255,** 306–323.

HELLER, F., CHEN, H., DOBSON, J. & HAAG, M. 1995. Permian-Triassic magnetostratigraphy – new results from South China. *Earth and Planetary Science Letters* **89**, 281-295.

HELLER, F., LOWRIE, W., HUANMEI, L. & JUNDA, W. 1988. Magnetostratigraphy of the Permo-Triassic boundary section at Shangsi (Guangyuan, Sichuan Province, China). *Earth and Planetary Science Letters* **88**, 348-356.

HELSLEY, C. E. 1965. Paleomagnetic results from the lower Permian Dunkard series of West Virginia. *Journal of Geophysical Research,* **70**, 413-424.

HENDERSON, C. M. & MEI, S. 2000. Preliminary cool water Permian conodont zonation in North Pangea: a review. *Permophiles*, **36**, 16-23.

HENDERSON, C.M., DAVYDOV, V.I. & WARDLAW, B.R. 2012. The Permian Period. *In:* GRADSTEIN, F. M., OGG, J. G., SCHMITZ, M. & OGG, G. (eds) The Geologic Time Scale, Vol II. Elsevier, 653-679.

HOUNSLOW, M.W. 2016. Geomagnetic reversal rates following Palaeozoic superchrons have a fast re-start mechanism. *Nature Communications*. DOI: 10.1038/ncomms12507.

HOUNSLOW, M. W. & NAWROCKI, J. 2008. Palaeomagnetism and magnetostratigraphy of the Permian and Triassic of Spitsbergen: a review of progress and challenges. *Polar Research*, **27**, 502-522.

HOUNSLOW, M.W. & MUTTONI, G. 2010. The geomagnetic polarity timescale for the Triassic: linkage to stage boundary definitions. *In*: LUCAS. S.G. (ed). *The Triassic Timescale*, Special Publication of the Geological Society, **334**, 61-102, London.

HOUNSLOW, M. W., PETERS, C., MØRK, A., WEITSCHAT, W. & VIGRAN, J. O. 2008. Biomagnetostratigraphy of the Vikinghøgda Formation, Svalbard (Arctic Norway), and the geomagnetic polarity timescale for the Lower Triassic. *Geological Society of America Bulletin*, **120**, 1305-1325.

HOUNSLOW M.W, MCINTOSH, G., EDWARDS, R. A., LAMING, D. J. C. & KARLOUKOVSKI, V. 2016. End of the Kiaman Superchron in the Permian of SW England: Magnetostratigraphy of the Aylesbeare Mudstone and Exeter groups. *Journal of the Geological Society*. doi:10.1144/jgs2015-141.

HOYT, J. H. & CHRONIC, B. J. 1961. Wolfcampian fusulinids from the Ingleside Formation, Owl Canyon, Colorado. *Journal of Paleontology*, **35**, 1089.

IDNURUM, M., KLOOTWIJK, C., THÉVENIAUT, H. & TRENCH, A. 1996. Magnetostratigraphy. *In*: Young, G.C & Laurie, J.R. (eds) *The Australian Phanaerozoic timescale,* Oxford University Press, 23-51.

IOSIFIDI, A. G. & KHRAMOV, A. N. 2009. Magnetostratigraphy of Upper Permian Sediments in the Southwestern Slope of Pai-Khoi (Khei-Yaga River Section): Evidence for the Global Permian–Triassic Crisis. *Izvestiya, Physics of the Solid Earth*, **45**, 3–13.

IOSIFIDI, A. G., MAC NIOCAILL, C., KHRAMOV, A. N., DEKKERS, M. J. & POPOV, V. V. 2010. Palaeogeographic implications of differential inclination shallowing in permo-carboniferous sediments from the donets basin, Ukraine. *Tectonophysics*, **490**, 229-240.

IRVING, E. 1971. Nomenclature in magnetic stratigraphy. *Geophysical Journal of the Royal Astronomical Society*, **24**, 529-531.

IRVING, E. & MONGER, J. W. H. 1987. Preliminary paleomagnetic results from the Permian Asitka Group, British Columbia. *Canadian Journal of Earth Sciences*, **24**, 1490-1497.

IRVING, E. & PARRY, L. G. 1963. The magnetism of some Permian rocks from New South Wales. *Geophysical Journal International*, **7**, 395-411.

IRVING, E. & PULLAIAH, G. 1976. Reversals of the geomagnetic field, magnetostratigraphy, and relative magnitude of paleosecular variation in the Phanerozoic. *Earth-Science Reviews*, **12**, 35-64.

JACOBS, J. A. 1963. *The earth's core and geomagnetism* (Vol. 1). Pergamon, New York.

JIN, Y.G., SHANG, Q.H. & CAO C.Q. 2000. Late Permian magnetostratigraphy and its global correlation. *Chinese Science Bulletin* **45**, 698-704.

JIN, Y.G., WANG, Y., HENDERSON, C., WARDLAW, B.R., SHEN, S. & CAO, C. 2006a. The global boundary stratotype section and point (GSSP) for the base of the Changhsingian Stage (Upper Permian). *Episodes* **29**, 175-182.

JIN, Y.G., SHEN, S., HENDERSON, C. M., WANG, X., WANG, W., WANG, Y., CAO, C. & SHANG, Q. 2006b. The Global Stratotype Section and Point (GSSP) for the boundary between the Capitanian and Wuchiapingian stage (Permian). *Episodes*, 29, 253.

JIRAH, S. & RUBIDGE, B. 2014. Refined stratigraphy of the Middle Permian Abrahamskraal Formation(Beaufort Group) in the southern Karoo Basin, *J. Afr. Earth Sci.,* **100**, 121–135.

JOHNSON, S.Y., SCHENK, C.J., ANDERS, D.L. & TUTTLE, M.L. 1990. Sedimentology and petroleum occurrence, Schoolhouse Member, Maroon Formation (Lower Permian): Northwestern Colorado. *American Association of Petroleum Geologists Bulletin*, **74**, 135–150.

KAMO, S. L., CZAMANSKE, G. K., AMELIN, Y., FEDORENKO, V. A., DAVIS, D. W. & TROFIMOV, V. R. 2003. Rapid eruption of Siberian flood-volcanic rocks and evidence for coincidence with the Permian–Triassic boundary and mass extinction at 251 Ma. *Earth and Planetary Science Letters*, **214**, 75-91.

KASUYA, A., ISOZAKI, Y. & IGO, H. 2012. Constraining paleo-latitude of a biogeographic boundary in mid-Panthalassa: Fusuline province shift on the Late Guadalupian (Permian) migrating seamount. *Gondwana Research*, **21**, 611-623.

KENT, D. V. & OLSEN, P. E. 1999. Astronomically tuned geomagnetic polarity timescale for the Late Triassic. *Journal of Geophysical Research: Solid Earth*, **104**, 12831-12841.

KHRAMOV, A. N. 1958. Paleomagnetic correlation of sedimentary rocks. Leningrad, Gostoptehizdat, Leningrad, 218pp [in Russian].

KHRAMOV, A. N. 1963a. Palaeomagnetic investigations of Upper Permian and Lower Triassic sections on the northern and eastern Russian Platform. *In:* KHRAMOV, A.N. (ed). *Palaeomagnetism of the Palaeozoic*. Transactions of the VNIGRI, **204**, 145-174 [in Russian].

KHRAMOV, A. N. 1963b. Palaeomagnetic investigations of the Upper Palaeozoic and the Triassic of the western part of the Donbass Basin. *In:* KHRAMOV, A.N. (ed). *Palaeomagnetism of the Palaeozoic*. Transactions of the VNIGRI, **204**, 97-117. [in Russian]

KHRAMOV, A. N. 1967. Magnetic field of the earth in the Late Palaeozoic. *Fiz. Zemli,* **1**, 86-108 [in Russian].

KHRAMOV, A. N. & DAVYDOV, V. I. 1984. Paleomagnetism of Upper Carboniferous and Lower Permian in the south of USSR and the problems of structure of the Kiama Hyperzone: *Transactions of VNIGRI*, St Petersburg, 55-73. [in Russian]

KHRAMOV, A. N. & DAVYDOV, V. I. 1993. Results of palaeomagnetic investigations. Permian system: guides to geological excursions in the Uralian type localities. *Occasional Publication ESRI, New Series*, **10**, 34-42.

KHRAMOV, A.N., KOMISSAROVA, R.A., IOSIFIDI, A.G. POPOV, V.V. & BAZHENOV, M.L. 2006. Upper Tatarian magnetostratigraphy of the Sukhona River sequence: a re-study. *In*: TROYAN, V.N., SEMENOV, V.S. & KUBYSHKINA, M.V. (eds) *Problems of Geocosmos* 6th International Conference St. Petersburg State University, St. Petersburg, 317–321.

KIRSCHVINK, J. L., ISOZAKI, Y., SHIBUYA, H., OTOFUJI, Y. I., RAUB, T. D., HILBURN, I. A. TERUHISA KASUYA, T., YOKOYAMA, M. & BONIFACI, M. 2015. Challenging the sensitivity limits of Paleomagnetism: Magnetostratigraphy of weakly magnetized Guadalupian–Lopingian (Permian) Limestone from Kyushu, Japan. *Palaeogeography, Palaeoclimatology, Palaeoecology,* **418**, 75-89.

KIRSCHVINK, J.L., KOPP, R.E., RAUB, T.D., BAUMGARTNER, C.T. & HOLT, J.W. 2008. Rapid, precise, and high-sensitivity acquisition of paleomagnetic and rock-magnetic data: development of a low-noise automatic sample changing system for superconducting rock magnetometers. *Geochem. Geophys. Geosyst.* **9,** 1–18.

KLOOTWIJK, C. T., SHAH, S. K., GERGAN, J., SHARMA, M. L., TIRKEY, B. & GUPTA, B. K. 1983. A palaeomagnetic reconnaissance of Kashmir, northwestern Himalaya, India. *Earth and Planetary Science Letters*, **63**, 305-324.

KLOOTWIJK, C.T., IDNURM, M., THEVENIAUT H. & TRENCH, A. 1994. Phanerozoic magnetostratigraphy: a contribution to the timescales project. Australian Geological Survey Organisation, Record 1994/45.

KORTE, C., JASPER, T., KOZUR, H. W. & VEIZER, J. 2005. $\delta^{18}O$ and $\delta^{13}C$ of Permian brachiopods: a record of seawater evolution and continental glaciation. *Palaeogeography, Palaeoclimatology, Palaeoecology*, **224**, 333-351.

KOTLYAR, G. V. 2015. Permian sections of southern Primorye: A link in correlation of stage units in the standard and general stratigraphic scales. *Russian Journal of Pacific Geology,* **9**, 254-273.

KOTLYAR, G.V & PRONINA-NESTELL, G.P. 2005. Report of the committee on the Permian system of Russian. *Permophiles* **46**, 9-13.

KOZUR, H. W. 2007. Biostratigraphy and event stratigraphy in Iran around the Permian–Triassic Boundary (PTB): implications for the causes of the PTB biotic crisis. *Global and Planetary change*, **55**, 155-176.

KRAINER, K., VACHARD, D. & LUCAS, S. 2003. Microfacies and microfossil assemblages (smaller foraminifers, algae, pseudoalgae) of the Hueco Group and Laborcita Formation (upper Pennsylvanian-lower Permian) south-central New Mexico, USA. *Rivista Italiana di Paleontologia e Stratigrafia*, **109**, 3-36.

KRASSILOV, V. & KARASEV, E. 2009. Paleofloristic evidence of climate change near and beyond the Permian–Triassic boundary. *Palaeogeography, Palaeoclimatology, Paleoecology*, **284**, 326–336.

KRUIVER, P. P., LANGEREIS, C. G., DEKKERS, M. J. & KRIJGSMAN, W. 2003. Rock-magnetic properties of multicomponent natural remanent magnetization in alluvial red beds (NE Spain). *Geophysical Journal International*, **153**, 317-332.

KRYZA, R., PIN, C., OBERC-DZIEDZIC, T., CROWLEY, Q. G. & LARIONOV, A. 2014. Deciphering the geochronology of a large granitoid pluton (Karkonosze Granite, SW Poland): an assessment of U–Pb zircon SIMS and Rb–Sr whole-rock dates relative to U–Pb zircon CA-ID-TIMS. *International Geology Review,* **56**, 756-782.

LAI, X., YANG, F., HALLAM, A. & WIGNALL, P.B. 1996. The Shangsi section candidate of the Global Stratotype section and point of the Permian-Triassic boundary. *In*: Yin, H.F. (ed) *The Paleozoic - Mesozoic Boundary*, China University of Geosciences Press, 113-124.

LAMBERT, L.L. WARDLAW, B.R. & HENDERSON, C.H. 2007. *Mesogondolella* and *Jinogondolella* (Conodonta): Multielement definition of the taxa that bracket the basal Guadalupian (Middle Permian Series) GSSP. *Palaeoworld* **16**, 208-221.

LANCI, L., TOHVER, E., WILSON, A. & FLINT, S. 2013. Upper Permian magnetic stratigraphy of the lower Beaufort group, Karoo basin. *Earth and Planetary Science Letters*, **375**, 123-134.

LANGEREIS, C. G., KRIJGSMAN, W., MUTTONI, G. & MENNING, M. 2010. Magnetostratigraphy–concepts, definitions, and applications. *Newsletters on Stratigraphy*, **43,** 207-233.

LAWTON, D.E. & ROBERTSON, P.P. 2003. The Johnston Gas Field, Blocks 43/26a, 43/27a, UK Southern North Sea. *In:* GLUYAS, J. & HICHENS, H.M. (eds), *United Kingdom Oil and Gas Fields, Commemorative Millennium Volume.* Geological Society Memoir, (London) **20**, 749-759.

LEGLER, B., GEBHARDT, U. & SCHNEIDER, J.W. 2005. Late Permian non marine to marine transitional profiles in central southern Permian Basin, northern Germany. *Int. Journal of Earth Sciences*, **94**, 851-862.

LE PAGE, B. A., BEAUCHAMP, B., PFEFFERKORN, H. W. & UTTING, J. 2003. Late Early Permian plant fossils from the Canadian High Arctic: a rare paleoenvironmental/climatic window in northwest Pangea. *Palaeogeography, Palaeoclimatology, Palaeoecology*, **191**, 345-372.

LI, H. & WANG, J. 1989. Magnetostratigraphy of the Permo-Triassic boundary section of Meishan of Changxing, Zhejang. *Science in China* **8**, 652-658.

LI, M., OGG, J. G. ZHANG, Y., HUANG, C., HINNOV, L., CHEN, Z-Q. & ZOU, Z. 2016. Astronomical tuning of the end –Permian extinction and the Early Triassic Epoch of South China and Germany. *Earth Planet. Sci. Lett*ers, **441**, 10-25.

LI, Z., CHEN, H., SONG, B., LI, Y., YANG, S. & YU, X. 2011. Temporal evolution of the Permian large igneous province in Tarim Basin in northwestern China. *Journal Asian Earth Sciences*, **42**, 917-927

LIU, C., PAN, Y. & ZHU, R. 2012. New paleomagnetic investigations of the Emeishan basalts in NE Yunnan, southwestern China: Constraints on eruption history. *Journal of Asian Earth Sciences,* **52**, 88-97.

LIU, Y.Y., ZHU, Y.M. & TIAN, W.H. 1999. New magnetostratigraphic results from the Meishan section, Changxing County, Zheijiang, China. *Earth Science Journal of China University of Geosciences* **24**, 151-154.

LOWRIE, W. & KENT, D.V. 2004. Geomagnetic polarity timescales and reversal frequency regimes. *In:* Channell, J.E.T., Kent, D.V., Lowrie, W. & Meert, J. (eds). *Timescales of the palaeomagnetic field,* pp. 117-129, America Geophysical Union.

LOZOVSKY, V. R. 1998. Chapter 7: The Permian- Triassic boundary. *In:* ESAULOVA, N.K., LOZOVSKY, V.R. & ROZANOV, A.Y. (eds). *Stratotypes and reference sections of the Upper Permian in the region of the Volga and Kama Rivers,* GEOS, 271-281.

LOZOVSKY V.R., KRASSILOV, V.A., AFONIN, S.A., BUROV, B.V. & YAROSHENKO, O.P. 2001. Transitional Permian-Triassic deposits in European Russia, and non-marine correlations. Natura Bresciana, Ann Mus. Civ. Sc. Nat., Brescia, **25**, 301-310.

LOZOVSKY, V. R. MINIKH, M. G. GRUNT, T. A. & KUKHTINOV, D. A. PONOMARENKO A. G. & SUKACHEVA, I. D. 2009. The Ufimian Stage of the East European Scale: Status, Validity, and Correlation Potential. *Stratigraphy and Geological Correlation* **17**, 602–614.

LOZOVSKY V.R. BALABANOV, YU. P. PONOMARENKO, A,G., NOVOKOV, I.V., BUSLOVICH, A.L. MORKOVIN, B.I. & YAROSHENKO, O.P. 2014. Stratigraphy, palaeomagnetism and petromagnetism of the Lower Triassic in the Moscow Syneclise. 1, Yug River Basin. *Bulletin of the Moscow Society of Naturalists. Geological series*, **89**, 61-72. [in Russian]

LUCAS, S. G. 2006. Global Permian tetrapod biostratigraphy and biochronology. *In:* LUCAS, S. G., CASSINIS, G. & SCHNEIDER, J. W. (eds). *Non-Marine Permian Biostratigraphy and Biochronology*. Geological Society, London, Special Publications, **265**, 65-93.

LUCAS, S. G. 2013. Vertebrate biostratigraphy and biochronology of the upper Paleozoic Dunkard Group, Pennsylvania–West Virginia–Ohio, USA. *International Journal of Coal Geology*, **119**, 79-87.

MACINTYRE, D. G., VILLENEUVE, M. E. & SCHIARIZZA, P. 2001. Timing and tectonic setting of Stikine Terrane magmatism, Babine-Takla lakes area, central British Columbia. *Canadian Journal of Earth Sciences,* **38**, 579-601.

MCMAHON, B. E. & STRANGWAY, D. W. 1968. Investigation of Kiaman Magnetic Divison in Colorado Redbeds. *Geophysical Journal International*, **15**, 265-285.

MAGNUS, G. & OPDYKE, N. D. 1991. A paleomagnetic investigation of the Minturn Formation, Colorado: a study in establishing the timing of remanence acquisition. *Tectonophysics*, **187**, 181-189.

MATUYAMA, M. 1929. On the direction of magnetisation of basalt in Japan, Tyosen and Manchuria. *Proceedings of the Imperial Academy*, **5**, 203-205.

MAY, W., HUTTENLOCKER, A. K., PARDO, J. D., BENCA, J. & SMALL, B. J. 2011. New Upper Pennsylvanian armored dissorophid records (Temnospondyli, Dissorophoidea) from the US midcontinent and the stratigraphic distributions of dissorophids. *Journal of Vertebrate Paleontology*, **31**, 907-912.

MCELHINNY, M. W. & BUREK, P. J. 1971. Mesozoic palaeomagnetic stratigraphy. *Nature*, **232**, 98 – 102.

MEI, S. & HENDERSON, C. M. 2002. Comments on some Permian conodont faunas reported from SE Asia and adjacent areas and their global correlation. *Journal of Asian Earth Sciences* **20**, 599-608.

MEI, S., HENDERSON, C. M. & WARDLAW, B. R., 2002. Evolution and distribution of the conodonts Sweetognathus and Iranognathus and related genera during the Permian, and their implications for climate change. *Palaeogeography, Palaeoclimatology, Palaeoecology,* **180**, 57–91.

MENG, X., HU, C., WANG, W. & LIU, H. 2000. Magnetostratigraphic Study of Meishan Permian-Triassic Section, Changxing, Zhejiang Province, China. *Journal of China University of Geosciences* **11**, 361-365.

MENNING, M. 1987. Magnetostratigraphy. *In:* LÜTZNER, H. (ed) *Sedimentary and Volcanic Rotliegend of the Saale Depression: Excursion Guidebook*. Symposimum on Rotliegend in Central Europe. Centr. Inst. Phys. Earth, Potsdam, 92-96.

MENNING, M. & JIN, Y. 1998. Comment on 'Permo-Triassic magnetostratigraphy in China: the type section near Taiyuan, Shanxi Province, North China' by B.J.J. Embleton, M.W. McElhinny, X. Ma, Z. Zhang & Z.X. Li. *Geophysical Journal International*, **133**, 213–216.

MENNING, M., KATZUNG, G. & LUTZNER, H. 1988. Magnetostratigraphic investigations in the Rotliegend (300-252 Ma) of central-Europe. *Zeitschrift fur geologische Wissenschaften*, **16**, 1045-1063.

MERCANTON, P.L. 1926. Inversion de l'inclinaison magnètique terrestre aux ages geologiques *Terrestrial Magnetism and Atmos. Elec*., **31**, 187.

MERTMANN, D. 2003. Evolution of the marine Permian carbonate platform in the Salt Range (Pakistan). *Palaeogeography, Palaeoclimatology, Palaeoecology* **191**, 373-384.

METCALFE, I., NICOLL, R.S. & WARDLAW, B.R. 2007. Conodont index fossil Hindeodus changxingensis Wang fingers greatest mass extinction event. *Palaeoworld* **16**, 202–207.

METCALFE, I., CROWLEY, J.L., NICOLL, R.S. & SCHMITZ, M. 2014. High-precision U-Pb CA-TIMS calibration of Middle Permian to Lower Triassic sequences, mass extinction and extreme climate-change in eastern Australian Gondwana. *Gondwana Research,* **28**, 61-81.

MILLER, J. D. & OPDYKE, N. D. 1985. Magnetostratigraphy of the Red Sandstone Creek section-Vail, Colorado. *Geophysical Research Letters*, **12**, 133-136.

MODIE, B. N. & LE HÉRISSÉ, A. 2009. Late Palaeozoic palynomorph assemblages from the Karoo Supergroup and their potential for biostratigraphic correlation, Kalahari Karoo Basin, Botswana. *Bulletin of Geosciences*, **84**, 337-358.

MOLOSTOVSKY, E. A., PEVZNER, M. A. & PECHERSKY, D. M. 1976. Phanerozoic magnetostratigraphic scale and regime of magnetic field reversals. In: Geomagnetic Investigations (Radiosvyaz', Moscow), 45–52 [in Russian].

MOLOSTOVSKY, E.A. 1996. Some aspects of magnetostratigraphic correlation. *Stratigraphy and Geological Correlation* **4**, 231-237.

MOLOSTOVSKY, E.A. 2005. Magnetostratigrphic correlation of Upper Permian Marine and Continental Formations. *Stratigraphy and Geological Correlation*, **13**, 49-58.

MOLOSTOVSKY, E.A., MOLOSTOVSKAYA, I.I. & MINIKH, M.G. 1998. Stratigraphic correlations of the Upper Permian and Triassic beds from the Volga-Ural and Cis-Caspian. *In:* CRASQUIN-SOLEAU S. & BARRIER, É. (eds), *Peri-Tethys memoir 3: Stratigraphy and Evolution of Peri-Tethyan platforms.* Mémoires du Muséum National d'histoire Naturelle, **177**, 35-44, Editions du Muséum.

MOURAVIEV, F.A. AREFIEV, M.P. SILANTIEV, V.V. BALABANOV, YU.P. BULANOV, V.V. GOLUBEV, V.K. MINIKH, A.V. MINIKH, M.G. KHAZIEV, R.R. FAKHRUTDINOV, E.I. MOZZHERIN. V.V. 2015. Monastery Ravine section: stratotype of the Urzhumian and limitotype of the Severodvinian Stage. *In:* Nurgaliev, D.K. Silantiev, V.V. Nikolaev S.V. a (eds). *Type and reference sections of the Middle and Upper Permian of the Volga and Kama River Regions.* A Field Guidebook of XVIII International Congress on Carboniferous and Permian. Kazan, Kazan University Press, 120-141.

MORRIS, N.J. 2013. *Stratigraphy and geochemistry of Lower Permian volcanics in the Sverdrup Basin, Northwest Ellesmere Island, Nunavut.* Unpubl. Msc. University of Calgary, Canada.

MUNDIL, R., LUDWIG, K.R., METCALFE, I. & RENNE, P.R. 2004. Age and timing of the Permian mass extinctions: U/Pb dating of closed-system zircons. *Science* **305**, 1760-1763.

MUNDIL, R., PALFY, J. RENNE, P.R. & BRACK, P. 2010. The Triassic timescale: new constraints and a review of geochronological data. *In:* LUCAS, S.G. (ed) *The Triassic Timescale,* Special Publication of the Geological Society, **334**, 41-60.

MURPHY, M. A. & SALVADOR, A. 1999. Special-International Stratigraphic Guide--An abridged version. *Episodes*, ***22***, 255-271.

NAKREM, H. A. 1994. Bryozoans from the Lower Permian Vøringen Member (Kapp Starostin Formation), Spitsbergen, Svalbard. *Norsk Polarinstitutt Skrifter,* **196**, 5-93.

NAKREM, H.A., RASMUSSEN, J.A. & SWIFT, A. 1991. Late Carboniferous to earliest Triassic conodonts of Svalbard. *Geonytt*, **1**, 38–39.

NAKREM, H. A., NILSSON, I. & MANGERUD, G. 1992. Permian biostratigraphy of Svalbard (Arctic Norway)- a review. *International Geology Review,* **34**, 933-959.

NAWROCKI, J. 1997. Permian to early Triassic magnetostratigraphy from the Central European Basin in Poland: Implications on regional and worldwide correlations. *Earth and Planetary Science Letters* **152**, 37-58.

NAWROCKI, J. 1999. Paleomagnetism of Permian through Early Triassic sequences in central Spitsbergen: implications for paleogeography. *Earth and Planetary Science Letters,* **169,** 59–70.

NAWROCKI, J. & GRABOWSKI, J. 2000. Palaeomagnetism of Permian through Early Triassic sequences in central Spitsbergen: contribution to magnetostratigraphy. *Geological Quarterly*, **44**, 109-118.

NEWELL, A.J. SENNIKOV, A.G., BENTON, M.J. MOLOSTOVSKAYA, I.A., GOLUBEV, V.K. MINIKH, A.V. & MINIKH, M.G. 2010. Disruption of playa–lacustrine depositional systems at the Permo-Triassic boundary: evidence from Vyazniki and Gorokhovets on the Russian Platform. *Journal of the Geological Society, London,* **167**, 695–716.

NICKLEN, B. L. 2011. *Establishing a Tephrochronologic Framework for the Middle Permian (Guadalupian) Type Area and Adjacent Portions of the Delaware Basin and Northwestern Shelf, West Texas and Southeastern New Mexico, USA*. Unpubl. PhD thesis, University of Cincinnati.

NILSSON, I. & DAVYDOV, V. I. 1997. Fusulinid biostratigraphy in Upper Carboniferous (Gzhelian) and Lower Permian (Asselian-Sakmarian) successions of Spitsbergen. Arctic Norway. *Permophiles*, **30**, 18-24.

OGG, J. G. 2012. Magnetostratigraphy. *In:* GRADSTEIN, F. M., OGG, J. G., SCHMITZ, M. D. & OGG, G.M. (eds). *The Geologic Time Scale 2012*, Elsevier, 85-114.

OGG, J.G., OGG, G. & GRADSTEIN F.M. 2008. *The concise geologic time scale*. Cambridge Univ. Press.

OLSZEWSKI, T. D. & ERWIN, D. H. 2009. Change and stability in Permian brachiopod communities from western Texas. *Palaios*, **24**, 27-40.

OPDYKE, N. D. 1995. Permo-Carboniferous magnetostratigraphy. *In*: BERGGREN, W. A., KENT, D. V., AUBRY, M. P. & HARDENBOL, J. (eds). *Geochronology, time scales and global stratigraphic correlation*. SEPM special publication **54**, 41-50.

OPDYKE, M. D. & CHANNELL, J. E. 1996. *Magnetic stratigraphy*. Academic Press, New York.

PAŠAVA, J., OSZCZEPALSKI, S. & DU, A. 2010. Re–Os age of non-mineralized black shale from the Kupferschiefer, Poland, and implications for metal enrichment. *Mineralium Deposita*, **45**, 189-199.

PARNELL, A.C., HASLETT, J., ALLEN, J.R.M., BUCK, C.E. & HUNTLEY, B. 2008. A flexible approach to assessing synchroneity of past events using Bayesian reconstructions of sedimentation history. *Quaternary Science Reviews*, **27**, 1872–1885.

PETERSON, D. N. & NAIRN, A. E. M. 1971. Palaeomagnetism of Permian redbeds from the south-western United States. *Geophysical Journal International*, **23**, 191-205.

PRUNER, P. 1992. Palaeomagnetism and palaeogeography of Mongolia from the Carboniferous to the Cretaceous-final report. *Physics of the Earth and Planetary Interiors*, **70**, 169-177.

RAKOTOSOLOFU, N.A., TORSVIK, T.H., ASHWAL, L.D., EIDE, E.A. & DE WIT, M.J. 1999. The Karoo Supergroup revisited and Madagascar-Africa fits. *Journal of African Earth Sciences,* **29**, 135-151.

RAMEZANI, J., SCHMITZ, M. D., DAVYDOV, V. I., BOWRING, S. A., SNYDER, W. S. & NORTHRUP, C. J. 2007. High-precision U–Pb zircon age constraints on the Carboniferous–Permian boundary in the southern Urals stratotype. *Earth and Planetary Science Letters*, **256**, 244-257.

RASNITSYN, A. P., SUKACHEVA, I. D. & ARISTOV, D. S. 2005. Permian insects of the Vorkuta Group in the Pechora Basin, and their stratigraphic implications. *Paleontological Journal*, **39**, 404–416. [Translated from Paleontologicheskii Zhurnal, No. 4, 2005, pp. 63–75.]

RETALLACK, G. J., SHELDON, N. D., CARR, P. F., FANNING, M., THOMPSON, C. A., WILLIAMS, M. L., JONES, B.G. & HUTTON, A. 2011. Multiple Early Triassic greenhouse crises impeded recovery from Late Permian mass extinction. *Palaeogeography, Palaeoclimatology, Palaeoecology*, **308**, 233-251.

ROCHA-CAMPOS, A. C., BASEI, M. A., NUTMAN, A. P., KLEIMAN, L. E., VARELA, R., LLAMBIAS, E., CANILEA, F.M. & DA ROSA, O. D. C. 2011. 30 million years of Permian volcanism recorded in the Choiyoi igneous province (W Argentina) and their source for younger ash fall deposits in the Paraná Basin: SHRIMP U–Pb zircon geochronology evidence. *Gondwana Research*, **19**, 509-523

ROSS, C. A. & MONGER, J. W. H. 1978. Carboniferous and Permian fusulinaceans from the Omineca Mountains, British Columbia. Contributions to Canadian Paleontology. *Geological Survey of Canada, Bulletin*, **267**, 43-63.

RUBIDGE, B. S., ERWIN, D. H., RAMEZANI, J., BOWRING, S. A. & DE KLERK, W. J. 2013. High-precision temporal calibration of Late Permian vertebrate biostratigraphy: U-Pb zircon constraints from the Karoo Supergroup, South Africa. *Geology*, **41**, 363-366.

RUSH, J. & KERANS, C. 2010. Stratigraphic response across a structurally dynamic shelf: the latest Guadalupian composite sequence at Walnut Canyon, New Mexico, USA . *Journal of Sedimentary Research* **80**, 808–828.

SADLER, P. M. & STRAUSS, D. J. 1990. Estimation of completeness of stratigraphical sections using empirical data and theoretical models. *Journal of the Geological Society*, *London* **147**, 471-485.

SAWIN, R. S., FRANSEEN, E. K., WEST, R. R., LUDVIGSON, G. A. & WATNEY, W. L. 2008. Clarification and changes in Permian stratigraphic nomenclature in Kansas (pp. 1-4). *Current Research in Earth Sciences, Bulletin* **254 (2)**, (http://www.kgs.ku.edu/Current/2008/Sawin/index.html), Kansas Geological Survey).

SCHMIDBERGER, S. S. & HEGNER, E. 1999. Geochemistry and isotope systematics of calc-alkaline volcanic rocks from the Saar-Nahe basin (SW Germany)–implications for Late-Variscan orogenic development. *Contributions to Mineralogy and Petrology*, **135**, 373-385.

SCHMITZ, M. D. & DAVYDOV, V. I. 2012. Quantitative radiometric and biostratigraphic calibration of the Pennsylvanian–Early Permian (Cisuralian) time scale and pan-Euramerican chronostratigraphic correlation. *Geological Society of America Bulletin*, **124**, 549-577.

SCHMITZ, M. D. 2012. Radiogenic isotope geochronology. *In:* GRADSTEIN, F. M., OGG, J. G., SCHMITZ, M. D. & OGG, G.M. (eds). *The Geologic Time Scale 2012*, 115-126, Elsevier.

SCHNEIDER, J. W., LUCAS, S. G. & BARRICK, J. E. 2013. The Early Permian age of the Dunkard Group, Appalachian basin, USA, based on spiloblattinid insect biostratigraphy. *International Journal of Coal Geology*, **119**, 88-92.

SCOTT, K.M. 2013. Carboniferous-Permian boundary in the Halgaito Formation, Cutler Group, Valley of the Gods and surrounding area, southeastern Utah. *In:* LUCAS, S.G.,. DIMICHELE, W.A., BARRICK, J.E., SCHNEIDER, J.W. & SPIELMANN, J.A. (eds), *The Carboniferous-Permian Transition*. New Mexico Museum of Natural History and Science, Bulletin, **60**, 398-409.

SENNIKOV, A.G. & GOLUBEV, V.K. 2006. Vyazniki Biotic Assemblage of the terminal Permian. *Paleontological Journal*, **40**, S475–S481.

SHARPS, R., MCWILLIAMS, M., LI, Y., COX, A., ZHANG, Z., ZHAI, Y., GAO, Z., LI, Y.& LI, Q. 1989. Lower Permian paleomagnetism of the Tarim block, northwestern China. *Earth Planetary Science Letters*, **92**, 275-291.

SHEN, S-Z & MEI, S.H. 2010. Lopingian (Late Permian) high-resolution conodont biostratigraphy in Iran with comparison to South China zonation. *Geol. J.* **45**, 135–161.

SHEN, S-Z., HENDERSON, C.M., BOWRING, S.A., CAO, C-Q., WANG, Y., ZHANG, H., ZHANG, Y-C. & MU, L. 2010. High resolution Lopingian (late Permian) timescale of South China. *Geological Journal* **45**, 122-134.

SHEN, S. Z., CROWLEY, J. L., WANG, Y., BOWRING, S. A., ERWIN, D. H., SADLER, P. M., CAO, C-Q., ROTHMAN, D.H., HENDERSON, C.M., RAMEZANI, J., ZHANG, H., SHEN, Y., WANG, X-D., WANG, W., MU, L., LI, W-Z., TANG, Y-G., LIU, X-L., LIU, L-J., ZENG, Y., JIANG, Y-F. & JIN Y-G. 2011. Calibrating the end-Permian mass extinction. *Science*, **334**, 1367-1372.

SILANTIEV, V.V. KOTLYAR, G.V. ZORINA, S.O. GOLUBEV, V.K. LIBERMAN. V.B. 2015a. The geological setting and Permian stratigraphy of the Volga and Kama river regions. *In:* NURGALIEV, D.K. SILANTIEV, V.V. NIKOLAEV S.V.A. (eds). *Type and reference sections of the Middle and Upper Permian of the Volga and Kama River Regions*. A field guidebook of XVIII International Congress on Carboniferous and Permian. Kazan, Kazan University Press, 10-23.

SILANTIEV, VV.V. AREFIEV, M.P. NURGALIEVA,N.G. MOURAVIEV,F.A. BULANOV, V.V. IVANOV, A.O. URAZAEVA , M.N. KHAZIEV, R.R. FAKHRUTDINOV, E.I. KUZINA D.M. 2015b. Cheremushka Section: parastratotype of the Urzhumian Stage. *In:* NURGALIEV, D.K. SILANTIEV, V.V. NIKOLAEV S.V. A (eds). *Type and reference sections of the Middle and Upper Permian of the Volga and Kama River Regions*. A Field Guidebook of XVIII International Congress on Carboniferous and Permian. Kazan, Kazan University Press, 70-119.

SILANTIEV, V.V. NURGALIEVA, N.G. MOURAVIEV, F.A. KABANOV, P.B. URAZAEVA, M.N. KHAZIEV, R.R. FAKHRUTDINOV, E.I. MOZZHERIN, V.V. EGOROVA K.A. 2015c. Elabuga section, Ufimian/Kazanian boundary. *In:* Nurgaliev, D.K. Silantiev, V.V. Nikolaev S.V. a (eds). *Type and reference sections of the Middle and Upper Permian of the Volga and Kama River Regions*. A field guidebook of XVIII International Congress on Carboniferous and Permian. Kazan, Kazan University Press, 144-153.

SINITO, A. M., VALENCIO, D. A. & VILAS, J. F. 1979. Palaeomagnetism of a sequence of Upper Palaeozoic—Lower Mesozoic red beds from Argentina. *Geophysical Journal International*, **58**, 237-247.

SŁOWAKIEWICZ, M., KIERSNOWSKI, H. & WAGNER, R. 2009. Correlation of the Middle and Upper Permian marine and terrestrial sedimentary sequences in Polish, German, and USA Western Interior Basins with reference to global time markers. *Palaeoworld*, **18**, 193-211.

SOREGHAN, G. L., ELMORE, R. D. & LEWCHUK, M. T. 2002. Sedimentologic-magnetic record of western Pangean climate in upper Paleozoic loessite (lower Cutler beds, Utah). *Geological Society of America Bulletin*, **114**, 1019-1035.

SOREGHAN, G. S., BENISON, K. C., FOSTER, T. M., ZAMBITO, J. & SOREGHAN, M. J. 2015. The paleoclimatic and geochronologic utility of coring red beds and evaporites: a case study from the RKB core (Permian, Kansas, USA). *International Journal of Earth Sciences*, **104**, 1589-1603.

SOSIPATROVA, G. P. 1967. Upper Paleozoic foraminifera of Spitsbergen. *In:* V. N. SOKOLOV (ed), *Stratigraphy of Spitsbergen*. Institut Geologii Arktiki, Leningrad, 125-163 [in Russian].

STEINER, M. B. 1988. Paleomagnetism of the Late Pennsylvanian and Permian: A test of the rotation of the Colorado Plateau. *Journal of Geophysical Research: Solid Earth*, **93**, 2201-2215.

STEINER, M. B. 2006. The magnetic polarity time scale across the Permian-Triassic boundary. *In*: LUCAS, S.G., CASSINIS, G. & SCHNEIDER, J.W. (Eds) *Non-marine Permian biostratigraphy and biochronology* Geological Society, London, Special Publications, **265,** 15-38.

STEINER, M.B., OGG, J., ZHANG, Z. & SUN, S. 1989. The Late Permian/early Triassic magnetic polarity time scale and plate motions of south China. *Journal Geophysical Research* **94**, 7343-7363.

STEMMERIK, L. 1988. Discussion. Brachiopod zonation and age of the Permian Kapp Starostin Formation (Central Spitsbergen). *Polar Research,* **6**, 179-180.

STEVENS L.G., HILTON, J., BOND, D.P.G., GLASSPOOL, I.J. & JARDINE, P.E. 2011. Radiation and extinction patterns in Permian floras from North China as indicators for environmental and climate change. *Journal of the Geological Society, London* **168**, 607–619.

SWEET, D.E., C.R. CARSRUD, A.J. WATTERS. 2015. Proposing an entirely Pennsylvanian age for the Fountain Formation through new lithostratigraphic correlation along the Front Range. *The Mountain Geologist*, **52**, 43-70.

SZURLIES, M., BACHMANN, G.H., MENNING, M., NOWACZYK, N.R. & KÄDING, K-C. 2003. Magnetostratigraphy and high resolution lithostratigraphy of the Permian- Triassic boundary interval in Central Germany. *Earth and Planetary Science Letters*, **212**, 263-278.

SZURLIES, M. 2013. Late Permian (Zechstein) magnetostratigraphy in western and central Europe. *In:* GASIEWICZ, A. & SŁOWAKIEWICZ, M. (eds) *Palaeozoic climate cycles: their evolutionary and sedimentological impact.* Geological Society, London, Special Publications, **376**, 73-85.

SUN, Y., LAI, X., JIANG, H., LUO, G., SUN, S., YAN, C. & WIGNALL, P.B. 2008. Guadalupian (Middle Permian) conodont Faunas at Shangsi section, Northeast Sichuan Province. *Journal of China University of Geosciences* **19**, 451-460.

SUN, Y., LAI, X., WIGNALL P.B., WIDDOWSON, M., ALI, J.R., JIANG, H., WANG, W., YAN, C., BOND, D.P.G. & V´EDRINE, S. 2010. Dating the onset and nature of the Middle Permian Emeishan large igneous province eruptions in SW China using conodont biostratigraphy and its bearing on mantle plume uplift models. *Lithos* **119**, 20-33.

SWIFT, A. 1986. The conodont *Merrillina divergens* (Bender & Stoppel) from the Upper Permian of England. *In*: Harwood, G.M. & Smith, D.B. (eds), *The English Zechstein and Related Topics*, Geological Society Special Publication **22**, 55-62.

SYMONS, D. T. A. 1990. Early Permian pole: Evidence from the Pictou red beds, Prince Edward Island, Canada. *Geology*, **18**, 234-237.

TALLING, P. & BURBANK, D. 1993. Assessment of uncertainties in magnetostratigraphic dating of strata. *In:* AISSAOUI, D.M., MCNEILL, D.F. & HURLEY, N.F. (eds), *Application of paleomagnetism to sedimentary geology* SEPM, Society for Sedimentary Geology, Tulsa USA, 59-70.

TAYLOR, G.K., TUCKER, C., TWITCHETT, R.J., KEARSEY, T., BENTON, M.J., NEWALL, A.J., SURKOV, M.V. & TVERDOKHLEBOV, V.P. 2009. Magnetostratigraphy of Permian/Triassic boundary sequences in the Cis-Urals, Russia: no evidence for a major temporal hiatus. *Earth and Planetary Science Letters* **281**, 36-47.

THOMPSON, R. 1972. Palaeomagnetic results from the Paganzo Basin of north-west Argentina. *Earth and Planetary Science Letters*, **15**, 145-156.

TOHVER, E., LANCI, L., WILSON, A., HANSMA, J. & FLINT, S. 2015. Magnetostratigraphic constraints on the age of the lower Beaufort Group, western Karoo basin, South Africa, and a critical analysis of existing U-Pb geochronological data. *Geochemistry, Geophysics, Geosystems*, **16**, 3649-3665.

TURNER, P. 1979. The palaeomagnetic evolution of continental red beds. *Geological Magazine*, **116**, 289-301.

TURNER, P., CHANDLER, P., ELLIS, D., LEVEILLE, G.P. & HEYWOOD, M.L. 1999. Remanance acquisition and magnetostratigraphy of the Leman Sandstone Formation: Jupiter Fields, southern North Sea. *In:* TARLING, D.H. & TURNER, P. (eds) *Palaeomagnetism and diagenesis in sediments*, Geological Society of London special publications, **151**, 109-124.

TVERDOKHLEBOV, V. P., TVERDOKHLEBOVA, G. I., MINIKH, A. V., SURKOV, M. V., & BENTON, M. J. 2005. Upper Permian vertebrates and their sedimentological context in the South Urals, Russia. *Earth-Science Reviews*, **69**, 27-77.

VALENCIO, D. A. 1980. Reversals and excursions of the geomagnetic field as defined by palaeomagnetic data from Upper Palaeozoic-Lower Mesozoic sediments and igneous rocks from Argentina. *Journal of Geomagnetism and Geoelectricity,* 32(Supplement3), SIII137-SIII142.

VALENCIO, D. A., VILAS, J. F. & MENDÍA, J. E. 1977. Palaeomagnetism of a sequence of red beds of the Middle and Upper Sections of Pagnazo Group (Argentina) and the correlation of Upper Palaeozoic-Lower Mesozoic rocks. *Geophysical Journal International*, **51**, 59-74.

VAN DER VOO, R., & TORSVIK, T. H. (2012). The history of remagnetization of sedimentary rocks: deceptions, developments and discoveries. *In*: ELMORE, R. D., MUXWORTHY, A. R., ALDANA, M.M. &MENA, M. (eds). *Remagnetization and Chemical Alteration of Sedimentary Rocks.* Geological Society, London, Special Publications, **371**, 23-53.

VOZÁROVÁ, A. & TÚNYI, I., 2003. Evidence of the Illawarra Reversal in the Permian sequence of the Hornic nappe (Western Carpathians, Slovakia). *Geologica Carpathica* **54**, 229–236.

WAHLMAN, G. P. & WEST, R. R. 2010. Fusulinids from the Howe Limestone Member (Red Eagle Limestone, Council Grove Group) in northeastern Kansas and their significance to the North American Carboniferous (Pennsylvanian)–Permian boundary. *Current Research in Earth Sciences, Bulletin* **258(4)**, 1-13 (http://www.kgs.ku.edu/Current/2010/Wahlman/index.html), Kansas Geological Survey.

WANG, C. & YANG, S. 1993. Brachiopod fauna around the Carboniferous-Permian boundary from the Balikelike Formation in Keping, Xinjiang. *Journal of Changchun University of Earth Sciences*, **23**, 1-9.

WARDLAW, B.R. & MEI, S. 1999. Refined conodont biostratigraphy of the Permian and lowest Triassic of the Salt and Khizor Ranges, Pakistan. *In*: YIN, H., & TONG, J. (eds), *Proceedings of the international conference on Pangea and the Palaeozoic-Mesozoic transition,* Wuhan China, China Univ. of Geosciences Press, 154-156.

WARDLAW, B.R. & POGUE, K.R. 1995. The Permian of Pakistan. *In*: SCHOLLE, P.A., PERYT, T.M., & ULMER-SCHOLLE, D.S. (eds). *The Permian of Northern Pangea 2, Sedimentary Basins and Economic Resources*, Springer-Verlag, 215-224.

WARD, P. D., BOTHA, J., BUICK, R., DE KOCK, M. O., ERWIN, D. H., GARRISON, G. H. *ET AL*. 2005. Abrupt and gradual extinction among Late Permian land vertebrates in the Karoo Basin, South Africa. *Science*, **307**, 709-714.

WATERHOUSE, J.B. 2010. Lopingian (Late Permian) stratigraphy of the Salt Range, Pakistan and Himalayan region. *Geol. J.* **45**, 264–284.

WESCOTT, W. A. & DIGGENS, J. N. 1998. Depositional history and stratigraphical evolution of the Sakamena Group (Middle Karoo Supergroup) in the southern Morondava Basin, Madagascar. *Journal of African Earth Sciences*, **27**, 461-479.

WESTFAHL , M., SURKIS, Y.F., GUREVICH, E.L. & KHRAMOV, A.N. 2005. Kiama-Illawarra geomagnetic reversal recorded in the Tatarian Stratotype (the Kazan region). *Izvestiya, Physics of the solid Earth* **41**, 634-653.

WINTERS, S. S. 1962. Lithology and stratigraphy of the Supai Formation, Fort Apache Indian Reservation, Arizona. *In*: WEBER, R. H. & PEIRCE, H. W. (eds), *Mogollon Rim Region (East-Central Arizona)*, New Mexico Geological Society 13th Annual Fall Field Conference Guidebook. New Mexico Geol. Society, 87-88.

WU, H., ZHANG, S., HINNOV, L. A., JIANG, G., FENG, Q., LI, H., & YANG, T. 2013. Time-calibrated Milankovitch cycles for the late Permian. *Nature Communications*, DOI: 10.1038/ncomms3452.

WYNNE, P. J., IRVING, E. & OSADETZ, K. 1983. Paleomagnetism of the Esayoo Formation (Permian) of northern Ellesmere Island: possible clue to the solution of the Nares Strait dilemma. *Tectonophysics*, **100**, 241-256.

XU. YI-G., WEI, X. LUO, Z-Y. LIU, H-Q. & CAO, J. 2014. The Early Permian Tarim Large Igneous Province: Main characteristics and a plume incubation model. *Lithos* **204**, 20–35

YIN, H., ZHANG, K., TONG, J., YANG, Z. & WU, S. 2001. The global stratotype section and point (GSSP) of the Permian-Triassic boundary. *Episodes* **24,** 102-114.

YUAN, D. X., SHEN, S. Z., HENDERSON, C. M., CHEN, J., ZHANG, H. & FENG, H. Z. 2014. Revised conodont-based integrated high-resolution timescale for the Changhsingian Stage and end-Permian extinction interval at the Meishan sections, South China. *Lithos*, **204**, 220-245.

ZHENG, L. YANG, Z. TONG, Y. & YUAN, W. 2010. Magnetostratigraphic constraints on two-stage eruptions of the Emeishan continental flood basalts. *Geochemistry Geophysics Geosystems*, **11**, doi:10.1029/2010GC003267.

ZHONG, Y. T., HE, B., MUNDIL, R., & XU, Y. G. 2014. CA-TIMS zircon U–Pb dating of felsic ignimbrite from the Binchuan section: implications for the termination age of Emeishan large igneous province. *Lithos*, **204**, 14-19.

ZIEGLER, A. M., REES, P. M. & NAUGOLNYKH, S. V. 2002. The Early Permian floras of Prince Edward Island, Canada: differentiating global from local effects of climate change. *Canadian Journal of Earth Sciences*, **39**, 223-238.

Figure Captions

Fig. 1. Lower Permian magnetic polarity data from Russia, Asia, South America and Africa. Ticks on the columns are sample positions. Data sources for magnetostratigraphy and supporting stratigraphic details: Tarim Basin Sharps *et al.* (1989), Li *et al.* (2011), Wang & Yang (1993) and Xu *et al.* (2014). South Ferghana composite from Davydov & Khramov (1991), with equivalent numbered foraminifera zones from the Urals successions, mapped using their Fig. 5 (See Table 2). Ouberg Pass, South Africa and SHRIMP dates from Lanci *et al.* (2013) and Modie & Le Hérissé (2009). Nikolskyi, Chernaja Rechka and Aidaralash from Khramov & Davydov (1984, 1994), Davydov *et al.* (1998) and Davydov & Leven (2003), with numbered foraminifera zones as indicated in Table 2. Paganzo Basin magnetostratigraphy and radiometric date from Valencio *et al.* (1977), Césari & Gutiérrez (2000) and Césari *et al.* (2011). SE Tatarstan composite, Kotlovka and Elabuga from Burov *et al.* (1998), Silantiev *et al.* (2015c). Khei-yaga River section from Iosifidi & Khramov (2009). Adz'va River section data from Balabanov (1998), with additional stratigraphy from

Rasnitsyn *et al.* (2005), Lozovsky *et al.* (2009) and Kotylar (2015). Stage base ages are those of Henderson *et al.* (2012).

Fig. 2. Lower Permian magnetic polarity data from Europe and North America. Ticks on the columns are sample positions. Data sources used are: Svalbard (Norway), magnetostratigraphy from Nawrocki & Grabowski (2000) and Hounslow & Nawrocki (2008), with additional stratigraphic details from Nakrem *et al.* (1992), Nilsson & Davydov (1997), Bond *et al.* (2015) and Ehrenberg *et al.* (2010). Lower Rotliegend (Germany), magnetostratigraphy from Menning (1987) and Menning *et al.* (1988), and additional stratigraphy from Schneider *et al.* (2013). Moab (Utah, USA) magnetostratigraphy from Gose & Helsely (1972), with additional age constraints from Soreghan *et al.* (2002), Condon (1997) and Lucas (2006). Dunkard Group (W. Virginia, USA) magnetostratigraphy from Helsley (1965) and Gose & Helsley (1972), with additional stratigraphy from Di Michael *et al.* (2013) and Lucas (2013). Red Sandstone Creek (Colorado, USA) magnetostratigraphy from Miller & Opdyke (1985), with additional stratigraphy from Johnson *et al.* (1990). Squaw Creek (Colorado, USA) magnetostratigraphy from Miller & Opdyke (1985). Foraminifera zone names on Svalbard column modified by Davydov *et al.* (2001), from Nilsson & Davydov (1997), stuck.=*Rauserites stuckenbergi*, jigul.=Jugulites jigulensis, sokensis=*Daixina sokensis*, robusta=*Schwagerina robusta*, furnishi=*Zigarella furnishi*, princeps=*Sch. princeps*, spherical=*Sch. sphaerica*, paralin=*Eoparafusulina paralinearis*. G.k= *Gerkeina komiensis, F.d=Frondicularia bajcurica* foraminifera assemblage zones. Stage base ages from Henderson *et al.* (2012).

Fig. 3. Summary of the mid and late Permian magnetostratigraphy from the Russian East European Basin successions west of the Urals (modified from Hounslow 2016). Boyevaya Gora, Tuyembetka and Sambullak sections are near Orenburg and are from Taylor *et al.* (2009). Murygino, Tetyushi, Cheremushka, Putyatino, Pizhma, Oparino sections are near the Kama, Volga and Vyatka Rivers (SW Tataria, Kazan region; Silantiev *et al.* 2015a, 2015b), some ~700 km NE of Orenburg area and are from Burov *et al.* (1998). Monastyrski (Volga River) section (Mouraview *et al.* 2015), from the Kazan region based on Gialanella *et al.* (1997), Burov *et al.* (1998), Balabanov (2014) and Westfhal *et al.* (2005). Sukhona River section from NE Russian, ~600 km North of Kazan is from Khramov *et al.* (2006). Khei-Yaga River section as in Fig. 2. Each section has a thickness scale in metres. Composite magnetochrons are also labelled with the Russian naming convention (Molostovsky, 1996; Molostovsky *et al.* 1998), and the Russian regional stratigraphy (Kotlyar & Pronina-Nestell, 2005). BH= borehole number.

Fig. 4. Summary of the mid and late Permian magnetostratigraphy from marine and non-marine sections (modified from Hounslow 2016). Meishan magnetic polarity composite from Fig. 8. Kyushu section magnetostratigraphy and fusulinid zones from Kirschvink *et al.* (2015). Linshui section magnetostratigraphy from Heller *et al.* (1995), other stratigraphy modified from that originally published (see text for details). Emeishan basalt magnetostratigraphy from Ali *et al.* (2002), Zheng *et al.* (2010), Liu *et al.* (2013) and Zhang *et al.* (2014) and associated stratigraphy from He *et al.* (2008) and Sun *et al.* (2010). The biostratigraphy of the Wulong section (Jin *et al.* 2000) is inadequately documented, but the magnetostratigraphy (Chen *et al.* 1994; Heller *et al.* 1995), appears to range into the lower Capitanian. The Shangsi magnetostratigraphy composite is from Fig. 5. The Taiyuan (a non-marine section) magnetostratigraphy is from Embleton *et al.* (1996), with additional stratigraphic details from Menning & Jin (1998) and Stevens *et al.* (2011). The Nammal Gorge section magnetostratigraphy is from Hagg and Heller (1991), with conodont ranges projected from nearby sections based on Wardlaw & Pogue (1995), Wardlaw & Mei (1999) and Waterhouse (2010). Abedah section magnetostratigraphy from Gallet *et al.* (2000) and Szurlies (2013) and its associated conodont biostratigraphy from Shen & Mei (2010). Fusulinids: Ps= *Palaeofusulina* spp., Nm= *Neoschwagerina margaritae* (Jin *et al.* 2000). Conodont zones: G2=*J. asserata* (base Wordian), G3=*J. postserrata* (base Capitianian), G5= *J.altudaensis* (mid Capitanian), G7= *J. xuanhanensis* (upper Capitanian). L1 to L12 are the standard Lopingian conodont zones from Shen *et al.* (2010).

Fig. 5. Summary of magnetic polarity data for the Shangsi section. The composite magnetostratigraphy on the right is derived from three magnetostratigraphic studies of Heller *et al.* (1988), Steiner *et al.* (1989) and Glen *et al.* (2009). Radiometric dates from the section are from Mundil *et al.* (2004) and Shen *et al.* (2010). Biostratigraphy is from Lai *et al.* (1996), Jin *et al.* (2000) and Sun *et al.* (2008). There are inconsistencies in the thickness of units between the three studies, but generally the datasets can be related using the bed number stratigraphy. Many of the uncertain (grey) intervals from the study of Glen *et al.* (2009) represent sample levels that yielded no polarity information. The cyclostratigraphy and conodont zonal boundaries are from Wu et al. (2013). Key as in Fig. 4. Ammonoid zones: T-S = *Tapashanites* - *Shevyrevites* assemblage Zone; P-P = *Pseudotirolites* - *Pleuronodoceras* assemblage Zone.

Fig. 6. Magnetic polarity data from North American and South African sections through the Middle Permian. West Texas/New Mexico data is a composite from several studies discussed in Steiner (2006), with the partly unpublished Guadalupian data from the backreef facies of the Guadalupe Mountains. The Guadalupe basinal facies (Apache Mts and Guadalupe Mts sections) from Burov

et al. (2002). Additional stratigraphic details from Lambert *et al.* (2007), Olszewski & Erwin (2009) and Rush & Kerans (2010). Radiometric dates from Bowring *et al.* (1998) and Nicklen (2011), related to the lithostratigraphy via sequence correlation of Rush & Kerans (2010). Rebecca K Bounds core magnetostratigraphy from Soreghan *et al.* (2015), and additional details from Sawin *et al.* (2008). Buffels River composite (South Africa) from Tohver *et al.* (2015) in which the grey (uncertain) intervals represent sampled intervals which yielded no polarity data. Individual section height scales on each section. The two options for correlation of the Abrahamskraal Fm data are discussed in the text.

Fig. 7. Magnetostratigraphic data from Upper Rotleigend- Zechstein equivalent, Permian age sections in Europe. Czaplinek, Piła and Jaworzna IG-1 well magnetostratigraphy composite derived from Nawrocki (1997) with additional stratigraphic details from Słowakiewicz *et al.* (2009). Mirow well 1/1a/74 from Menning *et al.* (1988) and Langereis *et al.* (2010). Obernsees well composite polarity re-interpretation is from Szurlies (2013). Schlierbachswald-4 and Everdingen 1 wells from Szurlies *et al.* (2003), Szurlies (2013). Southern North Sea data for the Leman Sandstone Fm from Turner *et al.* (1999) and Lawton & Robertson (2003). SW England coast section data from Hounslow *et al.* (2016).

Fig. 8. Summary of the Meishan section magnetic polarity data. The composite magnetic polarity is derived from the three published studies of the Meishan section from Li & Wang (1989), Liu *et al.* (1999) in Yuan *et al.* (2014) & Meng *et al.* (2000). Associated radiometric dates and biostratigraphy from Mundil *et al.* (2010), Shen *et al.* (2010), Jin *et al.* (2006a) and Burgess *et al.* (2014). The data for the polarity composite shown in Yin *et al.* (2001) has never been published. There is some ambiguity about how to relate these datasets, since thicknesses vary, and bed numbers are not shown in Li & Wang (1989) and Meng *et al.* (2000). Data relationships were attempted using the shale beds in the section logs.

Fig. 9. Geomagnetic polarity datasets for non-marine sections which span the Changhsingian-Induan boundary, compared to the data from the Shangsi section (which shows the clearest relationship between the magnetostratigraphy and a precise bio- and geochronology). Section data from Old Lootsberg and E-W Lootsberg from Gastaldo *et al.* (2015) and Ward *et al.* (2005) respectively- these are drawn using the same vertical scale. Polarity data for the Siberian traps using the composites in Fetisova *et al.* (2014), supported by magnetic and geochronologic data in Gurevitch *et al.* (2004) and Burgess & Bowring (2015). The Shangsi section data from Fig. 5. Cyclostratigraphic age on the base of LT1r from Li *et al.* (2016).

Fig. 10. Optimised composites (a, b, d,e) and age model for the Cisuralian (c) and early Guadalupian.. Optimised composites based on methodology in Hounslow (2016). A) and D) show the standard deviation (σ_T) for the levels used in the optimised scaling procedure (scaled to Ma, using the final age model). This is a measure of the correlated level misfit. The correlated levels are shown in b) and e). No σ_T values for a corresponding level shown in b) and e) indicate the level was not used to constrain the optimised model, but simply scaled with the section. B) and E) are the original section data shown on the y-axis (in a relative height scale), along with the final composite position of the levels on the x-axis. Scatter in the y-axis relates to the degree of between section mis-fit shown in the overlying panel as σ_T. Numbers in brackets next to section names are the D_j values of Hounslow (2016), which express the mis-fit of the section data to the optimised composite. i.e. the Karachtyr data has a mean residual of 14% per average 'chron width', for the optimised model. D_s is the average of the D_j values across all sections. C) The Bchron age model for the Carboniferous-Permian boundary, showing the scaling of optimised position to Ma, using the radiometric dates (magnetochrons in scale of optimised composite shown at the bottom). F) the radiometric dates used to scale the optimised composite scale. In c) and f) error bars on the y-axis and x-axis are the radiometric (σ_R) and stratigraphic (e_s) uncertainty values in Table 2.

Fig. 11. Bchron age model for the Kungurian to earliest Triassic. The optimised composite position scale that in Figure 10f ranging from the radiometric date at 296.1 Ma to GU2r, joined to that from GU2r to LT1n.2n from Hounslow (2016).

Fig. 12. Summary Permian geomagnetic polarity timescale. Chron scale in Ma derived from Bchron models in Fig. 10c and 11. Numbered fusulinid zones in the earliest Permian are those in Fig. 1 and detailed in Table 2. Standard conodont zones L2 to L12 from Shen *et al.* (2010), derived from data in Fig. 4. Selected other key biochronology from Figs. 2 & 4. Radiometric ages of stages indicated in Table 3.

Fig. 13. Confidence interval data for chron durations. A) Estimated magnetozone durations (and zone intervals) from each of the sections (blue triangles) used in the optimised composites (y-axis), versus the duration of the equivalent chron. Data for 173 magnetozones and zone intervals are shown. The 95% confidence intervals on the linear regression relationship using the ln-model (solid line). The 95% HPD limits, from Bchron for each of the Permian chrons are shown (as diamonds), along with a lines (dashed) expressing this variation with duration. B) Estimates of the 95% confidence intervals using uncertainty in the age model (gray line), using the approach of Agterberg (2004) and symmetrical 95% confidence intervals using the section magnetozone data (dashed lines) shown in a). The final 95% confidence interval model (black line) adds the

Agterberg estimates to the linear-model when chron duration >0.7 Ma and ln-model added to the Agterberg estimate when durations <0.5 Ma (that 0.5- 0.7 Ma is linearly interpolated). Regression and confidence intervals used the linear model routines in R, version 3.2.4 (Becker *et al.* 1988).

Location/ Age	Lithology, Lithostratigraphy	N_S. [N_{MZ}]	D_m/FT/ S	h.$_{MZ}$ (m)	Reference sources
Arizona, USA/mid Kungurian	Clastic red-beds, Schnebly Hill Fm	30[1?]	0/0/PP	?	Graham 1955.
Spitsbergen, Norway/ Kungurian	Cherts, spiculitic shales, Kapp Starostin Fm	4 [1]	1/0/MS	~12	Nawrocki & Grabowski 2000, Nawrocki 1999
Ellesmere Island, Canada/ early to mid Kungurian	Basaltic lavas, Esayoo Volcanics	5 [1]	1/0/PP	~10-30	Wynne *et al.* 1983, Morris 2013, LePage *et al.* 2003.
Prince Edward Island, Canada /Late Artkinskian	Red-beds, Pictou Group, Orby Head Fm.	9 [2]	2/0/PP	?	Symons 1990, Ziegler *et al.* 2002.
Oklahoma, USA/ mid Artkinskian	Red Sandstone, Garber Sandstone	7 [1]	2/0/PP	?	Peterson & Nairn 1971, Giles *et al.* 2013.
Spitsbergen, Norway/ late Artkinskian	Cherts, spiculitic shales, Kapp Starostin Fm	3 [1]	1/0/MS	~18	Nawrocki & Grabowski 2000; Nawrocki 1999
Paganzo Basin, Argentina/ Artinskian	Red beds, La Colina Fm	8[1]	2/0/MS	~15	Valencio *et al.* 1977, Valencio (1980, Césari *et al.* 2011, Césari & Gutiérrez 2000
British Columbia/ late Sakmarian – early Artinskian	Tuffs, Asitka Group	15[1?]	2/0/PP	?	Irving & Monger 1987, MacIntyre *et al.* 2001.
W. Virginia, USA/ Asselian	Dunkard Group, Washington Fm	2[1]	2/0/PP	?	Helsley 1965, Gose & Helsley 1972, Schneider *et al.* 2013.
Karachatyr, Tajikistan/ Asselian	Marine limestones and clastics	>=2?[1]	2/F+/MS	<200	Davydov & Khramov 1991.
Aidaralash, Kazakhstan/early Asselian	Marine limestones and clastics	2[1]	2/0/MS	10	Khramov & Davydov 1984,1993.
Saar-Nahe Basin, Germany/ 300-290 Ma (Sak.- Ass.)	Nohfelden & Donnersberg rhyolites	11[1?]	1/0/PP	?	Berthold *et al.* 1975, Schmidberger & Hegner 1999.
Thuringia, Germany/ Gzhelian?	Grey, coal bearing ssts, Manebach Fm	5[?]	2/0/MS	?	Menning 1987, Menning *et al.* 1988.
Aidaralash, Urals/late Gzhelian	Marine limestones and clastics	2[1?]	2/0/MS	<15	Khramov & Davydov 1984,1993.
Nikolskyi, Urals/late Gzhelian	Marine limestones and clastics	2?[2]	2/0/MS	<~20	Khramov & Davydov 1984,1993.
Spitsbergen, Norway/ late Gzhelian	Limestones, dolomites Tyrrellfjellet Mbr	2[1]	1/0/MS	~8	Nawrocki & Grabowski 2000, Nawrocki 1999.
Fergana, Tajikistan/ Gzhelian	Marine limestones and clastics	~6[3]	2/F+/MS	~3 to <300	Davydov & Khramov 1991.
Donets Basin, Suhoj-Jaz, Ukraine/ late Gzhelian	Red beds/ Kartamysh Suite	17[1]	0/F+/PP	<100	Khramov 1963b, Khramov & Davydov 1984, Davydov & Leven 2003, Iosifidi *et al.* 2010.

Table 1. Studies showing reliable normal polarity data in the early Permian and latest Carboniferous. N_s=Number of specimens with normal polarity. N.$_{MZ}$= number of normal magnetozones. h_{MZ}= normal magnetozone height, ?=unknown. Dm/FT/S= demagnetisation method/fold test/study type. D_m=1, if full demagnetisation applied to all samples, with principle component or great circle extraction, D_m=2, pilot demagnetisations of simple magnetisation behaviour, with stable point averaging, or single step. D_m=0, no demagnetisation. F+= fold test positive (or demonstrate pre-folding magnetisation), F-= fold test negative,F=0, no fold test. S=PP or MS for palaeopole or magnetostratigraphic study respectively.

1.Code, age (Ma)	2. ±2σ_R (Ma)	3. ±e_s	4. Location [estimated position]	5.Biostratigraphy, stratigraphy {position in biozone }	6. P_{out}	7. References
SH03, 260.74	0.9	10% of GU3n	36.3 m above base Wujiaping Fm, Shangsi, bed 8	Base Lopingian {base of LP0r}	0.12	Mundil *et al*. 2004, Zhong *et al*. 2014, Schmitz 2012.
JW1, 259.1	0.5+	10% of GU3n	Emeishan basalts, Zhaotong	~100 m below top of unit III {95% into GU3n}	0.45	Zhong *et al*. 2014.
GM-20, 262.58	0.45	100% of GU2r	20 m above Rader Limestone (Patterson Hills)	Within *Polydiexodina* fusulinid Zone, (i.e. ~ *J. postserrata* zone) {95% into GU2n}	0.03	Nicklen 2011.
OPA483, 264.6*	1.9	10% of GU1r	484 m above base of Abrahamskraal Fm, Ouberg Pass. S. Africa	Within mid *Eodicynodon* assemblage {75.4% into GU2r}	0.01	Lanci *et al*. 2013.
OPA292, 265.9*	1.4	5% of GU1n	195 m above base of Abrahamskraal Fm, Ouberg Pass. S. Africa	Within base *Eodicynodon* assemblage {86.7% into GU1n}	0.01	Lanci *et al*. 2013.
NH, 265.35	0.5	100% of GU1r.1n	Nipple Hill, Guadalupian Mts	37.2 m below base Capitanian, 2 m above top of the Hegler Member {base GU1r.1n}	0.04	Bowring *et al*. 1998, Nicklen 2011, (Fig. 1.8)
OPA230, 266.4*	1.8	5% of GU1n	132 m above base of Abrahamskraal Fm, Ouberg Pass. S. Africa	Within base *Eodicynodon* assemblage {97.4% into CI3r.2r}	0.01	Lanci *et al*. 2013.
GM-29, 266.50	0.24	100% of GU1r	below South Wells Limestone ("Monolith Canyon")	Within *J. asserrata* Zone {10% into MP1r}	0.17	Nicklen 2011.
OPA160, 267.1*	1.7	10% of CI3r.2r	62 m above base of Abrahamskraal Fm, Ouberg Pass. S. Africa	Within base *Eodicynodon* assemblage {69.1% into CI3r.2r}	0.00	Lanci *et al*. 2013.
OPA151, 268.5*	3.5	10% of CI3r.2r	52 m above base of Abrahamskraal Fm, Ouberg Pass. S. Africa	Within base *Eodicynodon* assemblage {65.0% into CI3r.2r}	0.01	Lanci *et al*. 2013.
PPAsh-1 296.09	0.35	300% of CI2n	La Colina Fm, Pagenzo basin, Argentina. [10's m above basalt flow/sill]	Pagenzo Group, *Fusacolpites fusus*–*Vitattina subsaccata* Interval Biozone	0.01	Gulbranson *et al*. 2010, Césari *et al*. 2011.
01DES212, 296.69	0.37	400% of CI1r.1n	Usolka section, Russia	Mid Asselian, {54% into zone 11}	0.01	Schmitz & Davydov 2012.
01DES202, 298.05	0.54	100% of CI1r.1n	Usolka section, Russia	Early Asselian, {83% into zone 10}	0.01	Ramezani *et al*. 2007.
01DES194, 298.49	0.34	100% of CI1r.1n	Usolka section, Russia	Earliest Asselian, {21% into zone 10}	0.01	Ramezani *et al*. 2007.
01DES144, 299.22	0.34	400% of CI1n	Usolka section, Russia	latest Gzhelian, {63% into zones 8 & 9}	0.01	Ramezani *et al*. 2007.
97USO-23.3, 300.22	0.35	30% of Zone 5	Usolka section, Russia	Mid Gzhelian, {83% into zone 5}	0.01	Schmitz & Davydov 2012.
01DES121, 301.29	0.36	30% of Zone 5	Usolka section, Russia	Mid Gzhelian, {61% into zone 5}	0.01	Schmitz & Davydov 2012.
01DES112, 301.82	0.36	30% of Zone 5	Usolka section, Russia	Mid Gzhelian, {26% into zone 5}	0.01	Schmitz & Davydov 2012.
01DES63, 303.10	0.36	30% of Zone 3	Usolka section, Russia	Basal Gzhelian, {40% into zone 3}	0.01	Schmitz & Davydov 2012.
97USO-2.7,303.54	0.39	30% of Zone 3	Usolka section, Russia	Basal Gzhelian, {10% into zone 3}	0.01	Schmitz & Davydov 2012.

Table 2. Permian radiometric dates used. **Column 1:** Analysis code and date (in Ma). **Column 2:** $\pm 2\sigma_R$ = two-sigma error on age. **Column 3**: $\pm e_s$= estimated stratigraphic error in placing the date onto the magnetostratigraphy in units of magnetochron or foraminifera zone widths. **Column 4:** section name, location. **Column 5:** Stratigraphic age or location, {..}= correlated position of date from base of chron, zone or interval. **Column 6:** P_{out}, probability (0 to 1.0) the date is an outlier (from Bchron); bigger values suggest more likely. For those dates not displayed here, but in supplementary Table 2 in Hounslow (2016), all have P_{out} <0.2 except those at 253.47 Ma, 251.1 Ma and 252.85 Ma giving P_{out} of 0.998, 0.992 and 0.207 respectively. **Column 7:** source reference for the radiometric and age information. Foraminifera zone numbers in Columns 3 and 5, based on Khramov & Davydov (1993), Davydov & Leven (2003), Schmitz & Davydov (2012): 2= *Rauserites quasiarcticus*, 3=*Daixina fragilis*, 4=*D. crispa*, 5=*D. ruzhenzevi*, 6 &7=*D. sokensis*, 8&9= *Ultradaixina bosbytauensis*, 10=*Sphaeroschwagerina aktjubensis* to *Sp. fusiformis*, zone 11= *Schwagerina nux* to *Pseudoschwagerina robusta*, 12=*Sp. gigas*, 13=*S. moelleri*, 14=*S. verneulli*, 15= *Ps. pilicatissima- Ps. urdalensis*. Nicklen (2011) used hand picked acicular, clear zircons, annealed at 900^{o}C for 48 hrs then chemically abraded and spiked with EARTH time tracer solution. GM-20 has 100 crystals picked, with the weighted mean using 2 multi-crystal and 2 single crystal analyses combined. GM-29 had 100 crystals separated, which produced a weighted mean using 8 concordant single crystals. *= Monto Carlo simulation of best fit SHRIMP ages and associated uncertainties.

Chron	Age (Ma)	Chron duration (Ma)	C_{95} (Ma)	σ_T (ka)	$\%D_{95}$	Chron	Age (Ma)	Chron duration (Ma)	C_{95} (Ma)	σ_T (ka)	$\%D_{95}$
LT1n.2n	251.444		0.28	-							
LT1n.1r	251.634	0.190	0.23	-	19.1	GU3n.an	262.129	2.297	0.89	-	9.6
LT1n.1n	252.242	0.608	0.23	40	15.1	GU3n.ar	262.160	0.031	0.87	-	31.4
LP3r.ar	252.54	0.298	0.17	-	16.8	GU3n	262.592	0.432	0.57	38	15.7
LP3r.an	252.571	0.031	0.17	-	31.4	GU2r	262.740	0.148	0.55	78	20.5
LP3r	252.668	0.097	0.19	28	23.2	GU2n.2n	263.134	0.394	0.84	73	15.9
LP3n	252.796	0.128	0.23	166	21.4	GU2n.1r	263.446	0.312	0.90	280	16.6
LP2r	253.196	0.400	0.34	99	15.9	GU2n.1n	264.375	0.929	0.95	346	12.5
LP2n.3n	253.242	0.046	0.37	20	28.7	GU1r	265.746	1.371	0.69	394	10.4
LP2n.2r	253.802	0.560	0.43	164	15.3	GU1n.3n	266.274	0.528	0.73	94	15.4
LP2n.2n	254.194	0.392	0.40	229	15.9	GU1n.2r	266.374	0.100	0.76	251	23.0
LP2n.1r	254.637	0.443	0.66	400	15.6	GU1n.2n	266.496	0.122	0.70	110	21.7
LP2n.an	254.876	0.239	0.88	-	17.8	GU1n.1r	266.566	0.070	0.70	77	25.6
LP2n.ar	255.106	0.230	0.99	-	18.0	GU1n	266.659	0.093	0.76	220	23.5
LP2n.1n	255.922	0.816	1.12	286	13.5	CI3r.2r	269.240	2.581	1.59	254	9.6
LP1r	257.584	1.662	0.75	424	9.9	CI3r.1n	269.542	0.302	1.61	355	16.7
LP1n.2n	258.002	0.418	0.58	177	15.8	CI3r.1r	275.386	5.844	2.02	132	9.6
LP1n.1r	258.072	0.070	0.58	111	25.6	CI3n	275.862	0.476	1.99	45	15.4
LP1n	258.214	0.142	0.66	115	20.8	CI2r	280.736	4.874	1.97	210	9.6
LP0r.ar	258.683	0.469	0.86	-	15.8	CI2n	281.242	0.506	2.26	184	15.5
LP0r.an	258.731	0.048	0.89	-	28.4	CI1r.2r	297.835	16.593	0.34	-	9.6
LP0r.3r	258.842	0.111	0.94	21	22.3	CI1r.1n	297.938	0.103	0.33	-	22.8
LP0r.2n	258.922	0.080	0.96	127	24.6	CI1r.1r	298.694	0.733	0.37	123	14.4
LP0r.2r	259.316	0.394	1.08	-	15.9	CI1n	298.774	0.081	0.37	140	24.5
LP0r.1n	259.396	0.080	1.10	-	24.6						
LP0r.1r	259.832	0.436	1.13	32	15.7						

Table 3. Permian chron base ages and durations. C_{95} : 95% Highest posterior density intervals on the age of the chron, estimated using Bchron in two age segments (shown in Fig. 10c and 11). σ_T : standard deviation of the chron position in the sections for the chron (from the optimisation method), scaled by the duration of the optimised chron. σ_T is a measure of the uncertainty in defining the chron position in the optimised GPTS. $\%D_{95}$ is the 95% confidence interval on the duration (expressed as the percent of the chron duration; Fig. 13). The age models define the base of the stages at the following: Gzhelian, 303.79 Ma; Asselian, 298.41 Ma; Sakmarian, 295.5 Ma; Artinskian, 290.1 Ma; Kungurian, 279.3 Ma; Roadian, 272.13 Ma; Wordian, c. 266.7Ma; Capitanian, c. 263.5 Ma; Wuchiapingian, 259.7 Ma; Changhsingian, 255.4 Ma; Induan 252.1 ±0.23Ma from which the relative position of the chrons in the stages can be determined. Age of some tentative subchrons designated were estimated using relative locations within the main chrons at the Monastyrski (for GU3n.ar), Wulong (for LP0r.1n), Linshui (for LP0r.an) and Everdingen (for LP3r.an) sections. The differing Wordian-Changhsingian age model and method to Hounslow (2016) gives slightly different age and uncertainty values for most of the data here.

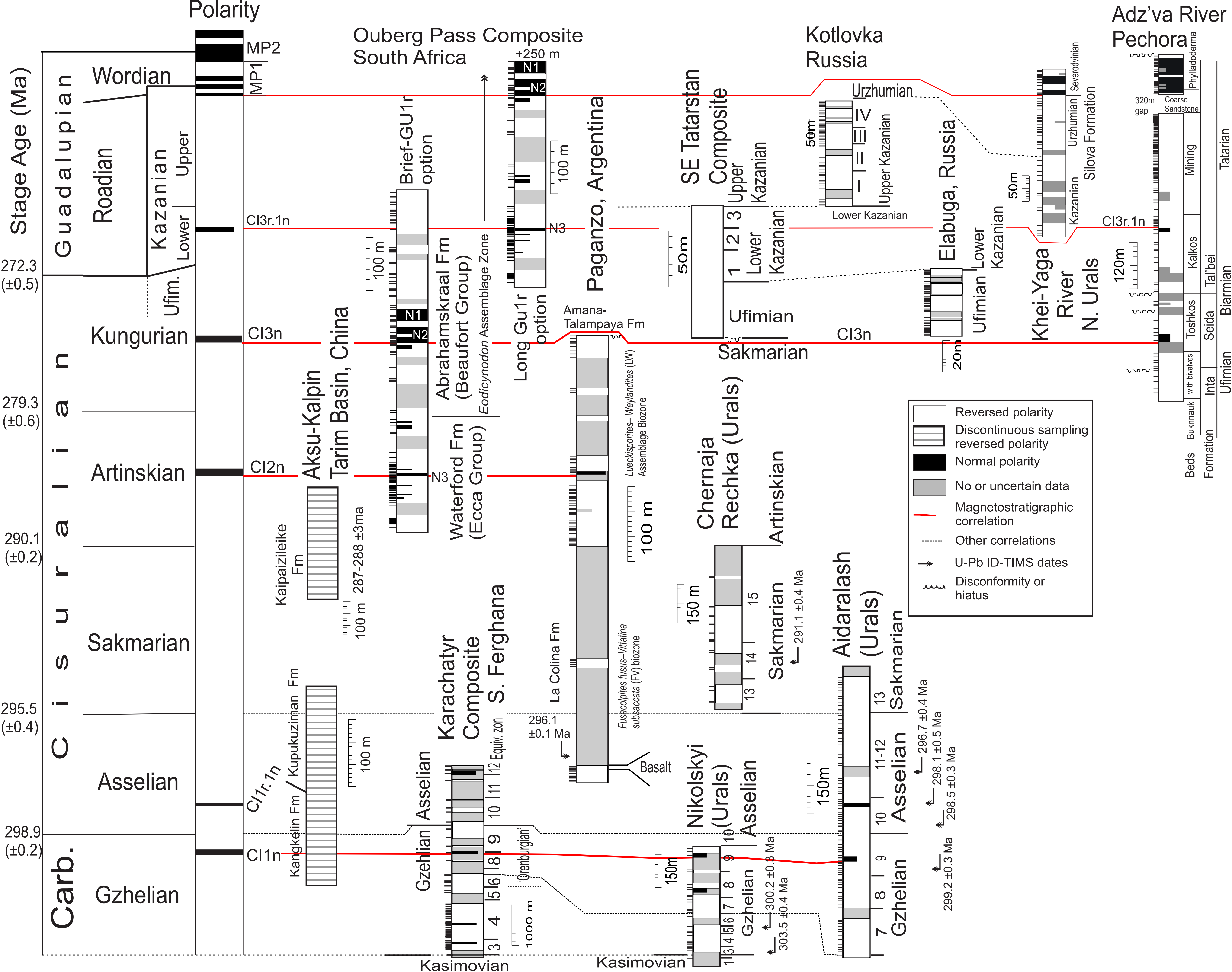

Stage Age (Ma)
Polarity
Guadalupian
Cisuralian
Carb.
Wordian
Roadian
Kazanian
Upper
Lower
Ufim.
Kungurian
Artinskian
Sakmarian
Asselian
Gzhelian
272.3 (±0.5)
279.3 (±0.6)
290.1 (±0.2)
295.5 (±0.4)
298.9 (±0.2)
MP2
MP1
CI3r.1n
CI3n
CI2n
CI1r.1n
CI1n
Ouberg Pass Composite South Africa
Brief-GU1r option
Long Gu1r option
Abrahamskraal Fm (Beaufort Group)
Waterford Fm (Ecca Group)
Eodicynodon Assemblage Zone
N1
N2
N3
+250 m
100 m
Paganzo, Argentina
Amana-Talampaya Fm
La Colina Fm
Lueckisporites–Weylandites (LW) Assemblage Biozone
Fusacolpites fusus–Vittatina subsaccata (FV) biozone
296.1 ±0.1 Ma
Basalt
Aksu-Kalpin Tarim Basin, China
Kaipaizileike Fm
287-288 ±3ma
Kupukuziman Fm
Kangkelin Fm
Karachatyr Composite S. Ferghana
Equiv. zon
'Orenburgian'
1000 m
Kasimovian
SE Tatarstan Composite
Upper Kazanian
Lower Kazanian
Ufimian
Sakmarian
50m
Kotlovka Russia
Urzhumian
Upper Kazanian
Lower Kazanian
IV
III
II
I
Elabuga, Russia
Lower Kazanian
Ufimian
20m
Chernaja Rechka (Urals)
Artinskian
Sakmarian
150 m
291.1 ±0.4 Ma
Nikolskyi (Urals)
Asselian
Gzhelian
300.2 ±0.3 Ma
303.5 ±0.4 Ma
Aidaralash (Urals)
296.7 ±0.4 Ma
298.1 ±0.5 Ma
298.5 ±0.3 Ma
299.2 ±0.3 Ma
Khei-Yaga River N. Urals
Silova Formation
Severodvinian
Urzhumian
Kazanian
Adz'va River Pechora
Phylladoderma
320m gap
Coarse Sandstone
Mining
Kalkos
Toshkos
Seida
Inta
with bivalves
Buknnauk
Beds
Formation
Tal'bei
Tatarian
Biarmian
Ufimian
120m
Reversed polarity
Discontinuous sampling reversed polarity
Normal polarity
No or uncertain data
Magnetostratigraphic correlation
Other correlations
U-Pb ID-TIMS dates
Disconformity or hiatus

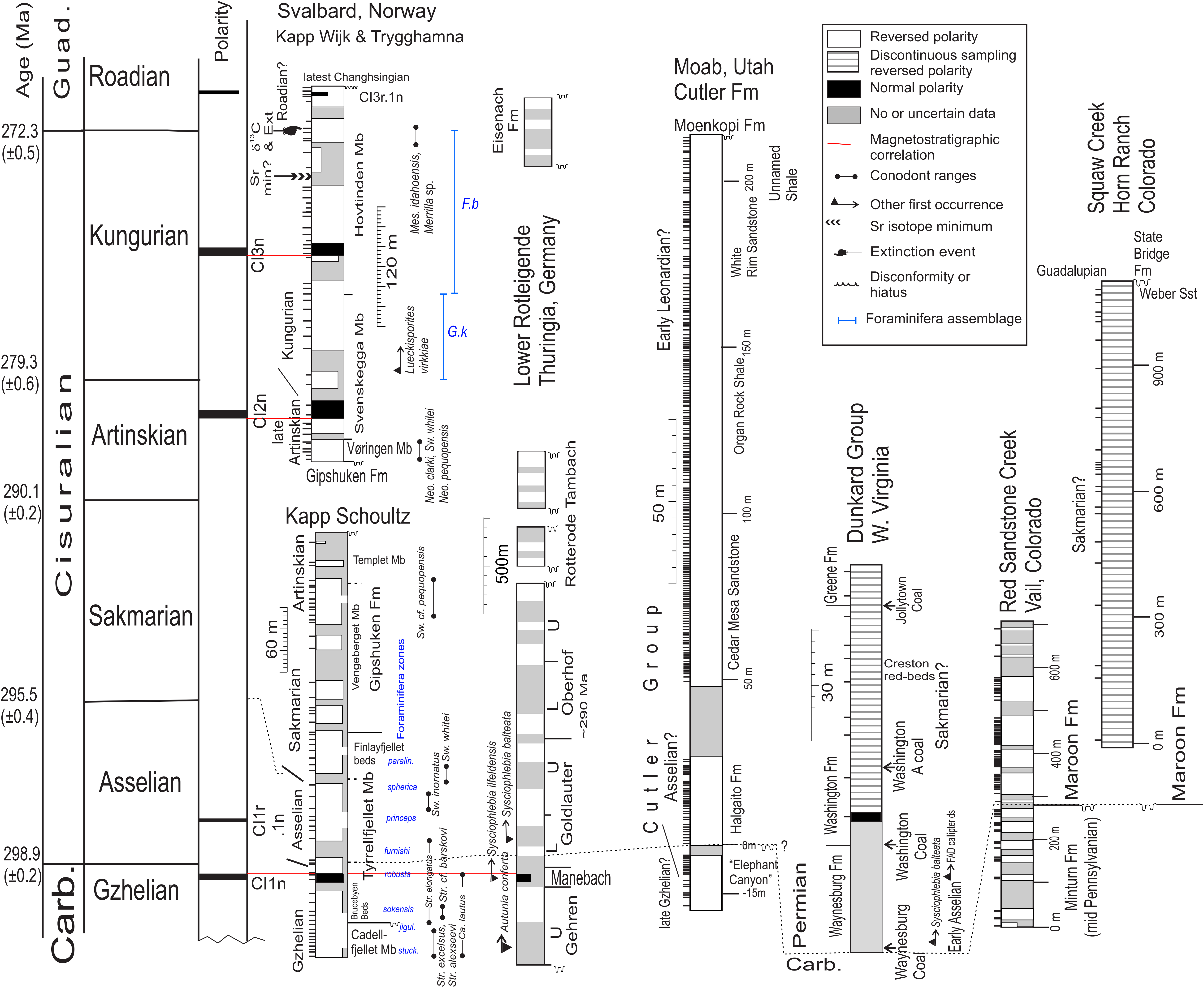

Svalbard, Norway
Kapp Wijk & Trygghamna
Kapp Schoultz
Lower Rotleigende Thuringia, Germany
Moab, Utah Cutler Fm
Dunkard Group W. Virginia
Red Sandstone Creek Vail, Colorado
Squaw Creek Horn Ranch Colorado
Age (Ma)
Polarity
Roadian
Kungurian
Artinskian
Sakmarian
Asselian
Gzhelian
Guad.
Cisuralian
Carb.
272.3 (±0.5)
279.3 (±0.6)
290.1 (±0.2)
295.5 (±0.4)
298.9 (±0.2)
Cl3r.1n
Cl3n
Cl2n
Cl1r.1n
Cl1n
latest Changhsingian
Hovtinden Mb
Svenskegga Mb
Vøringen Mb
Gipshuken Fm
Templet Mb
Vengeberget Mb
Finlayfjellet beds
Tyrrellfjellet Mb
Brucebyen Beds
Cadellfjellet Mb
Foraminifera zones
Eisenach Fm
Rotterode Tambach
Oberhof ~290 Ma
Goldlauter
Manebach
Gehren
Moenkopi Fm
Organ Rock Shale
White Rim Sandstone
Cedar Mesa Sandstone
Halgaito Fm
"Elephant Canyon"
Unnamed Shale
Cutler Group
Early Leonardian?
Greene Fm
Washington Fm
Waynesburg Fm
Jollytown Coal
Creston red-beds
Washington A coal
Washington Coal
Waynesburg Coal
Maroon Fm
Minturn Fm (mid Pennsylvanian)
State Bridge Fm
Weber Sst
Guadalupian
Reversed polarity
Discontinuous sampling reversed polarity
Normal polarity
No or uncertain data
Magnetostratigraphic correlation
Conodont ranges
Other first occurrence
Sr isotope minimum
Extinction event
Disconformity or hiatus
Foraminifera assemblage

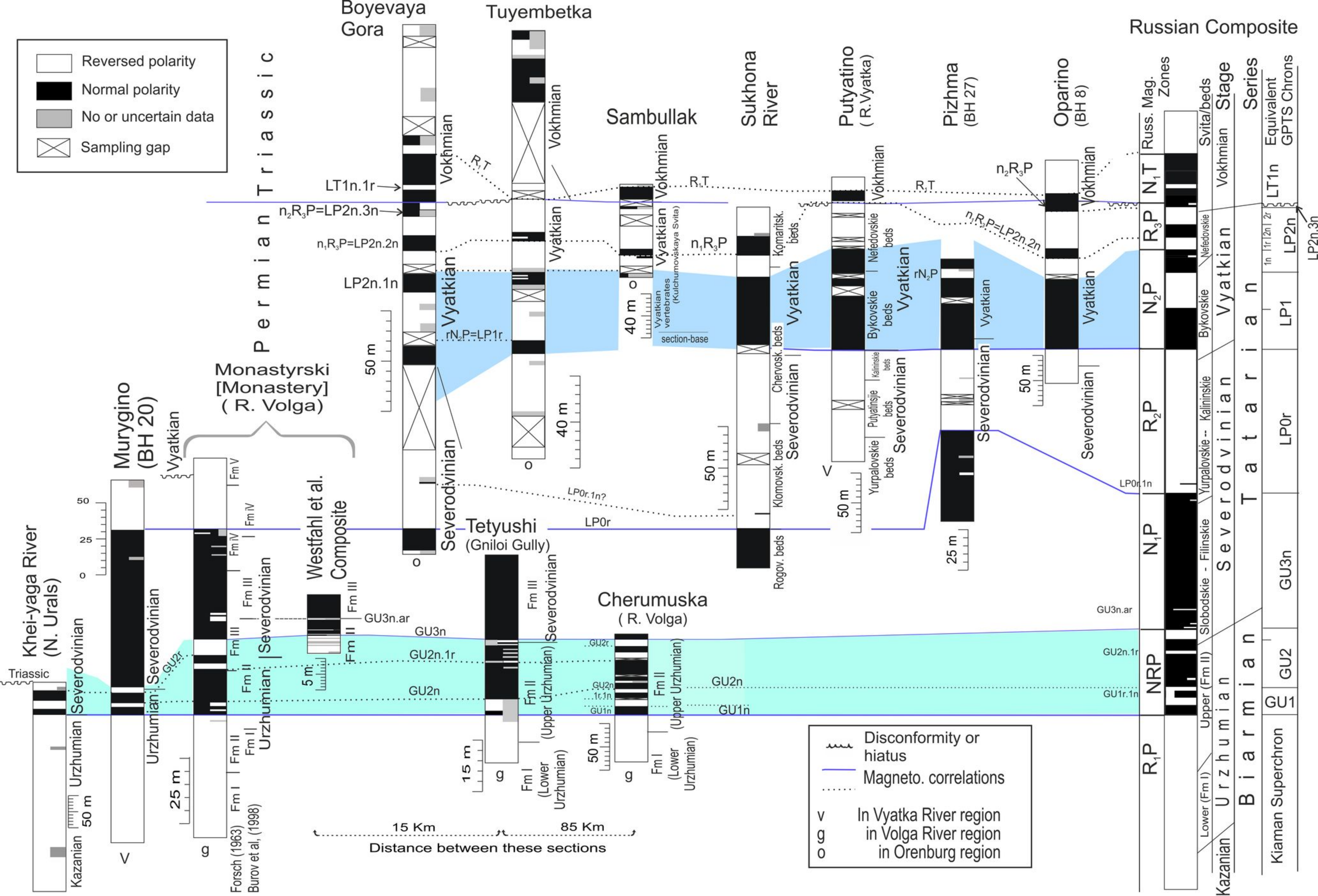
Reversed polarity
Normal polarity
No or uncertain data
Sampling gap
Boyevaya Gora
Tuyembetka
Sambullak
Sukhona River
Putyatino (R.Vyatka)
Pizhma (BH 27)
Oparino (BH 8)
Russian Composite
Permian
Triassic
Murygino (BH 20)
Monastyrski [Monastery] (R. Volga)
Westfahl et al. Composite
Tetyushi (Gniloi Gully)
Cherumuska (R. Volga)
Khei-yaga River (N. Urals)
Disconformity or hiatus
Magneto. correlations
v In Vyatka River region
g in Volga River region
o in Orenburg region
15 Km
85 Km
Distance between these sections
Russ. Mag. Zones
Svita/beds
Stage
Series
Equivalent GPTS Chrons
Vokhmian
Vyatkian
Severodvinian
Urzhumian
Kazanian
Tatarian
Biarmian
Kiaman Superchron
LT1n
LP2n
LP1
LP0r
GU3n
GU2
GU1
LP2n.3n
Nefedovskie
Bykovskie
Yurpalovskie -- Kalininskie
Slobodskie - Filinskie
Upper (Fm II)
Lower (Fm I)
Forsch (1963)
Burov et al, (1998)
section-base
Vyatkian vertebrates (Kuichumovskaya Svita)
LT1n.1r
LP2n.1n
rN2P=LP1r
LP0r.1n?
LP0r
GU3n.ar
GU3n
GU2n.1r
GU2n
GU1n
GU2r
GU1r.1n
Komaritsk. beds
Chervosk. beds
Klomovsk. beds
Rogov. beds
Kalininskie beds
Putyatinsjie beds
Yurpalovskie beds
Fm I
Fm II
Fm III
Fm IV
Fm V
Fm I (Lower Urzhumian)
Fm II (Upper Urzhumian)
50 m
40 m
25 m
15 m
5 m

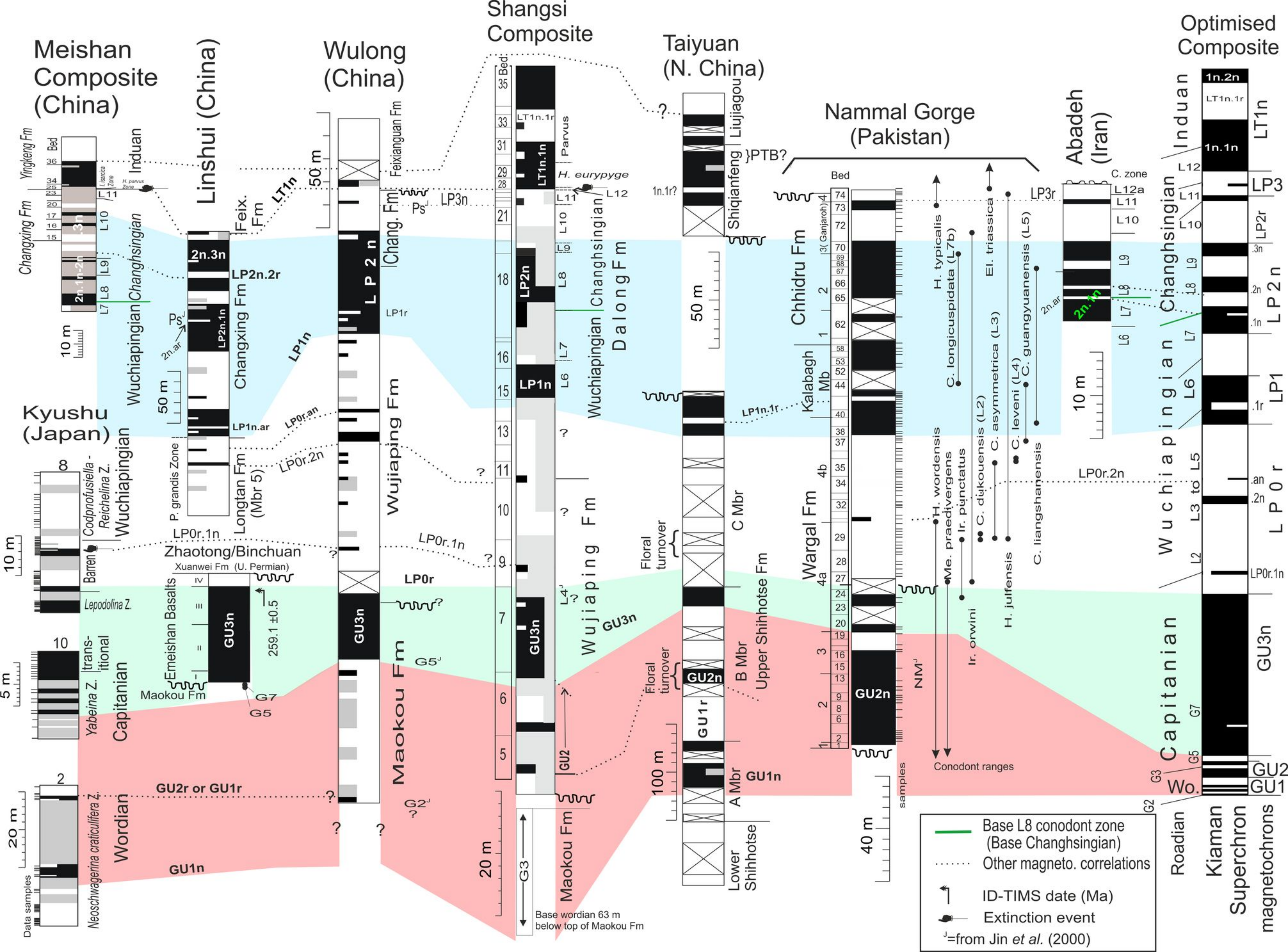

Meishan Composite (China)
Linshui (China)
Wulong (China)
Shangsi Composite
Taiyuan (N. China)
Nammal Gorge (Pakistan)
Abadeh (Iran)
Optimised Composite
Kyushu (Japan)
Zhaotong/Binchuan
Base L8 conodont zone (Base Changhsingian)
Other magneto. correlations
ID-TIMS date (Ma)
Extinction event
J=from Jin et al. (2000)
Conodont ranges
Base wordian 63 m below top of Maokou Fm
Kiaman Superchron
magnetochrons

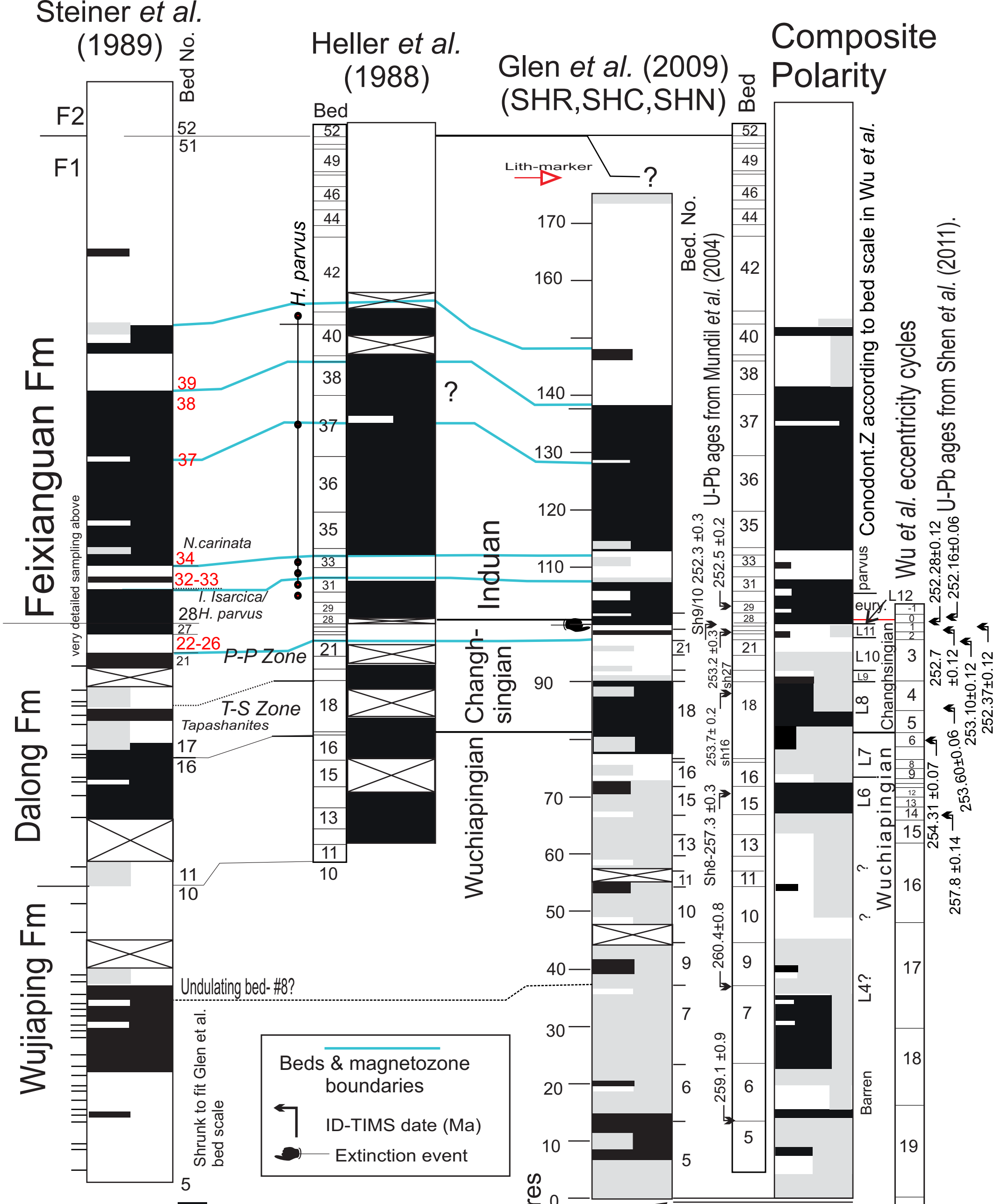

Dalong Fm: 42 m (Nicoll *et al.* 2002).
~49.5 m (Steiner *et al.* 1989)
~42 m (Heller *et al.* 1988)

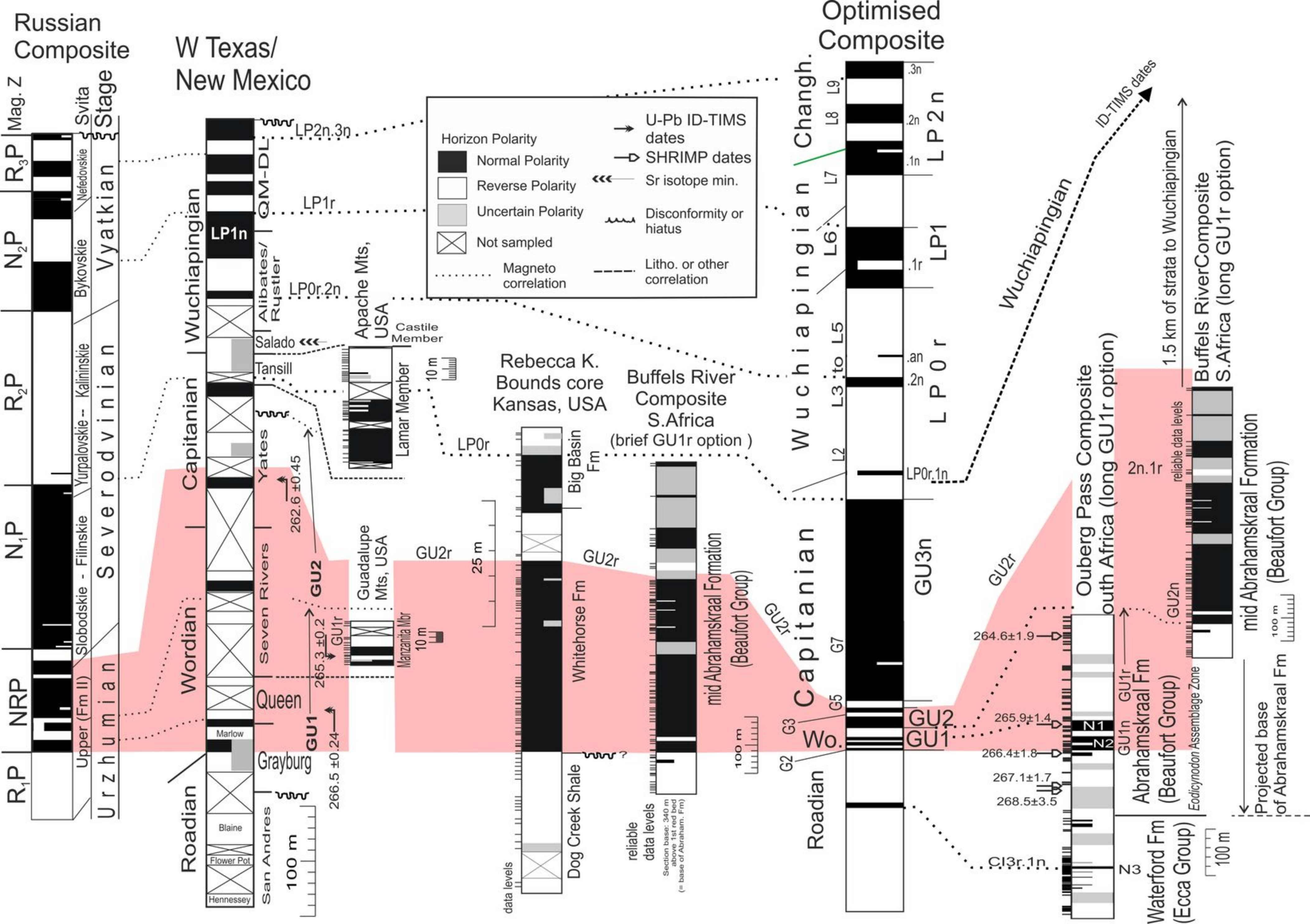

Russian Composite
W Texas/ New Mexico
Optimised Composite
Horizon Polarity
Normal Polarity
Reverse Polarity
Uncertain Polarity
Not sampled
Magneto correlation
U-Pb ID-TIMS dates
SHRIMP dates
Sr isotope min.
Disconformity or hiatus
Litho. or other correlation
Mag. Z
Svita
Stage
Nefedovskie
Vyatkian
Bykovskie
Kalininskie
Yurpalovskie -- Severodvinian
Slobodskie - Filinskie
Upper (Fm II)
Urzhumian
Wuchiapingian
Capitanian
Wordian
Roadian
LP1n
LP2n.3n
LP1r
LP0r.2n
LP0r
QM-DL
Alibates/ Rustler
Salado
Tansill
Yates
Seven Rivers
Queen
Grayburg
San Andres
Marlow
Blaine
Flower Pot
Hennessey
GU1
GU2
GU1r
GU2r
262.6 ±0.45
265.3 ±0.2
266.5 ±0.24
100 m
Apache Mts, USA
Castile Member
Lamar Member
10 m
Guadalupe Mts, USA
Manzanita Mbr
Rebecca K. Bounds core Kansas, USA
Big Basin Fm
Whitehorse Fm
Dog Creek Shale
25 m
data levels
Buffels River Composite S.Africa (brief GU1r option)
mid Abrahamskraal Formation (Beaufort Group)
reliable data levels
Section base: 340 m above 1st red bed (= base of Abraham. Fm)
Changh.
L9
L8
L7
L6
L5
L3 to L5
L2
LP 2 n
LP1
LP 0 r
.3n
.2n
.1n
.1r
.an
.2n
LP0r.1n
GU3n
GU2
GU1
G7
G5
G3
G2
Wo.
ID-TIMS dates
Wuchiapingian
Ouberg Pass Composite South Africa (long GU1r option)
264.6±1.9
265.9±1.4
266.4±1.8
267.1±1.7
268.5±3.5
N1
N2
N3
CI3r.1n
GU1r
GU1n
Abrahamskraal Fm (Beaufort Group)
Waterford Fm (Ecca Group)
Eodicynodon Assemblage Zone
1.5 km of strata to Wuchiapingian
Buffels RiverComposite S.Africa (long GU1r option)
2n.1r
GU2n
mid Abrahamskraal Formation (Beaufort Group)
Projected base of Abrahamskraal Fm

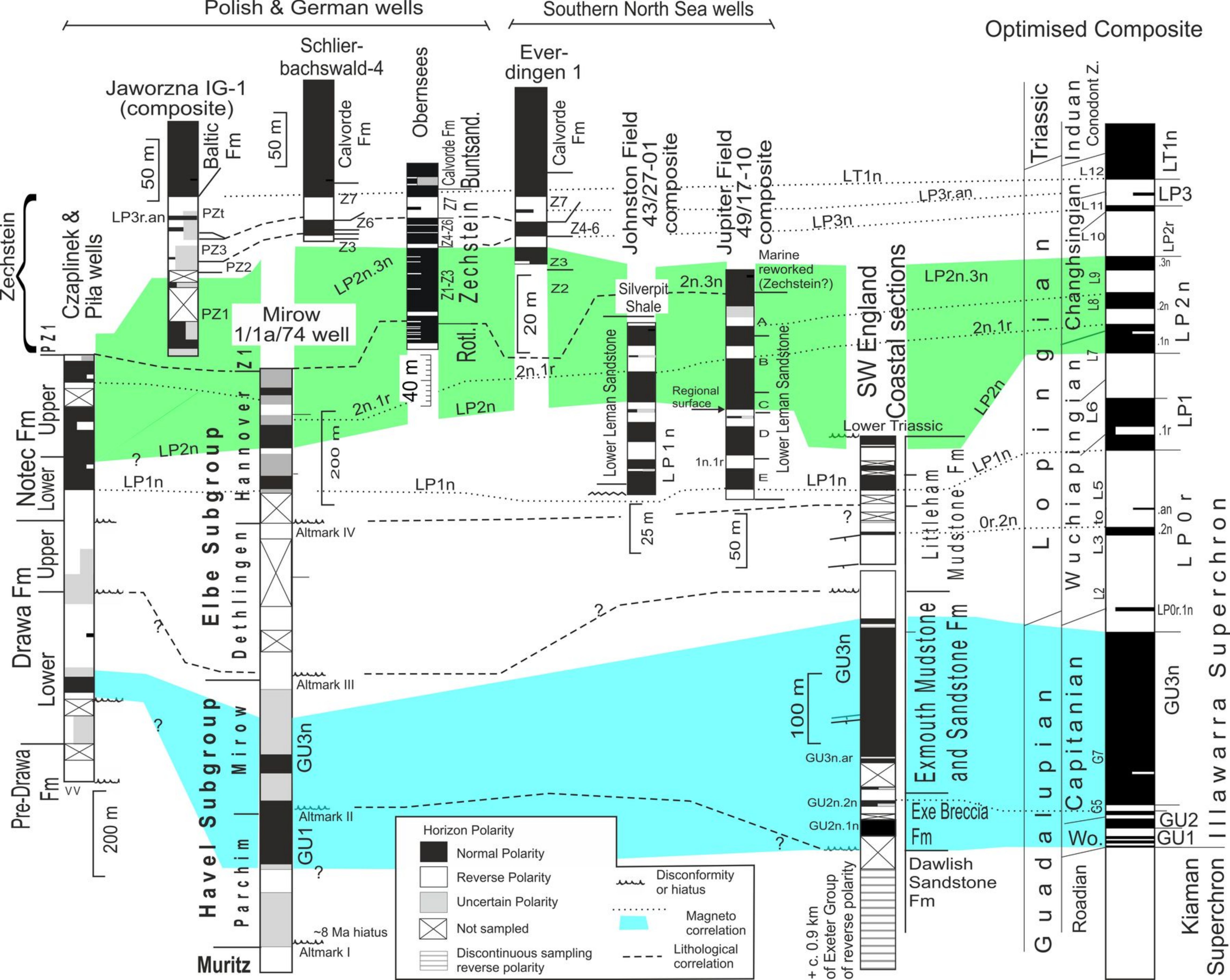

Polish & German wells
Southern North Sea wells
Optimised Composite
Jaworzna IG-1 (composite)
Schlier-bachswald-4
Obernsees
Ever-dingen 1
Johnston Field 43/27-01 composite
Jupiter Field 49/17-10 composite
SW England Coastal sections
Czaplinek & Piła wells
Mirow 1/1a/74 well
Zechstein
Baltic Fm
Calvorde Fm
Buntsand.
Zechstein
Rotl.
LT1n
LP3r.an
LP3n
LP2n.3n
2n.3n
2n.1r
LP2n
LP1n
0r.2n
Marine reworked (Zechstein?)
Silverpit Shale
Lower Leman Sandstone
Regional surface
Lower Triassic
Notec Fm
Drawa Fm
Pre-Drawa Fm
Upper
Lower
Elbe Subgroup
Havel Subgroup
Hannover
Dethlingen
Mirow
Parchim
Muritz
Altmark IV
Altmark III
Altmark II
Altmark I
~8 Ma hiatus
GU3n
GU1
GU3n.ar
GU2n.2n
GU2n.1n
Littleham Mudstone Fm
Exmouth Mudstone and Sandstone Fm
Exe Breccia Fm
Dawlish Sandstone Fm
+ c. 0.9 km of Exeter Group of reverse polarity
Triassic
Induan
Conodont Z.
Lopingian
Changhsingian
Wuchiapingian
Guadalupian
Capitanian
Wo.
Roadian
Illawarra Superchron
Kiaman Superchron
LP3
LP2r
LP2n
LP1
LP0r
LP0r.1n
GU2
GU1
Horizon Polarity
Normal Polarity
Reverse Polarity
Uncertain Polarity
Not sampled
Discontinuous sampling reverse polarity
Disconformity or hiatus
Magneto correlation
Lithological correlation
50 m
200 m
40 m
20 m
25 m
100 m

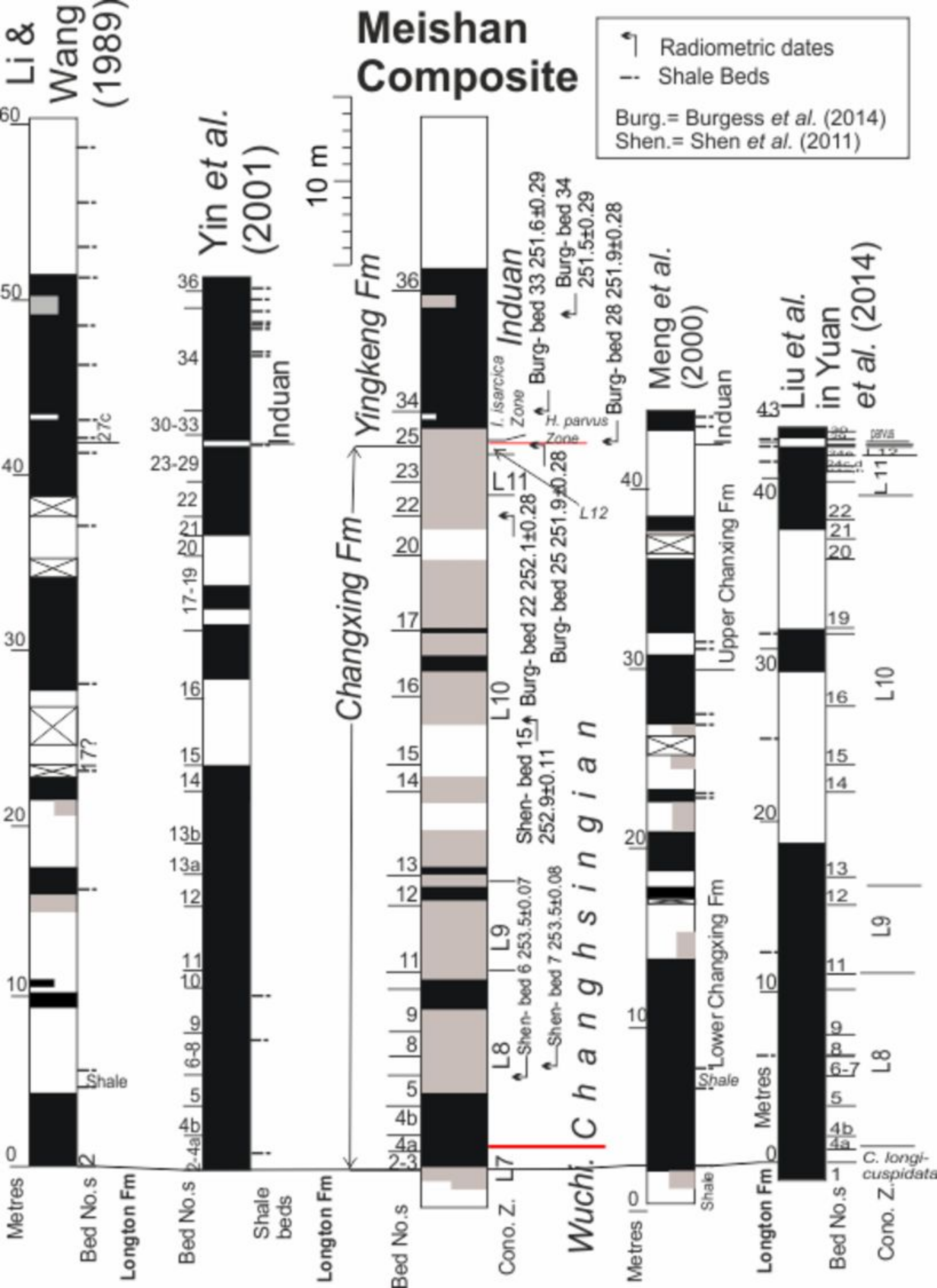

Meishan Composite
Radiometric dates
Shale Beds
Burg.= Burgess et al. (2014)
Shen.= Shen et al. (2011)
Li & Wang (1989)
Yin et al. (2001)
Meng et al. (2000)
Liu et al. in Yuan et al. (2014)
10 m
Induan
Yingkeng Fm
Changxing Fm
Upper Chanxing Fm
Lower Changxing Fm
Wuchi.
Changhsingian
I. isarcica Zone
H. parvus Zone
C. longicuspidata
Burg- bed 33 251.6±0.29
Burg- bed 34 251.5±0.29
Burg- bed 28 251.9±0.28
Burg- bed 25 251.9±0.28
Burg- bed 22 252.1±0.28
Burg- bed 15
Shen- bed 15 252.9±0.11
Shen- bed 6 253.5±0.07
Shen- bed 7 253.5±0.08
L7
L8
L9
L10
L11
L12
Shale
Metres
Bed No.s
Longton Fm
Shale beds
Cono. Z.

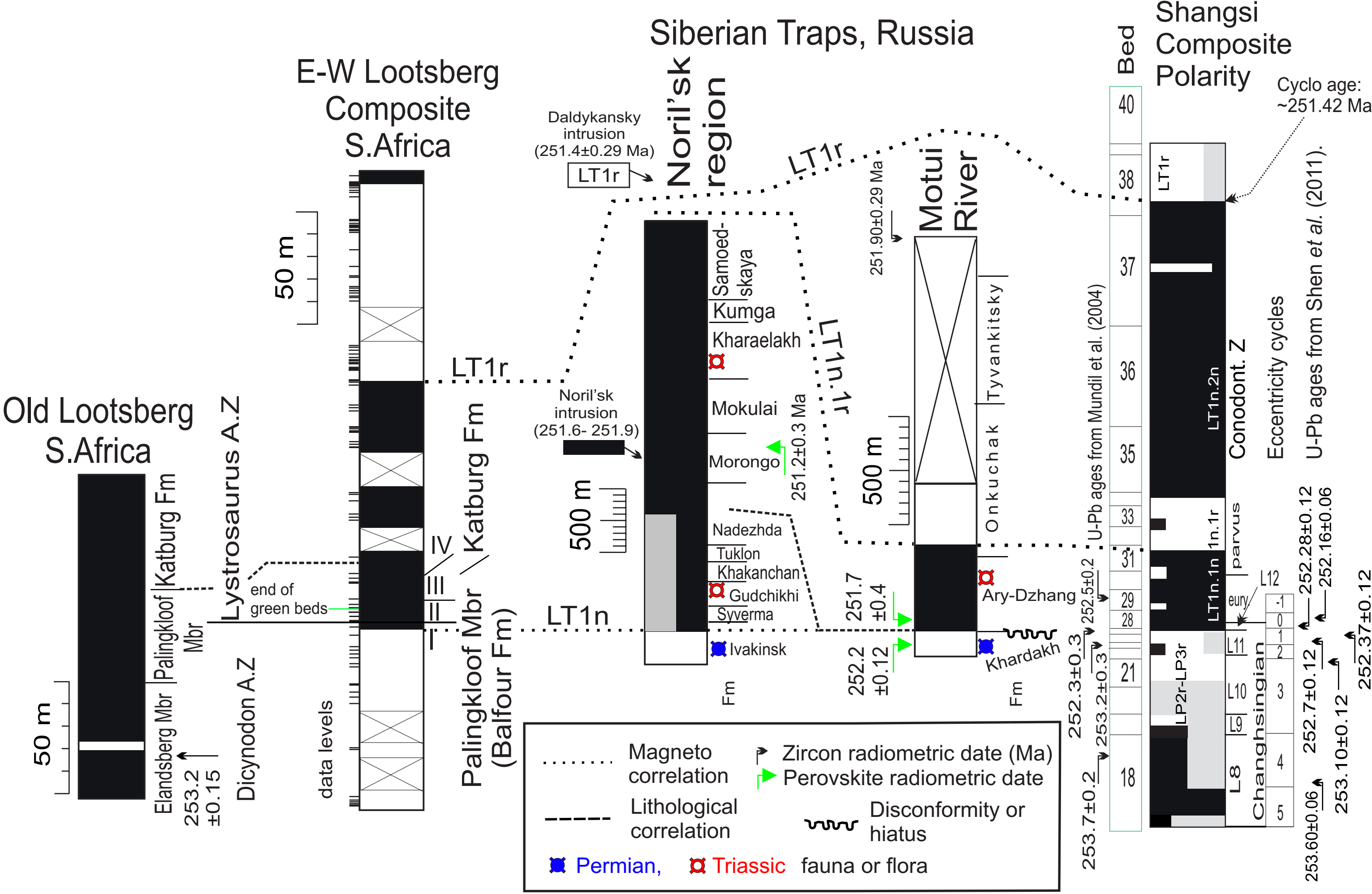
Old Lootsberg S.Africa
50 m
Katburg Fm
Palingkloof Mbr
Elandsberg Mbr
253.2 ±0.15
Lystrosaurus A.Z
Dicynodon A.Z
end of green beds
E-W Lootsberg Composite S.Africa
50 m
data levels
LT1r
LT1n
IV
III
II
I
Katburg Fm
Palingkloof Mbr (Balfour Fm)
Siberian Traps, Russia
Daldykansky intrusion (251.4±0.29 Ma)
LT1r
Noril'sk region
Noril'sk intrusion (251.6- 251.9)
500 m
Samoed-skaya
Kumga
Kharaelakh
Mokulai
Morongo
Nadezhda
Tuklon
Khakanchan
Gudchikhi
Syverma
Ivakinsk
Fm
251.2±0.3 Ma
LT1n.1r
251.7 ±0.4
252.2 ±0.12
251.90±0.29 Ma
Motui River
500 m
Tyvankitsky
Onkuchak
Ary-Dzhang
Khardakh
Fm
LT1r
Bed
40
38
37
36
35
33
31
29
28
21
18
U-Pb ages from Mundil et al. (2004)
252.5±0.2
252.3±0.3
253.2±0.3
253.7±0.2
Shangsi Composite Polarity
LT1r
LT1n.2n
1n.1r
LT1n.1n
LP2r-LP3r
Cyclo age: ~251.42 Ma
Conodont. Z
parvus
eury
L12
L11
L10
L9
L8
Changhsingian
Eccentricity cycles
-1
0
1
2
3
4
5
U-Pb ages from Shen et al. (2011).
252.28±0.12
252.16±0.06
252.37±0.12
252.7±0.12
253.10±0.12
253.60±0.06
Magneto correlation
Lithological correlation
Zircon radiometric date (Ma)
Perovskite radiometric date
Disconformity or hiatus
Permian, Triassic fauna or flora

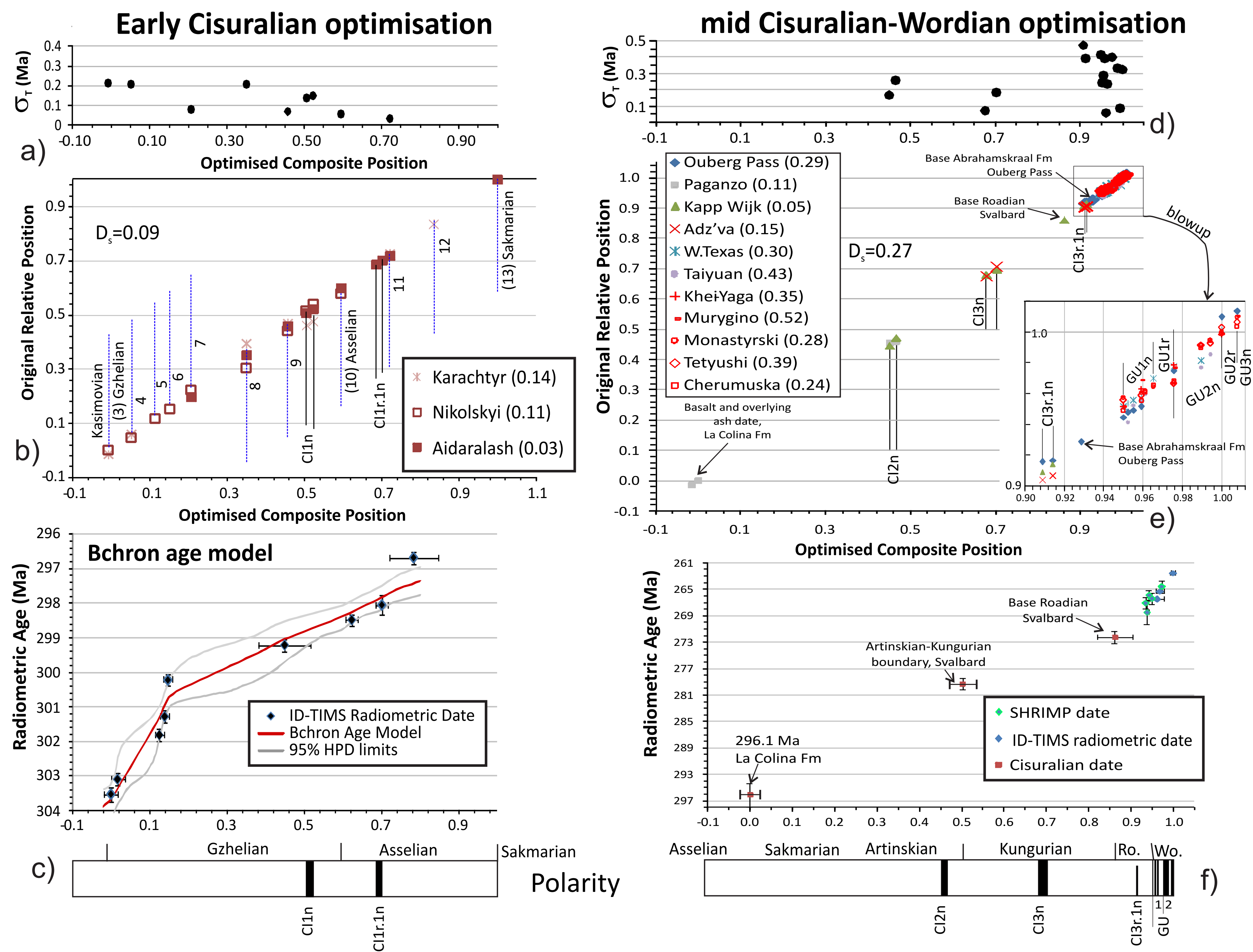

Early Cisuralian optimisation
mid Cisuralian-Wordian optimisation
σT (Ma)
Optimised Composite Position
Original Relative Position
Ds=0.09
Ds=0.27
Karachtyr (0.14)
Nikolskyi (0.11)
Aidaralash (0.03)
Ouberg Pass (0.29)
Paganzo (0.11)
Kapp Wijk (0.05)
Adz'va (0.15)
W.Texas (0.30)
Taiyuan (0.43)
Khei-Yaga (0.35)
Murygino (0.52)
Monastyrski (0.28)
Tetyushi (0.39)
Cherumuska (0.24)
Base Abrahamskraal Fm Ouberg Pass
Base Roadian Svalbard
Basalt and overlying ash date, La Colina Fm
blowup
Bchron age model
Radiometric Age (Ma)
ID-TIMS Radiometric Date
Bchron Age Model
95% HPD limits
SHRIMP date
ID-TIMS radiometric date
Cisuralian date
Artinskian-Kungurian boundary, Svalbard
296.1 Ma La Colina Fm
Kasimovian
(3) Gzhelian
(10) Asselian
(13) Sakmarian
Gzhelian
Asselian
Sakmarian
Artinskian
Kungurian
Ro.
Wo.
Polarity
Cl1n
Cl1r.1n
Cl2n
Cl3n
Cl3r.1n
GU1n
GU1r
GU2n
GU2r
GU3n
a)
b)
c)
d)
e)
f)

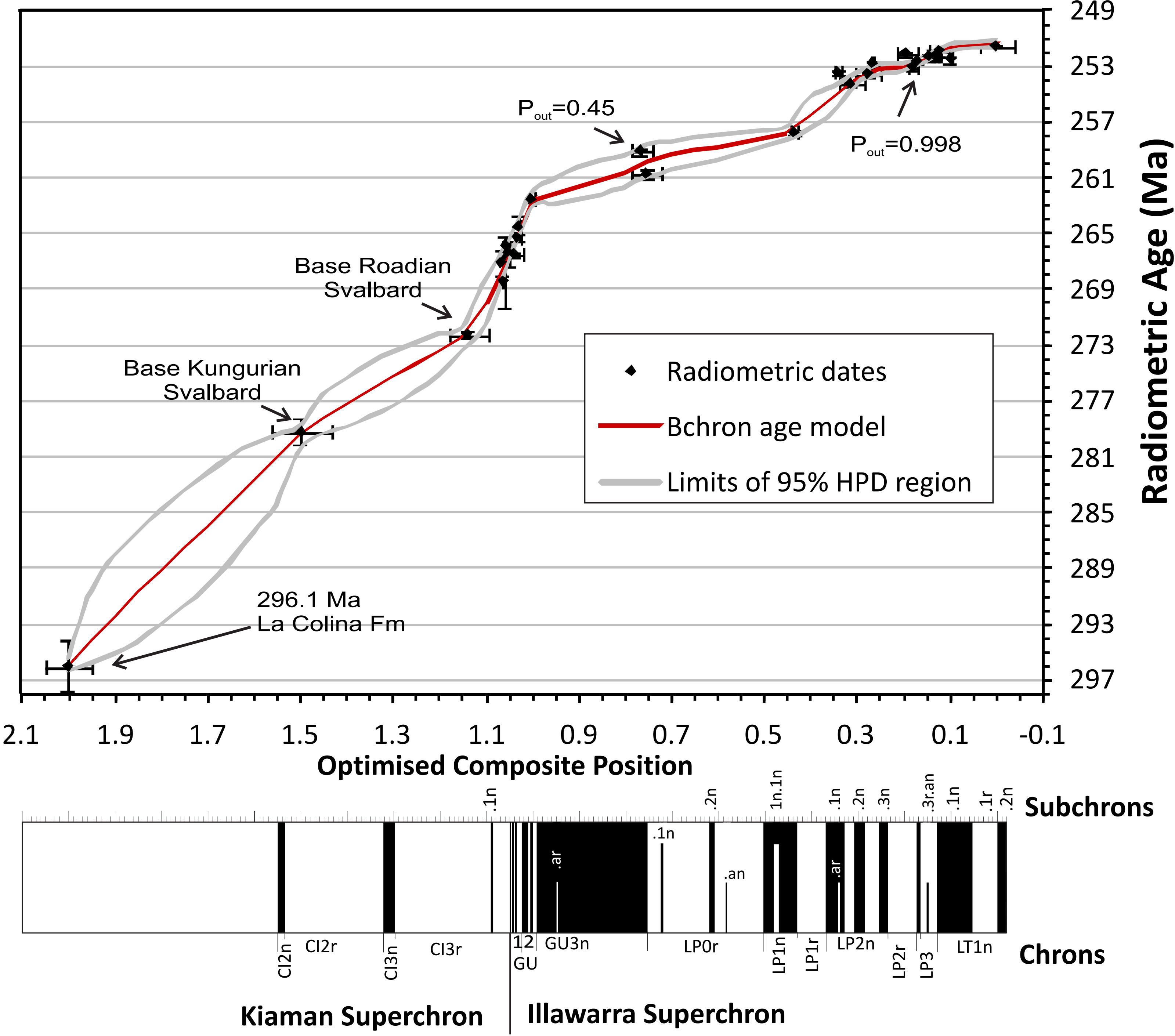

Pout=0.45
Pout=0.998
Base Roadian
Svalbard
Base Kungurian
Svalbard
296.1 Ma
La Colina Fm
Radiometric dates
Bchron age model
Limits of 95% HPD region
Radiometric Age (Ma)
249
253
257
261
265
269
273
277
281
285
289
293
297
2.1
1.9
1.7
1.5
1.3
1.1
0.9
0.7
0.5
0.3
0.1
-0.1
Optimised Composite Position
Subchrons
Chrons
.1n
.2n
1n.1n
.1n
.2n
.3n
.3r.an
.1n
.1r
.2n
.1n
.ar
.an
.ar
CI2n
CI2r
CI3n
CI3r
1
2
GU
GU3n
LP0r
LP1n
LP1r
LP2n
LP2r
LP3
LT1n
Kiaman Superchron
Illawarra Superchron

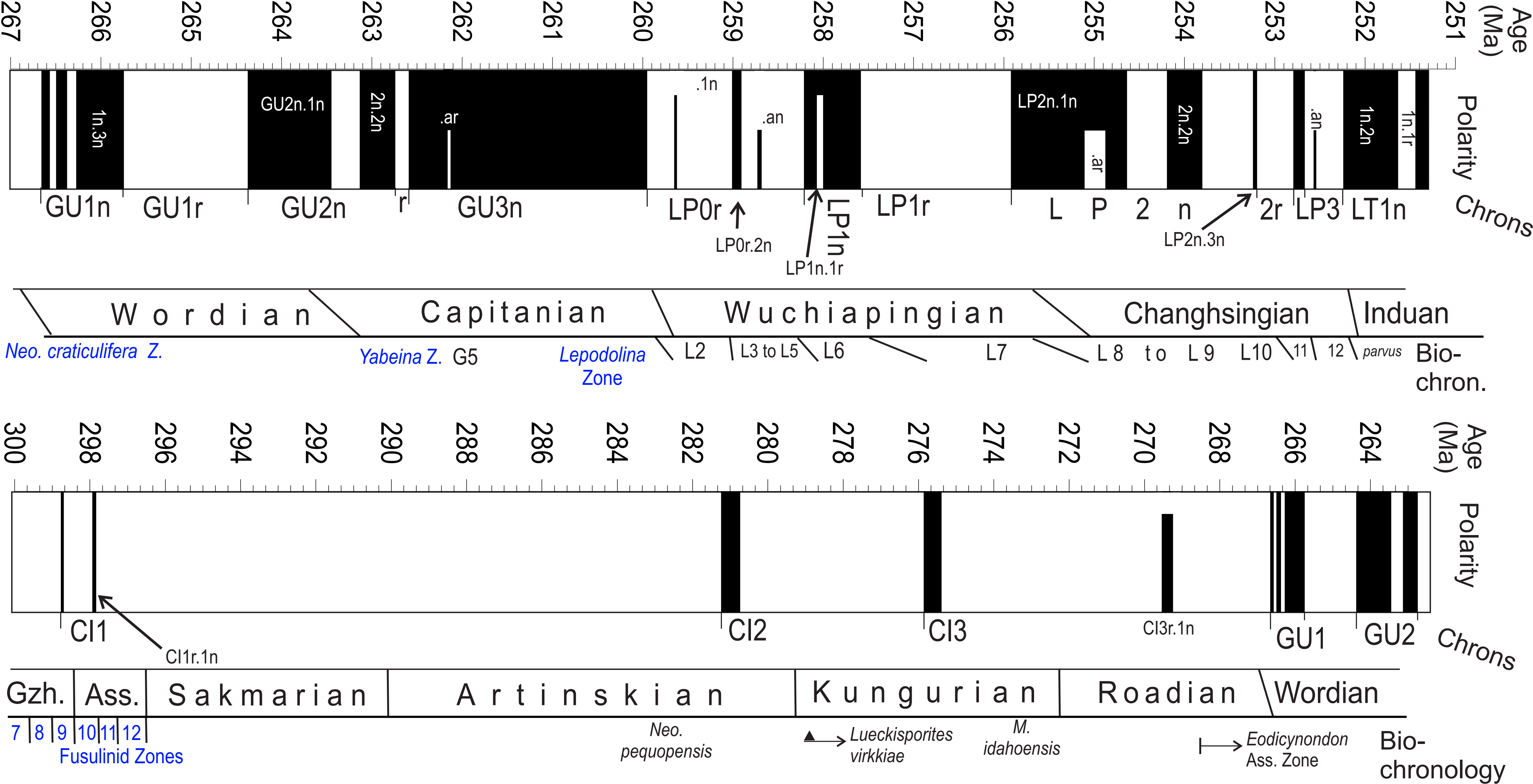
Age (Ma)
Polarity
Chrons
GU1n GU1r GU2n r GU3n LP0r LP1r L P 2 n 2r LP3 LT1n
LP0r.2n
LP1n
LP1n.1r
LP2n.3n
GU2n.1n
LP2n.1n
Wordian Capitanian Wuchiapingian Changhsingian Induan
Neo. craticulifera Z.
Yabeina Z. G5
Lepodolina Zone
L2 L3 to L5 L6 L7 L8 to L9 L10 11 12 parvus
Bio-chron.
Polarity
Chrons
CI1 CI1r.1n CI2 CI3 CI3r.1n GU1 GU2
Gzh. Ass. Sakmarian Artinskian Kungurian Roadian Wordian
7 8 9 10 11 12
Fusulinid Zones
Neo. pequopensis
Lueckisporites virkkiae
M. idahoensis
Eodicynondon Ass. Zone
Bio-chronology

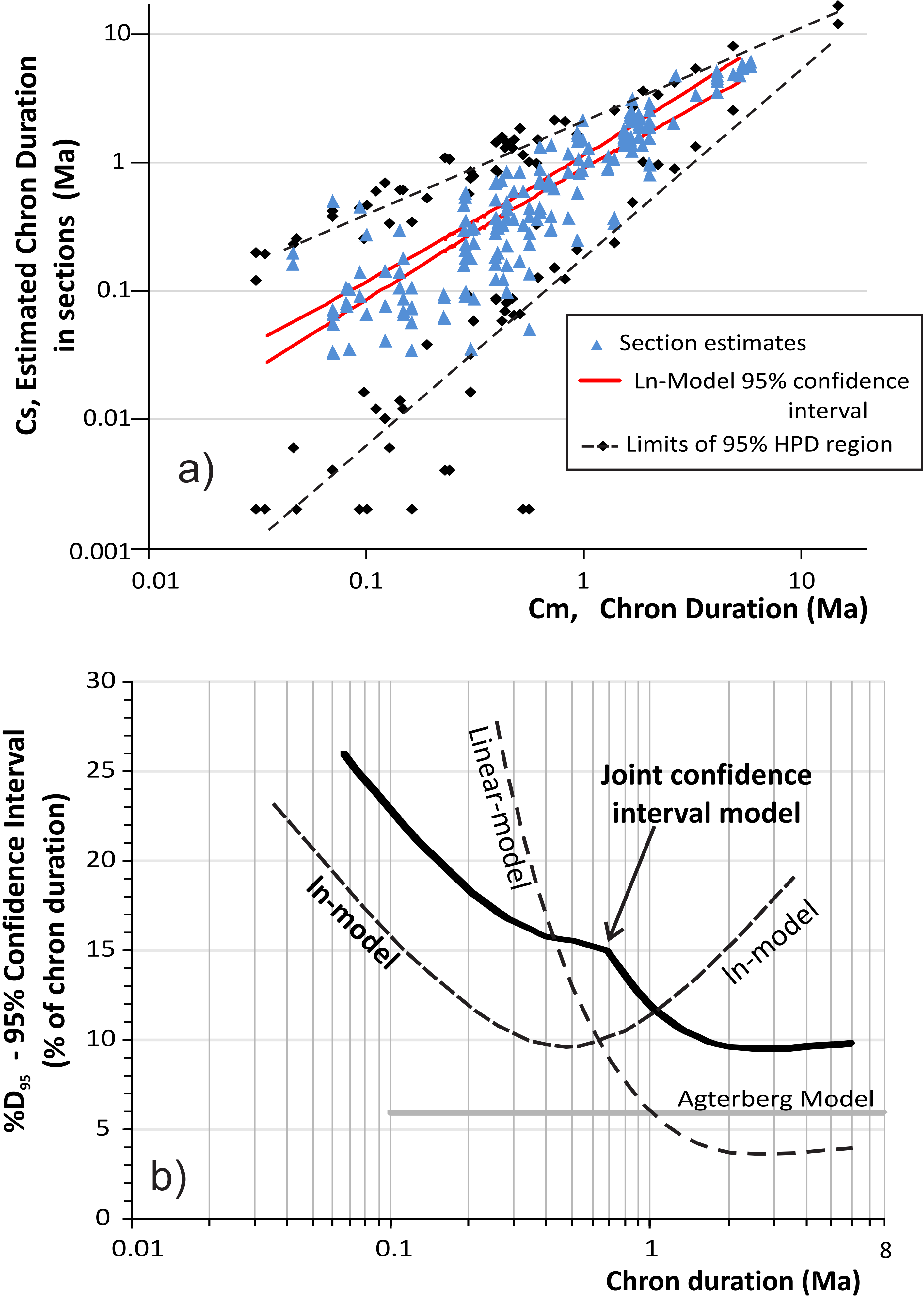
Cs, Estimated Chron Duration in sections (Ma)
10
1
0.1
0.01
0.001
0.01
0.1
1
10
Cm, Chron Duration (Ma)
a)
Section estimates
Ln-Model 95% confidence interval
Limits of 95% HPD region
%D95 - 95% Confidence Interval (% of chron duration)
30
25
20
15
10
5
0
0.01
0.1
1
8
Chron duration (Ma)
Linear-model
Joint confidence interval model
ln-model
ln-model
Agterberg Model
b)